UC Riverside

UC Riverside Electronic Theses and Dissertations

Title

Optimizing Immunity Against SARS-CoV-2 and Influenza Viruses

Permalink

https://escholarship.org/uc/item/0rg4c6rf

Author

Dulin, Harrison

Publication Date

2022

Peer reviewed|Thesis/dissertation

eScholarship.org Powered by the California Digital Library
University of California

UNIVERSITY OF CALIFORNIA
RIVERSIDE

Optimizing Immunity Against SARS-CoV-2 and Influenza Viruses

A Dissertation submitted in partial satisfaction
of the requirements for the degree of

Doctor of Philosophy

in

Cell, Molecular, and Developmental Biology

by

Harrison Westcott Dulin

June 2022

Dissertation Committee:
Dr. Rong Hai, Chairperson
Dr. Shou-wei Ding
Dr. Juliet Morrison

Copyright by
Harrison Westcott Dulin
2022

The Dissertation of Harrison Westcott Dulin is approved:

Committee Chairperson

University of California, Riverside

ACKNOWLEDGEMENTS

"Who is wise and understanding among you? Let them show it by their good life, by deeds done in the humility that comes from wisdom." - James 3:13

Thank you to Dr. Shou-wei Ding and Dr. Meera Nair for mentoring me during my rotations as a first-year graduate student. They were a huge help in getting me started as a brand-new scientist.

Thank you to Dr. Morris Maduro, Dr. David Lo, Dr. Marcus Kaul, Dr. Juliet Morrison, and Dr. Shou-wei Ding for serving on my qualifying exam committee. The input I received was very helpful and provided me a wonderful opportunity to grow in my thinking as a scientist. Thank you to Dr. Weifeng Gu for serving on my Guidance Committee every year.

Thank you to all the professors who worked with me while I was a teaching assistant to help me become a more proficient science communicator.

Thank you to the various labs who helped me with my experiments. Thank you to Dr. Huiwang Ai for his input on unnatural amino acids. Thank you to Dr. Nathan Hendricks and Dr. Quanqing Zhang for their help with the mass spec and size exclusion chromatography experiments. Thank you to Dr. Boxiao Wang and Dr. Linfeng Gao for showing me how to purify proteins. Thank you to Dr. Emma Wilson, Edward Viscarra, and Dr. Rachel Behar for teaching me about Flow Cytometry and letting me use their machines. Thank you to Dr. Gary Chen for his assistance with the mouse work. Thank you to Tran Phan and Arrmund Neal for their help in the BSL3 lab.

Thank you to everyone in the Hai Lab, first and foremost to Dr. Rong Hai who I have had the privilege of working with for over 5 years. Thank you to my fellow graduate students Dr. Stephanie Thurmond and Jerald Chavez, who are both way smarter than me and provided excellent feedback on my experiments. Thank you to the many undergraduates who I have had the pleasure of working with over the years whose assistance made all my experiments possible.

Thank you to my mom Dr. Wendy Dulin for being awesome. Thank you to my church community who regularly prayed for me. And thank you to my God, who meets all my needs according to the riches of His glory in Christ Jesus.

ABSTRACT OF THE DISSERTATION

Optimizing Immunity Against SARS-CoV-2 and Influenza Viruses

by

Harrison Westcott Dulin

Doctor of Philosophy, Graduate Program in Cell, Molecular, and Developmental Biology
University of California, Riverside, June 2022
Dr. Rong Hai, Chairperson

Emerging and reemerging viruses remain a significant threat to human health. Multiple viral outbreaks have occurred since the start of the twenty-first century. Particularly concerning is the emergence of novel pandemic viruses such as the 2009 H1N1 influenza virus and SARS-CoV-2 coronavirus. Adaptive immune responses to these viruses provide a major mode of protection against virus infection and disease. Antibodies against the hemagglutinin protein of influenza viruses and the spike protein of SARS-CoV-2 play an essential role in providing protection, since they can block virus entry into host cells and neutralize virus infection. However, these responses are often suboptimal. This dissertation examines how different modifications to viral proteins effects anti-viral immune responses. We tested the effect of nitration of influenza virus proteins on virus infectivity and immunogenicity. *In vitro* nitration of influenza virus proteins was found to reduce infectivity of multiple strains of influenza viruses. Additionally, chemical *in vitro* nitration of influenza HA protein led to reduced antibody responses against unmodified HA protein. However, nitration of influenza HA protein *in*

vivo was not observed. While overall nitration of the influenza HA protein reduced antibody responses to the HA protein, it was hypothesized that modifications of specific amino acids of the HA protein could increase antibody responses to HA. Mutants of HA incorporating the unnatural amino acid p-nitrophenylalanine were generated and used for vaccination. However, increased antibody responses to the HA protein were not observed in unnatural amino acid mutants. Finally, we examined the ability of pre-existing immunity to influenza viruses to boost antibody responses to a novel vaccine antigen: the SARS-CoV-2 spike protein. We found that a fusion protein vaccine made of the receptor-binding domain of spike and the influenza NP protein generated accelerated antibody responses against spike in mice with pre-existing immunity to influenza virus. The knowledge gained in these studies will help guide the optimization of vaccine strategies for better immune responses against novel emerging viral pathogens.

TABLE OF CONTENTS

LIST OF FIGURES

Chapter 1:

Introduction

INTRODUCTION

Viruses have evolved a wide range of strategies to facilitate infection and replication in hosts organisms. In return, host organisms have evolved multiple different strategies to prevent virus infection. In this arms race between hosts and pathogens, humans are unique among all other organisms in their development of a powerful prophylactic and highly specific antiviral tool: vaccines. Vaccination in humans allows for the development of adaptive immune responses specific to the virus of interest, and these adaptive immune responses can form immune memory that protects the vaccinated individual upon exposure to the virus. This introductory chapter will familiarize the reader with the basics of replication and pathogenesis of influenza viruses and SARS-CoV-2, the responses of the adaptive immune system to virus infection, how the virology and immunology knowledge is applied in the development of vaccines against influenza and SARS-CoV-2 viruses, and the current challenges in influenza and SARS-CoV-2 vaccination.

INFLUENZA VIRUS REPLICATION

Influenza viruses are respiratory pathogens that are spread primarily by airborne transmission from one person to another. Influenza viruses are enveloped viruses containing a negative-sense, single-stranded RNA genome split into 8 separate segments. Three viral proteins are visible on the surface of the virion: the hemagglutinin (HA)

glycoprotein, the neuraminidase (NA) glycoprotein, and the ion channel (M2) protein. HA trimers make up the majority of the protein on the virion surface (about 80%), and HA plays a major role in virus infection and anti-viral antibody responses[1]. The replication cycle of the virus begins upon attachment of the virion to host cells. HA facilitates infection of host cells by binding to sialic acid receptors on the surface of epithelial cells that line the respiratory tract of the host. Differences in affinity between different HA proteins and different sialic acid receptors plays a major role in determining the species specificity of different influenza viruses[1,2]. Once HA has bound its sialic acid receptor, virus entry into the cell is triggered by receptor-mediated endocytosis. Once inside the cell, fusion of the virus membrane with the endosomal membrane is required for the release of the virus genome and polymerase enzymes into the cytoplasm. Fusion is mediated by the HA protein, which undergoes major structural changes to facilitate fusion. The HA protein is cleaved by trypsin or trypsin-like proteases into two separate proteins, HA1 and HA2[1,3]. Cleavage produces a "fusion peptide" at the N-terminus of HA2. The fusion peptide is hydrophobic and capable of integrating into host membranes but is sequestered in the interior of the HA trimer prior to virion endocytosis[4,5]. Following endocytosis and virion entry into the cell, endosomal pH drops, and pH-driven structural changes in HA expose the fusion peptide and reposition the HA trimer to bring the two membranes together[6,7].

Fusion results in the release of the viral genome into the cytoplasm. The viral genome is made up of 8 separate segments of ribonucleoprotein (RNP) complexes consisting of the virus RNA bound to four different virus proteins: NP, PB1, PB2, and

PA. The virus nucleocapsid protein (NP) binds to the virus RNA at regular intervals and facilitates import of the RNP into the nucleus, the site of virus genome replication[8]. PB1, PB2, and PA associates with the 5' and 3' ends of the virus RNA, and these three proteins form a heterotrimer that functions as the viral polymerase[9]. The genome of influenza viruses is negative sense and therefore cannot be translated directly into protein. Positive-sense RNA is synthesized by the viral polymerase. The positive-sense RNA can then be used as a template for making more negative-sense RNA or can be translated to produce virus proteins.

Once synthesis of the new viral proteins and RNA is complete, the different components of the virion must be brought together to form the new virus particle. The viral M1 protein facilitates export of the new RNPs from the nucleus to the inner side of the cell membrane, where the M1 protein interacts with the inner-membrane tails of the virus transmembrane proteins HA, NA, and M2[10]. To facilitate budding of new virus particles, newly synthesized NA protein enzymatically cleaves sialic acid on the surface of the cell to prevent attachment of newly made viruses to the already-infected cell[1]. Once budding is complete, the replication cycle begins again when the virus binds to a new host cell.

SARS-COV-2 REPLICATION

SARS-CoV-2 is an enveloped, positive-sense, single stranded RNA virus. It is transmitted in either respiratory droplets or aerosols. Once inside the respiratory tract, the replication cycle of the virus is initiated by the binding of virus particles to the surface of host airway epithelial cells. The surface of the SARS-CoV-2 virus is studded with trimers

of the virus spike glycoprotein that allows for attachment of the virus to host cells. Spike is a large protein between 180kD-200kD and is divided into S1 and S2 domains[11]. The S1 domain contains the receptor binding domain (RBD) of the protein, which interacts directly with angiotensin-converting enzyme 2 (ACE2) on the surface of host cells[12]. ACE2 is highly expressed in epithelial cells in the lung and digestive tract, and the presence of ACE2 in part determines the tissue trophism of SARS-CoV-2. Attachment of virion to the host cell triggers receptor-mediated endocytosis of the virus. Similar to the HA protein of influenza viruses, spike facilitates the fusion of the virus envelope with the endosomal membrane but must first be proteolytically cleaved into S1 and S2. The host proteases TMPRSS2 and cathepsin L can both fulfill the cleavage requirement for S protein[13,14]. The N-terminus of the S2 protein has a hydrophobic fusion peptide that functions similarly to the fusion peptide of the influenza HA protein. Fusion of the viral envelope with the endosomal membrane releases the virus genome into the cytoplasm of the cell[15].

The genome of SARS-CoV-2 consists of an RNP made up of the single strand of viral RNA coated in nucleocapsid (N) protein. The SARS-CoV-2 genome is positive-sense and can be directly translated into protein. Uncoating of the RNA allows for translation of two open reading frames ORF1a and ORF1b[16]. These open reading frames are translated as long polyproteins that are then proteolytically cleaved into 16 different non-structural proteins that make up the virus polymerase and accessory proteins that form the virus replication and transcription complex (RTC). The genome is transcribed into a negative-sense copy of the viral genome that is then used as a template to produce

more copies of genomic positive-sense RNA as well as a series of sub-genomic RNAs. The sub-genomic RNAs code for the four main structural proteins of the virus, including the spike protein, as well as several non-structural proteins that modulate various molecular pathways inside the cell[13,17].

Virus structural proteins are synthesized in the ER and progress through the cellular secretory pathway to the ER–Golgi intermediate compartment (ERGIC). Genomic RNA coated in N protein interacts with the structural proteins to produce the new virus particle, which buds into the lumen of the secretory vesicle. The virus then exits the cell by a lysosomal exocytosis pathway, and the replication cycle begins again when the virus binds to a new host cell[18,19].

VIRAL PATHOGENESIS

Pathogenesis of COVID-19 and influenza disease is driven by direct cell death from virus infection and by immune responses to infection. Accumulated death of respiratory tract epithelial cells, particularly alveolar epithelial cells, results in damage to the airway and alveoli. Direct cell death and fluid leakage into the alveoli can interfere with gas exchange and lead to acute respiratory distress syndrome (ARDS), which if not resolved will lead to death by hypoxemia[20,21].

Virus proteins can play major roles in cell death, either by directly interfering with host cellular processes or by activating innate immune pathways that trigger apoptosis in the infected cell. The influenza virus protein PB1-F2 can induce cell death by directly interfering with mitochondrial function via membrane disruption[22,23]. The SARS-CoV-2 nsp1 protein binds directly with the 40S ribosomal subunit to prevent

binding of mRNAs to the ribosome, shutting down host cell translation[17]. Recognition of virus RNA by cellular pattern recognition receptors can lead to the activation of the inflammasome in macrophages and epithelial cells. Inflammasome activation following infection with influenza virus or SARS-CoV-2 leads to the cleavage of pro-apoptotic caspases inside the cell in a process called pyroptosis[24,25]. Activation of innate immune sensers in the cell promotes expression of pro-inflammatory cytokines such as interferons, TNFα, IL-1β, and IL-6. These cytokines help recruit immune cells to the site of infection and weaken the lining of the airway vasculature. This allows for easier egress of immune cells from the circulatory system into the lung tissue, but also promotes fluid leakage into the lung, inhibiting gas exchange. The damage to the vasculature can further activate clotting factors, and coagulation dysfunction is a major contributory factor to COVID-19 mortality[26,27].

Recruitment of immune cells to the cite of infection can further the progression of cell death. Activated Natural Killer (NK) cells, cytotoxic T cells, neutrophils, and macrophages that infiltrate the lung release harmful molecules that damage and kill surrounding cells. NK cells release perforins and granzymes that trigger apoptosis in nearby cells. NK cells have been shown to contribute to the pathogenesis of influenza in mice, and elevated levels of NK cells have been observed in the lungs during autopsies of COVID-19 patients[28,29]. Neutrophils release their chromatin into the environment in response to cytokine stimulation, a process called NETosis. The NETs release by the neutrophils can trigger thrombosis and may be a contributing factor to the coagulation disfunction seen in COVID-19[30]. Additionally, activated macrophages and neutrophils

have increased production of reactive nitrogen and reactive oxygen species (RNS and ROS). These are highly reactive molecules that can damage cellular macromolecules, leading to cellular disfunction and contributing to pathogenesis[31–33].

ADAPTIVE IMMUNE RESPONSES TO INFLUENZA AND SARS-COV-2 VIRUSES

Adaptive immune responses to virus infections are mediated by two broad cell types: B cells and T cells. These two classes of immune cells can mount highly specific defenses against individual viruses. B cell mediated immunity comes from the secretion of antibodies by activated, pathogen-specific plasma cells. T cell mediated immunity comes from the recognition of pathogenic peptides bound to MHC molecules on the surface of cells. The presence of pathogen-specific antibodies and pathogen-specific T cells are used as correlates of protection against disease[34,35].

T cell activation requires two signals. The first signal comes from the recognition of antigenic peptides bound to MHC molecules displayed on the surface of antigen-presenting cells by the T Cell Receptor (TCR) on the surface of the T cell. The two main classes of T cells are CD4 positive and CD8 positive T cells. CD4 positive helper T cells recognize antigen bound to MHC class II molecules, while CD8 positive cytotoxic T cells recognize antigen bound to MHC class I molecules. The second signal required for T cell activation comes from the interaction of co-stimulatory molecules such as CD28 on the T cell with CD80/86 on the surface of antigen-presenting cells. Additional cytokine signals can skew the activation of the T cells toward unique gene expression profiles that equip the T cells to better fight specific pathogens. The Th1 class of helper T cells are

associated with better clearance of viral pathogens and are marked by the production of IL-2 and IFNγ cytokines[36]. CD4 positive helper T cells play a key role in the activation of virus-specific B cells, while CD8 positive cytotoxic T cells can eliminate virus-infected cells through the release of cytotoxic molecules such as granzymes and perforins.

Activation of B cells is a multi-step process that typically requires T cell help. (Figure 1). It was first noted that B cell activation in response to protein antigens is T cell dependent when it was discovered that separation of B and T cells no longer lead to the production of antibodies following *in vitro* stimulation[37–39]. It was discovered that just like APCs, B cells could present protein antigen on their surface bound to MHC, and antigen-specific T cells could be activated by antigen presented by B cells.[40] However, rather than displaying antigen in a non-specific manner, B cells specifically present antigen that is recognized by their B cell receptor (BCR). Antigen that binds to the B cell receptor on a naïve B cell is endocytosed and processed in the lysosome into antigenic peptides. These antigenic peptides are loaded onto MHC class II molecules for display to helper T cells, which then become activated to secrete stimulatory cytokines such as IFNγ and IL4. In addition to secreted factors, direct contact between the B and T cell is required. Mice lacking the activated T cell surface marker CD40 fail to mount strong antibody responses to antigens[41]. CD40 interacts with CD40L on B cells to stimulate B cell activation and class switching. Initial B cell activation produces antibodies of the IgM type, but class switching allows for the production of antibodies of the more stable IgG type or the mucosal IgA type. Further T cell help allows B cells to undergo somatic

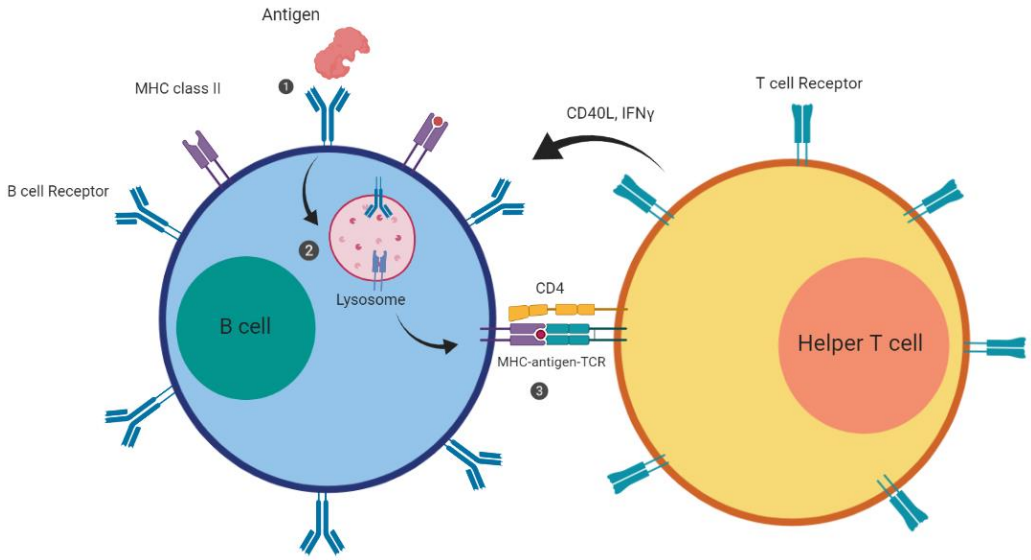

Figure 1. T-cell dependent B cell activation. (1) Antigen is recognized by the B cell receptor (BCR). (2) The BCR bound to antigen is endocytosed and fuses with the lysosome. In the lysosome, the antigenic protein is digested by proteases into peptides that can be recognized by MHC class II. (3) Peptides that are recognized by MHC class II are displayed on the surface of the cell. Helper T cells with antigen-specific T-cell receptors (TCRs) recognize antigen bound to MHC class II and signal to the B cell to become active.

hypermutation of their BCR, a process that leads to greater antigen affinity[42,43]. Activated B cells eventually differentiate into plasma cells that produce high levels of specific antibodies that can protect against virus infection.

The protective role of adaptive immune responses to influenza viruses focuses primarily on the antibody response to virus proteins, primarily to the main virus surface glycoproteins HA and NA. HA and NA are displayed on the surface of virus particles and on the surface of virus-infected cells. HA and NA are therefore directly accessible for antibody recognition. Influenza virus proteins such as NP and the polymerase proteins are internal proteins, found inside the cell or inside the virus particle, and are therefore not directly accessible for binding to antibodies. Nevertheless, antibodies against these proteins are still produced after infection, though the protective role of these antibodies

remains unclear[44]. A direct protective role of antibodies targeting HA comes from the ability of HA antibodies to block the binding of HA to sialic acid receptors on the surface of host cells, preventing virus-induced cell death and the activation of many innate immune responses. These neutralizing antibodies are therefore seen as the main effector of protection against influenza disease. However, non-neutralizing antibodies can still play a role in combating infection. Antibodies targeting the stalk-domain of HA can prevent the conformational changes required for virus fusion with the host cell membrane[45]. Antibodies targeting NA can prevent the enzymatic function of NA, preventing budding of viruses from infected cells[46]. Additionally, antibodies bound to HA or NA on the surface of infected cells can be recognized by immune cells such as NK cells that express Fc receptors. Antibody recognition triggers antibody-dependent cellular cytotoxicity (ADCC), whereby NK cells can kill virus-infected cells[47]. T cell responses to influenza are also protective against influenza virus infections, particularly the cytotoxic CD8 cells, though these responses are often only partially protective[48]. Influenza-specific CD4 positive cells are also protective against influenza, but to a much lesser extent, and mainly influence their protective role through their effect on B cell activation[49]. Due to their ability to recognize antigens displayed on MHC molecules, T cells can recognize internal viral antigens, and NP responses have been shown to make up the largest fraction of the T cell response in mouse models of influenza infection[50]. The internal virus proteins are more conserved between different influenza virus lineages compared to the surface antigens. T-cells may therefore play a major role in providing protection against divergent influenza viruses[51,52].

Adaptive immune responses against SARS-CoV-2 have also focused on antibodies, especially antibodies against the spike protein. Spike is the main surface protein of the virion and is therefore readily accessible to bind spike-specific antibodies. Antibodies against the spike RBD can block attachment of spike to ACE2, preventing attachment of virus to host cells. These neutralizing antibodies are therefore viewed as the main protector against COVID-19. Non-neutralizing antibodies that bind to spike may also play a role in preventing infection by blocking the structural changes in spike required for membrane fusion. While antibodies to spike are crucial in combating SARS-CoV-2 infection, agammaglobulinemia patients who contracted COVID-19 where able to recover from virus infection without the need for supplemental oxygen, despite their inability to mount antibody responses to the virus[53]. This suggests that while antibody responses are crucial, other protective factors can play a role in preventing the development of severe COVID-19. Much attention has been paid to the protective role of cross-reactive T cells that recognize conserved epitopes between SARS-CoV-2 and circulating common-cold coronaviruses, though the extent to which these T cells are protective remains unclear[54].

Protective roles for antibody responses and T cell responses to viral infections has made these adaptive immune responses key metrics in assessing the potential of virus vaccines. Numerous vaccine platforms have been developed with the goal of producing high titers of virus-specific antibodies and T cells. The next two sections cover the main vaccine platforms currently in use and in development for combating influenza and

COVID-19. They include inactivated vaccines, live-attenuated vaccines, virus-vectored vaccines, protein vaccines, and nucleic acid vaccines.

VACCINE STRATEGIES AGAINST INFLUENZA VIRUSES

In the 1935, it was discovered that influenza viruses could be propagated in embryonated chicken eggs[55]. Viruses harvested from infected eggs could be chemically inactivated and safely used for vaccination. Inactivated vaccines made from virus grown in chicken eggs were first approved for use by the US military in the 1940s and have since been the standard method of preparing influenza vaccines. The virus is typically first inactivated by formalin treatment, which cross-links virus proteins, and then the virus envelope is digested to produce "split" virus vaccines [56]. While these are the standard vaccines used in influenza virus vaccination, inactivated vaccines suffer from poor immunogenicity, particularly in the US where many of the vaccines do not contain adjuvant. Additionally, since the virus is delivered intramuscularly, inactivated vaccines typically do not produce mucosal IgA responses in the upper airway. T cell responses to inactivated vaccines are poor since antigen display to T cells is limited to APCs that can take up virus proteins. Finally, the presence of egg macromolecules can lead to high levels of reactogenicity of the vaccine. To bypass production of virus in eggs, virus for use in inactivated virus vaccines can also be grown in cell cultures of MDCK cells, but this production method is more expensive than the current egg-based platform[57].

While it is certainly safer to use inactivated virus vaccines, other vaccine platforms seek to induce stronger immune responses, particularly mucosal responses, by using live-attenuated virus vaccines. Live-attenuated virus vaccines are given intranasally

and can infect epithelial cells in the upper airway. However, the attenuation of the virus results in poor virus replication, particularly in the lower respiratory tract, so the vaccinated person does not develop influenza disease from the vaccine. The Flumist vaccine from AstraZeneca is the only live-attenuated vaccine currently used in the United States[58,59]. However, the vaccine has not been recommended by the CDC during some past flu seasons due to lower-than-expected vaccine effectiveness during the 2009 influenza pandemic[60]. Potentially, cross-reactive antibodies to the vaccine can neutralize the virus before it has a chance to propagate in the upper airway, reducing the overall amount of virus antigen produced and lowering immune responses to the vaccine.

A modification of the live-virus vaccine approach is virus-vectored vaccines. This strategy involves inserting influenza virus genes into already attenuated virus vectors for expression of influenza virus proteins. These vaccines have the benefit of expressing virus genes inside infected cells for antigen display in MHC class I molecules for better T cell activation. Examples of the virus-vectored vaccines for influenza include modified vaccinia virus Ankara (MVA) vectors and adenovirus vectors[61,62]. However, these vaccines have not progressed yet to phase III clinical trials.

Platforms that don't rely on the propagation of influenza viruses have also been developed. Protein or peptide-based vaccines utilize purified influenza virus proteins for immunization without the need to grow the live virus. One such platform involves cloning the HA gene into a baculovirus genome for expression in insect cells. The Flublok vaccine from Sanofi Pasteur makes use of this approach and has been approved for use in the United States[63,64]. Other protein-based platforms aim to increase the

immunogenicity of purified HA proteins by displaying them in nanoparticle structures. NanoFlu, developed by NovaVax, has completed Phase III clinical trials and showed increased cellular and humoral responses compared to inactivated virus vaccine[65]. Additional platforms have targeted the evolutionarily conserved internal virus proteins. The M-001 vaccine developed by Biondvax contains epitopes from the HA, NP, and M1 influenza proteins. A Phase III trial of the vaccine was completed in 2020, but the trail failed to meet its primary efficacy endpoints[66].

The final category of influenza vaccines is nucleic acid vaccines. Like the live attenuated and virus-vectored vaccines, the nucleic acid vaccines are designed to enhance cellular immune responses by expressing virus antigens inside host cells. Additionally, nucleic acid vaccine production is simpler than protein purification, making these vaccines useful in pandemic scenarios where rapid production of vaccine is desirable. There is no currently approved nucleic acid vaccine for influenza, but the approval of the RNA vaccines for SARS-CoV-2 may led to an approved influenza RNA vaccine in the near future.

VACCINE STRATEGIES AGAINST SARS-COV-2

The severity of the SARS-CoV-2 pandemic drew nearly every vaccine maker into the race for an effective vaccine. The WHO currently lists 198 COVID-19 vaccines in pre-clinical development and 161 vaccines in clinical development[67]. Most of these vaccines can be classified into the same categories used for influenza viruses: live-attenuated vaccines, inactivated virus vaccines, virus vectored vaccines, protein vaccines, or nucleic acid vaccines.

Safety issues have made the development of live-attenuated COVID-19 vaccines challenging. Nevertheless, modern genetic technologies have greatly reduced the timescale necessary to produce a live-attenuated virus vaccine. Prior to the 21st century, live-attenuated vaccines were produced by serially passaging viruses in animals or animal tissue with the hope that as the virus developed mutations to better propagate in the animal tissue, it would lose its pathogenicity in humans. This strategy produced several successful vaccines, including the 17D yellow fever virus vaccine and polio live-attenuated vaccines. However, passaging the virus repeatedly through animal tissue was time-consuming and relied on chance to produce the desired mutations. The development of modern genetic technologies, particularly virus rescue systems that allow for precise manipulation of virus genomes, has allowed researchers to make attenuating mutations to the virus genome at will. One such strategy is codon deoptimization, where virus codons are mutated to be less suited for translation in human cells. Codagenix Inc and the Free University of Berlin have generated codon deoptimized SARS-CoV-2 viruses and demonstrated their effectiveness as vaccines in preclinical studies[68,69].

The main inactivated vaccines against COVID-19 are CoronaVac developed by Sinovac and the BBIBP COVID-19 vaccine developed by Sinopharm. CoronaVac is the most widely used coronavirus vaccine in the world, with nearly 1 billion doses administered to date. The inactivated vaccines make use of virus propagated in Vero cells and inactivated with β-propiolactone[70]. The vaccines were shown to be effective in preventing severe disease and death, but had lower effectiveness compared to the RNA

vaccines[71]. A benefit of the inactivated vaccines is their ability to be shipped at 4°C, which allows for easier transport and distribution.

Virus vectored vaccines against COVID-19 include the Covishield vaccine developed by Oxford/AstraZeneca, the Jcovden vaccine developed by Jansen/J&J, and the Russian Sputnik V vaccine. These vaccines make use of adenovirus vectors for expressing the spike protein of SARS-CoV-2 and were originally designed to provide protection after a single vaccine dose. The vaccines were shown to be protective against severe disease and death, but with lower effectiveness compared to the RNA vaccines[72–74]. Additional boosters of the vaccines increased their effectiveness. However, safety concerns around the Jansen and Oxford/AstraZeneca vaccines were raised after the vaccines were associated with a low risk of vaccine-induced immune thrombotic thrombocytopenia (VITT), which has limited the use of these vaccines[75].

Protein vaccines against SARS-CoV-2 make up the largest fraction of vaccines in clinical trials listed by the WHO, with over 50 vaccine candidates having progressed to some form of clinical testing[76]. These vaccines use purified spike protein or spike RBD protein as the vaccine antigen. A wide range of strategies have been employed to manufacture these vaccines and increase their immunogenicity. Platforms in use to produce spike or spike RBD include bacteria cells, yeast cells, insect cells, and mammalian cells[77–80]. Different chemical vaccine adjuvants have been used such as aluminum hydroxide and MF59. The inclusion of dimerization and trimerization domains in the spike protein, as well as presentation in nanoparticles, are further strategies designed to increase the immunogenicity of the vaccine[65,81–84]. Additionally, vaccines

making use of the full-length spike protein included mutations to fix the structure of spike in its pre-fusion state, which corresponds to the structure found on virus particles[85]. While protein-based vaccines have not been approved for use in the US, several protein vaccines including the Novavax nanoparticle vaccine have completed phase III clinical trials and shown to be effective in preventing severe disease and death[86].

The biggest upstarts in the race to produce an effective COVID-19 vaccine are the RNA vaccines produced by Pfizer/BioNTech and Moderna. These were the first nucleic acid-based vaccines approved for human use and showed high efficacy against severe disease and death. The vaccines make use of RNAs encoding for the spike protein encapsulated in lipid nanoparticles. The nanoparticles allow for uptake of the vaccine by host cells, whereupon the mRNA is translated to produce the spike protein. Production of the spike protein by the host cells allows for antigen presentation in MHC class I and removes a manufacturing step in vaccine production. The relative ease of production of RNA vaccines led to their rapid authorization in the US barely a year after the start of the pandemic, and they remain the most widely used vaccines in this country[87–90].

INFLUENZA AND SARS-COV-2 VACCINE CHALLENGES

Despite the successes of vaccines against influenza viruses and SARS-CoV-2, many challenges remain. One of the main concerns is how effective current vaccines will be against new virus strains and variants. This has been a concern in the influenza field for decades and has led to the pursuit of a universal influenza vaccine that would provide broad protection against divergent strains and subtypes of influenza viruses. Strategies include targeting the conserved stalk domain of the HA protein and the conserved

internal virus proteins. Variants are already proving to be a challenge in the ongoing SARS-CoV-2 pandemic. New variants such as the Omicron variant contain multiple mutations in the spike protein, allowing for escape from vaccine-derived antibody responses[91,92]. Additionally, concerns about future emerging novel coronaviruses have led to calls for universal coronavirus vaccines that would protect against all current and future novel coronaviruses[93–95].

An additional concern with current vaccine strategies for both influenza viruses and SARS-CoV-2 is the waning of antibody responses over time. Circulating antibody responses decline after about 6 months with the current SARS-CoV-2 vaccines, which corresponds with decreased effectiveness of the vaccines[96,97]. The current strategy to combat wanning immunity is to give additional boosters of the original vaccines. However, more targeted vaccine strategies designed to increase long-term immunity to both influenza and SARS-CoV-2 viruses are needed.

Another concern with the current vaccines is the multi-dose vaccine regimen needed for full protection. In the case of seasonal influenza vaccines, which suffer from poor vaccine effectiveness, a case could be made that a single dose regimen of the seasonal influenza vaccine is not sufficiently immunogenic to provide robust protection against disease. In the case of SARS-CoV-2, it was disappointing that the virus-vectored vaccines designed to be single dose "one-and-done" vaccines proved not as effective as the multi-dose RNA vaccines. The current vaccine strategies that require multiple vaccinations, including additional boosters, leave people vulnerable to disease during the

weeks after the first vaccination. Vaccine strategies to boost immunity after a single dose will be important in future pandemic scenarios.

Finally, a challenge with current influenza and SARS-CoV-2 vaccines is poor immunogenicity in very young and very old populations. Children and the elderly are at greater risk of influenza disease than other age groups. The elderly are especially vulnerable to COVID-19, with over 80% of deaths in the US occurring in this age group[76]. To protect elderly populations from influenza, the US issues the high-dose Fluzone vaccine for people 65 and older or recommends the adjuvanted influenza vaccines. People over the age of 50 are also encouraged to get a fourth dose of SARS-CoV-2 RNA vaccine[98]. While children remain at low risk for developing severe COVID-19, vaccines for this age group could play a major role in controlling the virus. However, vaccines in children under 5 years old have not been approved in the US, and an initial two-dose regimen of Moderna's RNA vaccine was only 37% effective against disease[99]. Vaccines that provide increased immunogenicity and protection in these age groups are therefore a remaining challenge in the field.

SUMMARY

Influenza viruses and coronaviruses remain a global threat to public health. Much work has been done elucidating the mechanisms of virus infection and pathogenesis, as well as the ways the immune system responds to control infections. Adaptive immune responses, particularly antibody responses, remain the gold standard in providing protection from these viruses, and the number of effective vaccine strategies designed to elicit these protective responses are numerous. Nevertheless, there is still a need to

develop vaccines with greater immunogenicity and effectiveness. The remaining chapters of this dissertation detail studies undertaken to better optimize immune responses to influenza viruses and SARS-CoV-2. The results obtained from these studies will aid the development of improved vaccination strategies against emerging viruses.

REFERENCES

1. Russell, R. J., Gamblin, S. J. & Skehel, J. J. Influenza glycoproteins: Hemagglutinin and neuraminidase. in *Textbook of Influenza* (eds. Webster, R. G., Monto, A. S., Braciale, T. J. & Lamb, R. A.) 67–100 (John Wiley & Sons, Ltd, 2013). doi:10.1002/9781118636817.ch5.

2. Rogers, G. N. & Paulson, J. C. Receptor determinants of human and animal influenza virus isolates: Differences in receptor specificity of the H3 hemagglutinin based on species of origin. *Virology* **127**, 361–373 (1983).

3. Sui, J. *et al.* Structural and Functional Bases for Broad-Spectrum Neutralization of Avian and Human Influenza A Viruses. *Nat Struct Mol Biol* **16**, 265–273 (2009).

4. Cross, K. J., Langley, W. A., Russell, R. J., Skehel, J. J. & Steinhauer, D. A. Composition and functions of the influenza fusion peptide. *Protein Pept Lett* **16**, 766–778 (2009).

5. Cohen, F. S. & Melikyan, G. B. Implications of a fusion peptide structure. *Nat Struct Mol Biol* **8**, 653–655 (2001).

6. Han, X., Bushweller, J. H., Cafiso, D. S. & Tamm, L. K. Membrane structure and fusion-triggering conformational change of the fusion domain from influenza hemagglutinin. *Nat Struct Mol Biol* **8**, 715–720 (2001).

7. Skehel, J. J. & Wiley, D. C. Receptor Binding and Membrane Fusion in Virus Entry: The Influenza Hemagglutinin. *Annual Review of Biochemistry* **69**, 531–569 (2000).

8. Neumann, G., Castrucci, M. R. & Kawaoka, Y. Nuclear import and export of influenza virus nucleoprotein. *J Virol* **71**, 9690–9700 (1997).

9. Mehle, A. & McCullers, J. A. Structure and function of the influenza virus replication machinery and PB1-F2. in *Textbook of Influenza* (eds. Webster, R. G., Monto, A. S., Braciale, T. J. & Lamb, R. A.) 133–145 (John Wiley & Sons, Ltd, 2013). doi:10.1002/9781118636817.ch8.

10. Nayak, D., Shivakoti, S., Balogun, R. A., Lee, G. & Zhou, Z. H. Structure, disassembly, assembly, and budding of influenza viruses. in *Textbook of Influenza* (eds. Webster, R. G., Monto, A. S., Braciale, T. J. & Lamb, R. A.) 35–56 (John Wiley & Sons, Ltd, 2013). doi:10.1002/9781118636817.ch3.

11. Walls, A. C. *et al.* Structure, Function, and Antigenicity of the SARS-CoV-2 Spike Glycoprotein. *Cell* **181**, 281-292.e6 (2020).

12. Lan, J. *et al.* Structure of the SARS-CoV-2 spike receptor-binding domain bound to the ACE2 receptor. *Nature* **581**, 215–220 (2020).

13. V'kovski, P., Kratzel, A., Steiner, S., Stalder, H. & Thiel, V. Coronavirus biology and replication: implications for SARS-CoV-2. *Nat Rev Microbiol* **19**, 155–170 (2021).

14. Emrani, J. *et al.* SARS-COV-2, infection, transmission, transcription, translation, proteins, and treatment: A review. *International Journal of Biological Macromolecules* **193**, 1249–1273 (2021).

15. Harrison, A. G., Lin, T. & Wang, P. Mechanisms of SARS-CoV-2 Transmission and Pathogenesis. *Trends in Immunology* **41**, 1100–1115 (2020).

16. Malone, B., Urakova, N., Snijder, E. J. & Campbell, E. A. Structures and functions of coronavirus replication–transcription complexes and their relevance for SARS-CoV-2 drug design. *Nat Rev Mol Cell Biol* **23**, 21–39 (2022).

17. Thoms, M. *et al.* Structural basis for translational shutdown and immune evasion by the Nsp1 protein of SARS-CoV-2. *Science* **369**, 1249–1255 (2020).

18. Ghosh, S. *et al.* β-Coronaviruses Use Lysosomes for Egress Instead of the Biosynthetic Secretory Pathway. *Cell* **183**, 1520-1535.e14 (2020).

19. Zhang, H. & Zhang, H. Entry, egress and vertical transmission of SARS-CoV-2. *Journal of Molecular Cell Biology* **13**, 168–174 (2021).

20. Klenk, H. D., Garten, W. & Matrosovich, M. Pathogenesis. in *Textbook of Influenza* (eds. Webster, R. G., Monto, A. S., Braciale, T. J. & Lamb, R. A.) 157–172 (John Wiley & Sons, Ltd, 2013). doi:10.1002/9781118636817.ch10.

21. Lamers, M. M. & Haagmans, B. L. SARS-CoV-2 pathogenesis. *Nat Rev Microbiol* **20**, 270–284 (2022).

22. Chen, W. *et al.* A novel influenza A virus mitochondrial protein that induces cell death. *Nat Med* **7**, 1306–1312 (2001).

23. Zamarin, D., García-Sastre, A., Xiao, X., Wang, R. & Palese, P. Influenza virus PB1-F2 protein induces cell death through mitochondrial ANT3 and VDAC1. *PLoS Pathog* **1**, e4 (2005).

24. Lee, S., Hirohama, M., Noguchi, M., Nagata, K. & Kawaguchi, A. Influenza A Virus Infection Triggers Pyroptosis and Apoptosis of Respiratory Epithelial Cells through the Type I Interferon Signaling Pathway in a Mutually Exclusive Manner. *Journal of Virology* **92**, e00396-18 (2018).

25. Ferreira, A. C. *et al.* SARS-CoV-2 engages inflammasome and pyroptosis in human primary monocytes. *Cell Death Discov.* **7**, 1–12 (2021).

26. Ye, Q., Wang, B. & Mao, J. The pathogenesis and treatment of the `Cytokine Storm' in COVID-19. *Journal of Infection* **80**, 607–613 (2020).

27. Merad, M., Blish, C. A., Sallusto, F. & Iwasaki, A. The immunology and immunopathology of COVID-19. *Science* **375**, 1122–1127 (2022).

28. Wilk, A. J. *et al.* A single-cell atlas of the peripheral immune response in patients with severe COVID-19. *Nat Med* **26**, 1070–1076 (2020).

29. Zhou, G., Juang, S. W. W. & Kane, K. P. NK cells exacerbate the pathology of influenza virus infection in mice. *Eur J Immunol* **43**, 929–938 (2013).

30. Skendros, P. *et al.* Complement and tissue factor–enriched neutrophil extracellular traps are key drivers in COVID-19 immunothrombosis. *J Clin Invest* **130**, 6151–6157 (2020).

31. Perrone, L. A., Belser, J. A., Wadford, D. A., Katz, J. M. & Tumpey, T. M. Inducible Nitric Oxide Contributes to Viral Pathogenesis Following Highly Pathogenic Influenza Virus Infection in Mice. *The Journal of Infectious Diseases* **207**, 1576–1584 (2013).

32. Zablockienė, B., Ambrozaitis, A., Kačergius, T. & Gravenstein, S. Implication of nitric oxide in the pathogenesis of influenza virus infection. *Biologija* **58**, (2012).

33. Akaike, T. *et al.* Pathogenesis of influenza virus-induced pneumonia: involvement of both nitric oxide and oxygen radicals. *Proceedings of the National Academy of Sciences* **93**, 2448–2453 (1996).

34. Feng, S. *et al.* Correlates of protection against symptomatic and asymptomatic SARS-CoV-2 infection. *Nat Med* **27**, 2032–2040 (2021).

35. Trombetta, C. M. & Montomoli, E. Influenza immunology evaluation and correlates of protection: a focus on vaccines. *Expert Rev Vaccines* **15**, 967–976 (2016).

36. Mosmann, T. R. & Coffman, R. L. TH1 and TH2 Cells: Different Patterns of Lymphokine Secretion Lead to Different Functional Properties. *Annual Review of Immunology* **7**, 145–173 (1989).

37. Persson, U., Bick, P. H., Hammarström, L., Möller, E. & Smith, C. I. Different requirements for T cells responding to various doses of concanavalin A. *Scand J Immunol* **8**, 291–301 (1978).

38. Hammarström, L., Bird, A. G., Britton, S. & Smith, C. I. Pokeweed mitogen induced differentiation of human B cells: evaluation by a protein A haemolytic plaque assay. *Immunology* **38**, 181–189 (1979).

39. Paige, C. J. & Skarvall, H. Plaque formation by B cell colonies. *J Immunol Methods* **52**, 51–61 (1982).

40. Lanzavecchia, A. Antigen-specific interaction between T and B cells. *Nature* **314**, 537–539 (1985).

41. Kawabe, T. *et al.* The immune responses in CD40-deficient mice: Impaired immunoglobulin class switching and germinal center formation. *Immunity* **1**, 167–178 (1994).

42. Di Noia, J. M. & Neuberger, M. S. Molecular Mechanisms of Antibody Somatic Hypermutation. *Annual Review of Biochemistry* **76**, 1–22 (2007).

43. Neuberger, M. S. & Milstein, C. Somatic hypermutation. *Current Opinion in Immunology* **7**, 248–254 (1995).

44. Padilla-Quirarte, H. O., Lopez-Guerrero, D. V., Gutierrez-Xicotencatl, L. & Esquivel-Guadarrama, F. Protective Antibodies Against Influenza Proteins. *Frontiers in Immunology* **10**, (2019).

45. Liu, W.-C., Nachbagauer, R., Krammer, F. & Albrecht, R. A. Assessment of Influenza Virus Hemagglutinin Stalk-Specific Antibody Responses. in *Influenza Virus: Methods and Protocols* (ed. Yamauchi, Y.) 487–511 (Springer, 2018). doi:10.1007/978-1-4939-8678-1_23.

46. Marcelin, G., Sandbulte, M. R. & Webby, R. J. Contribution of antibody production against neuraminidase to the protection afforded by influenza vaccines. *Rev Med Virol* **22**, 267–279 (2012).

47. Jegaskanda, S. *et al.* Cross-Reactive Influenza-Specific Antibody-Dependent Cellular Cytotoxicity Antibodies in the Absence of Neutralizing Antibodies. *The Journal of Immunology* **190**, 1837–1848 (2013).

48. Nguyen, H. H., van Ginkel, F. W., Vu, H. L., McGhee, J. R. & Mestecky, J. Heterosubtypic Immunity to Influenza A Virus Infection Requires B Cells but Not CD8+ Cytotoxic T Lymphocytes. *J Infect Dis* **183**, 368–376 (2001).

49. Topham, D. J. & Doherty, P. C. Clearance of an Influenza A Virus by CD4+ T Cells Is Inefficient in the Absence of B Cells. *Journal of Virology* **72**, 882–885 (1998).

50. Sant, A. J., DiPiazza, A. T., Nayak, J., Rattan, A. & Richards, K. CD4 T cells in protection from influenza virus: Viral antigen specificity and functional potential. *Immunol Rev* **284**, 91–105 (2018).

51. Hemann, E. A., Kang, S.-M. & Legge, K. L. Protective CD8 T cell mediated immunity against influenza A virus infection following influenza virus-like particle vaccination. *J Immunol* **191**, 2486–2494 (2013).

52. Turner, S. J., Doherty, P. C. & Kelso, A. Cell-mediated immunity. in *Textbook of Influenza* (eds. Webster, R. G., Monto, A. S., Braciale, T. J. & Lamb, R. A.) 298–310 (John Wiley & Sons, Ltd, 2013). doi:10.1002/9781118636817.ch19.

53. Soresina, A. *et al.* Two X-linked agammaglobulinemia patients develop pneumonia as COVID-19 manifestation but recover. *Pediatr Allergy Immunol* (2020) doi:10.1111/pai.13263.

54. Loyal, L. *et al.* Cross-reactive CD4+ T cells enhance SARS-CoV-2 immune responses upon infection and vaccination. *Science* (2021).

55. Brauer, R. & Chen, P. Influenza Virus Propagation in Embryonated Chicken Eggs. *J Vis Exp* 52421 (2015) doi:10.3791/52421.

56. Sridhar, S., Brokstad, K. A. & Cox, R. J. Influenza Vaccination Strategies: Comparing Inactivated and Live Attenuated Influenza Vaccines. *Vaccines (Basel)* **3**, 373–389 (2015).

57. Harding, A. T. & Heaton, N. S. Efforts to Improve the Seasonal Influenza Vaccine. *Vaccines (Basel)* **6**, E19 (2018).

58. Toback, S. L. *et al.* Quadrivalent Ann Arbor strain live-attenuated influenza vaccine. *Expert Rev Vaccines* **11**, 1293–1303 (2012).

59. Block, S. L., Yi, T., Sheldon, E., Dubovsky, F. & Falloon, J. A randomized, double-blind noninferiority study of quadrivalent live attenuated influenza vaccine in adults. *Vaccine* **29**, 9391–9397 (2011).

60. Live Attenuated Influenza Vaccine [LAIV] (The Nasal Spray Flu Vaccine) | CDC. https://www.cdc.gov/flu/prevent/nasalspray.htm (2021).

61. Kreijtz, J. H. C. M. *et al.* Safety and immunogenicity of a modified-vaccinia-virus-Ankara-based influenza A H5N1 vaccine: a randomised, double-blind phase 1/2a clinical trial. *Lancet Infect Dis* **14**, 1196–1207 (2014).

62. Gurwith, M. *et al.* Safety and immunogenicity of an oral, replicating adenovirus serotype 4 vector vaccine for H5N1 influenza: a randomised, double-blind, placebo-controlled, phase 1 study. *Lancet Infect Dis* **13**, 238–250 (2013).

63. Cox, M. M. J., Patriarca, P. A. & Treanor, J. FluBlok, a recombinant hemagglutinin influenza vaccine. *Influenza Other Respir Viruses* **2**, 211–219 (2008).

64. Cox, M. M. J., Izikson, R., Post, P. & Dunkle, L. Safety, efficacy, and immunogenicity of Flublok in the prevention of seasonal influenza in adults. *Ther Adv Vaccines* **3**, 97–108 (2015).

65. Shinde, V. *et al.* Comparison of the safety and immunogenicity of a novel Matrix-M-adjuvanted nanoparticle influenza vaccine with a quadrivalent seasonal influenza vaccine in older adults: a phase 3 randomised controlled trial. *The Lancet Infectious Diseases* **22**, 73–84 (2022).

66. BiondVax Pharmaceuticals ltd. *A Pivotal Multi-center, Randomized, Modified Double-blind, Placebo-controlled Phase 3 Trial to Assess the Safety and Clinical Efficacy of M-001 Influenza Vaccine Administered Intra-muscularly Twice in Older Adults and Elderly (≥50 Years).* https://clinicaltrials.gov/ct2/show/NCT03450915 (2021).

67. COVID-19 vaccine tracker and landscape. https://www.who.int/publications/m/item/draft-landscape-of-covid-19-candidate-vaccines.

68. Trimpert, J. *et al.* Live attenuated virus vaccine protects against SARS-CoV-2 variants of concern B.1.1.7 (Alpha) and B.1.351 (Beta). *Science Advances* **7**, eabk0172 (2021).

69. Wang, Y. *et al.* Scalable live-attenuated SARS-CoV-2 vaccine candidate demonstrates preclinical safety and efficacy. *Proceedings of the National Academy of Sciences* **118**, e2102775118 (2021).

70. Wang, H. *et al.* Development of an Inactivated Vaccine Candidate, BBIBP-CorV, with Potent Protection against SARS-CoV-2. *Cell* **182**, 713-721.e9 (2020).

71. Mallapaty, S. WHO approval of Chinese CoronaVac COVID vaccine will be crucial to curbing pandemic. *Nature* **594**, 161–162 (2021).

72. Greinacher, A. *et al.* Thrombotic Thrombocytopenia after ChAdOx1 nCov-19 Vaccination. *New England Journal of Medicine* **0**, null (2021).

73. Sadoff, J. *et al.* Safety and Efficacy of Single-Dose Ad26.COV2.S Vaccine against Covid-19. *New England Journal of Medicine* **384**, 2187–2201 (2021).

74. Jones, I. & Roy, P. Sputnik V COVID-19 vaccine candidate appears safe and effective. *The Lancet* **397**, 642–643 (2021).

75. Cines, D. B. & Bussel, J. B. SARS-CoV-2 Vaccine–Induced Immune Thrombotic Thrombocytopenia. *New England Journal of Medicine* **384**, 2254–2256 (2021).

76. COVID-19 Provisional Counts - Weekly Updates by Select Demographic and Geographic Characteristics. https://www.cdc.gov/nchs/nvss/vsrr/covid_weekly/index.htm (2022).

77. Tai, W. *et al.* A novel receptor-binding domain (RBD)-based mRNA vaccine against SARS-CoV-2. *Cell Res* **30**, 932–935 (2020).

78. Yang, J. *et al.* A vaccine targeting the RBD of the S protein of SARS-CoV-2 induces protective immunity. *Nature* **586**, 572–577 (2020).

79. He, Y. *et al.* Purification and characterization of the receptor-binding domain of SARS-CoV-2 spike protein from Escherichia coli. *Engineering in Life Sciences* **21**, 453–460 (2021).

80. Chen, W.-H. *et al.* Yeast-expressed recombinant SARS-CoV-2 receptor binding domain RBD203-N1 as a COVID-19 protein vaccine candidate. *Protein Expression and Purification* **190**, 106003 (2022).

81. Liu, Z. *et al.* RBD-Fc-based COVID-19 vaccine candidate induces highly potent SARS-CoV-2 neutralizing antibody response. *Sig Transduct Target Ther* **5**, 1–10 (2020).

82. Joyce, M. G. *et al.* SARS-CoV-2 ferritin nanoparticle vaccines elicit broad SARS coronavirus immunogenicity. *Cell Reports* **37**, 110143 (2021).

83. Keech, C. *et al.* Phase 1–2 Trial of a SARS-CoV-2 Recombinant Spike Protein Nanoparticle Vaccine. *N Engl J Med* **383**, 2320–2332 (2020).

84. Dai, L. *et al.* Efficacy and Safety of the RBD-Dimer–Based Covid-19 Vaccine ZF2001 in Adults. *New England Journal of Medicine* **0**, null (2022).

85. Hsieh, C.-L. *et al.* Structure-based design of prefusion-stabilized SARS-CoV-2 spikes. *Science* **369**, 1501–1505 (2020).

86. Heath, P. T. *et al.* Safety and Efficacy of NVX-CoV2373 Covid-19 Vaccine. *New England Journal of Medicine* **385**, 1172–1183 (2021).

87. Chung, H. *et al.* Effectiveness of BNT162b2 and mRNA-1273 covid-19 vaccines against symptomatic SARS-CoV-2 infection and severe covid-19 outcomes in Ontario, Canada: test negative design study. *BMJ* **374**, n1943 (2021).

88. Corbett, K. S. *et al.* Evaluation of the mRNA-1273 Vaccine against SARS-CoV-2 in Nonhuman Primates. *New England Journal of Medicine* **383**, 1544–1555 (2020).

89. Barda, N. *et al.* Effectiveness of a third dose of the BNT162b2 mRNA COVID-19 vaccine for preventing severe outcomes in Israel: an observational study. *The Lancet* (2021) doi:10.1016/S0140-6736(21)02249-2.

90. Tang, P. *et al.* BNT162b2 and mRNA-1273 COVID-19 vaccine effectiveness against the SARS-CoV-2 Delta variant in Qatar. *Nat Med* **27**, 2136–2143 (2021).

91. Tian, D., Sun, Y., Xu, H. & Ye, Q. The emergence and epidemic characteristics of the highly mutated SARS-CoV-2 Omicron variant. *Journal of Medical Virology* **94**, 2376–2383 (2022).

92. Yu, J. *et al.* Neutralization of the SARS-CoV-2 Omicron BA.1 and BA.2 Variants. *New England Journal of Medicine* **386**, 1579–1580 (2022).

93. Koff, W. C. & Berkley, S. F. A universal coronavirus vaccine. *Science* **371**, 759–759 (2021).

94. Dai, L. *et al.* A Universal Design of Betacoronavirus Vaccines against COVID-19, MERS, and SARS. *Cell* **182**, 722-733.e11 (2020).

95. Morens, D. M., Taubenberger, J. K. & Fauci, A. S. Universal Coronavirus Vaccines — An Urgent Need. *New England Journal of Medicine* **386**, 297–299 (2022).

96. Abu-Raddad, L. J., Chemaitelly, H. & Bertollini, R. Waning mRNA-1273 Vaccine Effectiveness against SARS-CoV-2 Infection in Qatar. *New England Journal of Medicine* **386**, 1091–1093 (2022).

97. Chemaitelly, H. *et al.* Waning of BNT162b2 Vaccine Protection against SARS-CoV-2 Infection in Qatar. *New England Journal of Medicine* **0**, null (2021).

98. Coronavirus Disease 2019. *Centers for Disease Control and Prevention* https://www.cdc.gov/media/releases/2022/s0328-covid-19-boosters.html (2022).

99. Moderna Files for Authorization of Its COVID-19 Vaccine in Young Children Six Months to Under Six Years of Age. https://www.accesswire.com/699210/Moderna-Files-for-Authorization-of-Its-COVID-19-Vaccine-in-Young-Children-Six-Months-to-Under-Six-Years-of-Age.

Chapter 2:
Investigations of *In Vitro* and *In Vivo* Nitration of Influenza Hemagglutinin Protein

ABSTRACT

Influenza viruses are deadly respiratory pathogens of special importance due to their long history of global pandemics. During influenza virus infections, the host responds by producing interferons, which activate interferon-stimulated genes (ISGs) inside target cells. One of these ISGs is inducible nitric oxide synthase (iNOS). iNOS produces nitric oxide (NO) from arginine and molecular oxygen inside the cell. NO can react with superoxide radicals to form reactive nitrogen species, principally peroxynitrite. While much work has been done studying the many roles of nitric oxide in influenza virus infections, the direct effect of peroxynitrite on influenza virus proteins has not been determined. Manipulations of NO, either by knocking out iNOS or chemically inhibiting NO, produced no change in virus titers in mouse models of influenza infection. However, peroxynitrite has a known antimicrobial effect on various bacteria and parasites, and the reason for its lack of antimicrobial effect on influenza virus titers *in vivo* remains unclear. Therefore, we wished to test the direct effect of nitration of influenza virus proteins. We examined the impact of nitration on virus infectivity, replication, and immunogenicity. We observed that the nitration of influenza A virus proteins decreases virus infectivity and replication *ex vivo*. We also show that the nitration of influenza hemagglutinin protein can reduce antibody responses to native virus protein. However, our study also suggests that nitration of influenza virus proteins in vivo is likely not extensive enough to

inhibit virus functions substantially. These findings will help clarify the role of peroxynitrite during influenza virus infections.

INTRODUCTION

Influenza virus infections remain a global health threat, responsible for seasonal epidemics and four major pandemics since the start of the last century, despite the availability of vaccines and antiviral medications. Influenza viruses are respiratory agents, infecting epithelial cells along the respiratory tract. Damage from virus infection can compromise lung function, which can prove fatal. The damage to the lungs during virus infection is due to a combination of direct cell death from virus infection and immune responses to the virus. One of the innate immune factors activated by virus infection is inducible nitric oxide synthase (iNOS), an interferon-stimulated gene product (ISG). Murine and human macrophages and neutrophils that infiltrate the lung during infection upregulate iNOS in response to interferon signaling[1–3], and iNOS in turn synthesizes nitric oxide (NO) from cellular L-arginine and molecular oxygen[4,5].

The roles of NO in microbial infection are diverse and seemingly paradoxical. NO acts as a signaling molecule through NO-sensitive guanylyl cyclase (NO-GC), which promotes vascular relaxation and pulmonary vasodilation, improving blood flow to the lungs and lung function[6,7]. NO has also been implicated in the modulation of immune responses during infection. iNOS knock-out mice exhibit reduced proinflammatory cytokine profiles in the lung during infection compared to iNOS competent mice[8]. Additionally, NO is required for Th17 cell differentiation[9], and NO has been implicated in B cell activation and plasma cell survival[10,11]. On the other hand, NO can react with

superoxide radials to form highly reactive nitrogen species (RNS), principally peroxynitrite[12,13]. Peroxynitrite and other radical species can react with macromolecules such as proteins, lipids, and nucleic acids. When reacting with proteins, RNS can oxidize serine residues and nitrate tyrosine residues to give nitrotyrosine, aminotyrosine, cysteine-sulfinic acid, cysteine-sulfonic acid, and S-nitrosothiol[14,15]. These modifications can alter protein function, and extensive nitration of cellular macromolecules can produce nitrative stress inside the cell. This damage to the cell has been linked to cellular stress and cell death[16].

Following influenza virus infection, protein nitration in the lungs is observed in both mice and humans by immunohistochemical staining for nitrotyrosine, indicating nitrative stress inside lung cells[17–19]. This nitrative stress has been linked directly to the pathogenesis of influenza disease in mice. iNOS knock-out mice have increased survival following infection with influenza virus compared to iNOS competent mice[17,20]. This has also been observed with other pathogens such as Sendai virus, Dengue virus, and *Cryptococcus gattii*[1,21–24]. The increased survival of iNOS knock-out mice has been attributed to the reduced damage to the lung from reactive nitrogen species, principally peroxynitrite[1,25]. In addition to host macromolecules, peroxynitrite can also react with viral proteins, which can compromise protein function. Nitration of HIV reverse transcriptase *in vitro* and nitration of Coxsackievirus protease 3C inhibits enzyme function through the nitration of amino acids in the enzyme active site[26, 27]. Nitration of the SARS-CoV-1 spike (S) protein reduces the cell-cell fusion activity mediated by S protein, which is associated with decreasing amounts of S protein palmitoylation[28]. We

hypothesized that nitration of influenza virus proteins could similarly alter protein function and, in turn, virus replication dynamics. However, more information is needed on the interaction between reactive nitrogen species and influenza virus proteins. The multiple roles of NO *in vivo* can possibly affect viruses in ways beyond direct nitration of virus proteins by peroxynitrite. We therefore wished to test if direct nitration of influenza virus proteins was sufficient to cripple virus infectivity and replication by *in vitro* nitration of influenza virions.

Additionally, post-translational modifications to influenza proteins such as glycosylation of hemagglutinin (HA) can affect antibody responses to HA[29, 30]. Modification of B-cell epitopes can inhibit the recognition of virus antigen and reduce antibody responses to unmodified antigen. We hypothesized nitration of HA could result in similar alterations in antibody responses. We therefore set out to examine the effects of nitration of influenza HA on antibody responses to HA protein. Finally, we sought to look for the *in vivo* nitration of influenza HA protein during infection. There are many reports showing the presence of nitrotyrosine, a marker for nitration, in the lung following influenza virus infection[17–19]. However, these reports rely on immunohistochemical staining of the tissue for nitrotyrosine. Since peroxynitrite is a highly reactive nitrogen species that can react with either host or virus macromolecules, immunohistochemical staining of the lung tissue does not demonstrate direct nitration of virus macromolecules. To the best of our knowledge, this is the first report of experiments to detect the direct nitration of influenza virus proteins in infected lungs. We immunoprecipitated HA protein from mouse lung followed by mass spectrometry (mass

spec) analysis to check for nitration of HA *in vivo.* In summary, we found that direct nitration of influenza virus *in vitro* has a deleterious effect on virus infectivity and replication dynamics. We also found that vaccination with nitrated HA protein reduces antibody responses to wild-type HA. However, although we detected immunoprecipitated HA protein from mouse lung, our mass spec analysis did not detect nitration of HA. We conclude with a discussion of the interplay between peroxynitrite, host macromolecules, and virus proteins.

RESULTS

In vitro nitration of Hemagglutinin protein and influenza virion

To understand the direct effects of nitration of influenza A virus proteins, we needed to separate the roles of NO as an innate immune response factor and signaling molecule from its role as a contributor to the formation of RNS. We therefore took an *in vitro* approach to directly nitrate influenza virus proteins. We used SIN-1 (3-morpholino-sydnonimine), which produces peroxynitrite under physiological conditions, to nitrate influenza virus proteins *in vitro*[31]. We confirmed the presence of nitrotyrosine modification of HA by western blot (Figure 2A, 1B) and mass spec analysis (Figure 2C-F). The treated virions and proteins were used to study the effects of nitration on virus infectivity and the antibody response to virus proteins.

SIN-1 treatment of influenza virus reduces virus infectivity and replication

Mass spec analysis of the SIN-1 treated influenza virus revealed nitration of tyrosine residues at positions Y214 and Y222, which are in the receptor-binding domain of HA[32] (Figure 2C). We hypothesized that nitration of the receptor-binding domain

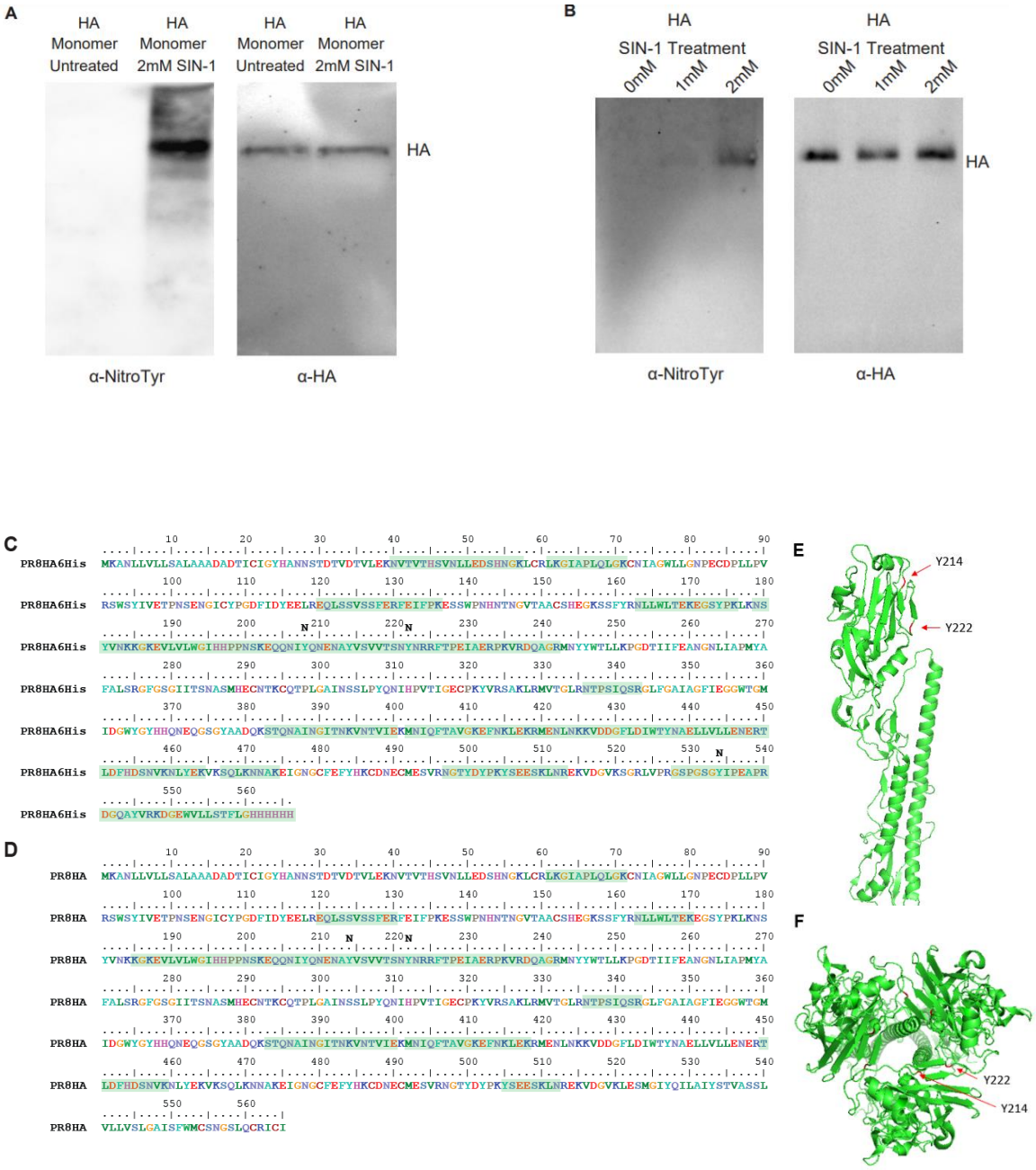

Figure 2. In vitro nitration of influenza HA protein and influenza virion with SIN-1. (A) Western Blot confirming the nitrotyrosine modification of HA monomer. (B) Western blot confirming the nitrotyrosine modification of influenza virion HA. (C) Mass spectrometry coverage and confirmation of nitrotyrosine modification of HA trimer (48.9% coverage) (D) Mass spectrometry coverage and confirmation of nitrotyrosine modification of influenza virion HA (26.6% coverage). (E and F) Structural representation of the HA monomer (E) and trimer (F) showing the Nitrotyrosine sites modified in (D).

might reduce influenza virus infectivity and hinder virus replication. To determine the effect of SIN-1 treatment on the ability of influenza viruses to infect cells, PR8, NL09, and X31 strains of purified influenza virus were treated overnight with either 0mM, 1mM, or 2mM SIN-1 in PBS. Infectious virus concentrations were determined by a standard plaque assay analysis. SIN-1 treatment in PBS resulted in significantly fewer plaques compared to untreated virus (Figure 3A). To further study the effect of SIN-1 treatment on virus infectivity and replication, we performed influenza virus growth curves in the presence of SIN-1. SIN-1 significantly reduced the replication of influenza virus in MDCK cells (Figure 3B, $p<0.05$). Furthermore, we performed a growth curve with influenza viruses pre-treated with SIN-1. PR8, NL09, and X31 were treated overnight with 2mM or 1mM SIN-1, and then allowed to infect MDCK cells for the virus growth curve. The pre-infection SIN-1 treatment gave significantly reduced virus titers (Figure 3C, $p<0.05$). To better mimic *in vivo* nitration conditions, which contain macromolecules other than virus proteins, we treated PR8 virus with SIN-1 in the presence of increasing amounts of BSA, which acted as a non-viral target for nitration. SIN-1 treatment in the presence of 1.25% or 2.5% BSA resulted in no change in plaque titers compared to untreated virus (Figure 4). This supports the notion that nitration of influenza viruses reduces virus infectivity and replication, but this effect may be mitigated by the presence of other host macromolecules.

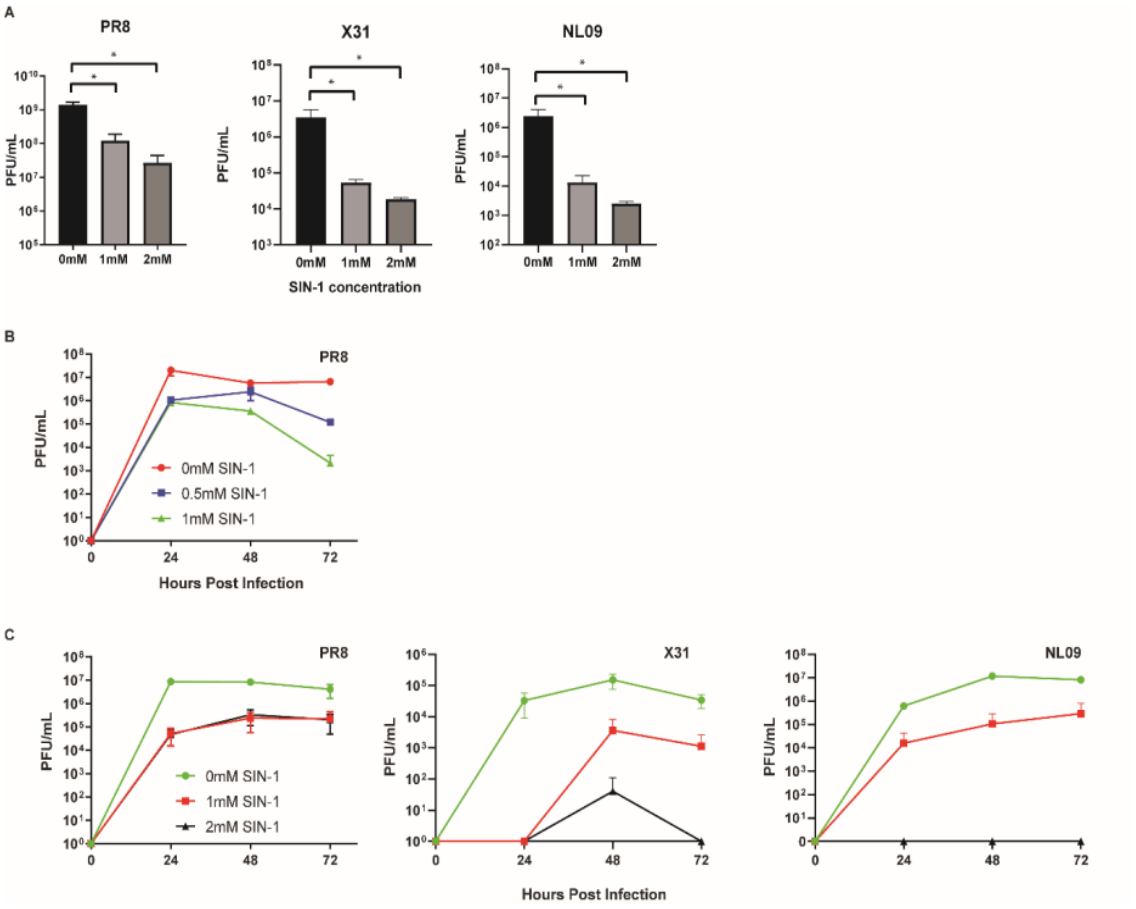

Figure 3. **SIN-1 treatment of influenza virions.** (A) Plaque assay titers of infectious virus following overnight SIN-1 treatment. Statistical significance was determined by two-tailed unpaired t-test: (* $p<0.05$). (B) Growth curve of PR8 virus with SIN-1 included in growth media. (C) Growth curves of influenza viruses pre-treated with SIN-1.

SIN-1 treatment of HA protein lowers virus-specific antibody responses

The head domain of the PR8 influenza HA protein contains 5 immunodominant antigenic regions: Sa, Sb, Ca_1, Ca_2, and Cb[33]. Our mass spec analysis of the SIN-1 treated purified HA protein showed nitration of tyrosine residue Y208, which is within the Sb antigenic region (Figure 2C). We therefore hypothesized that nitration of influenza virus proteins could alter antibody epitopes and reduce antibody responses to native virus

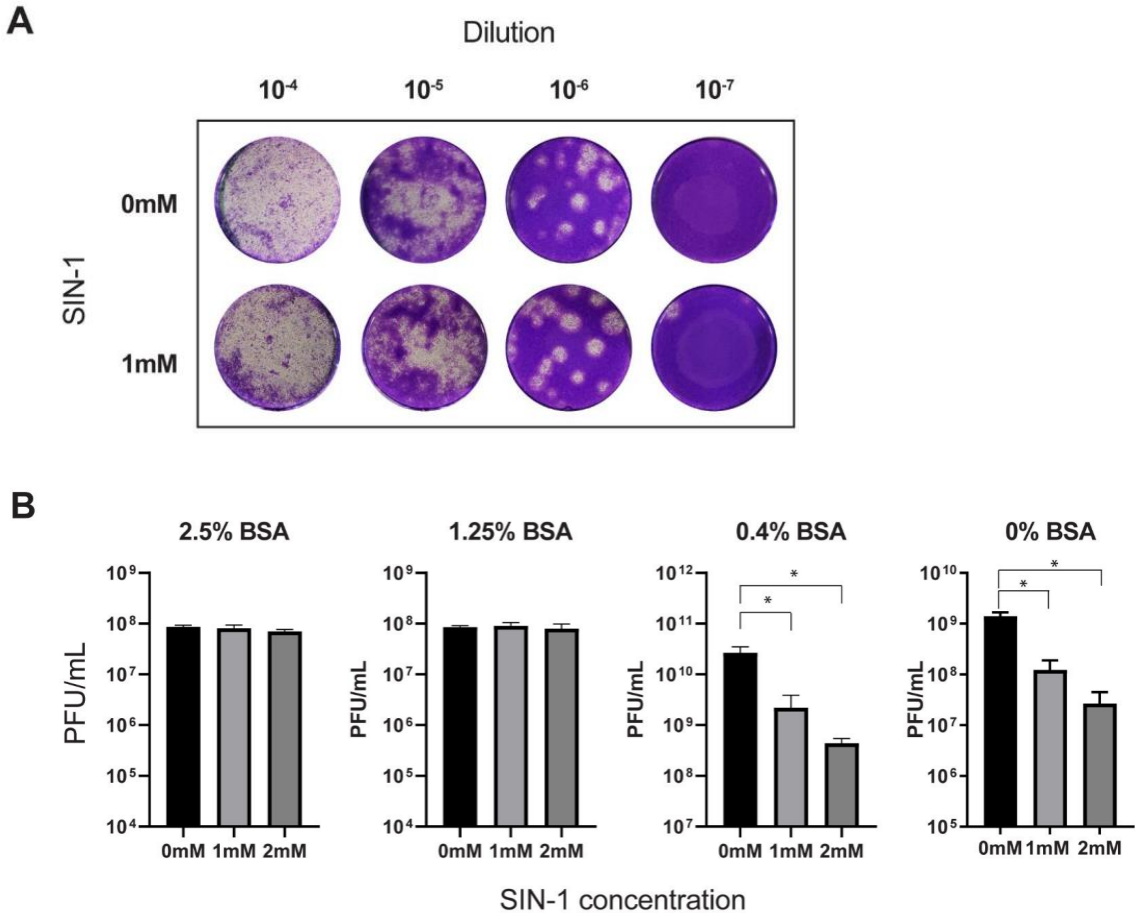

Figure 4. SIN-1 treatment of PR8 influenza virus in the presence of BSA. (A) Representative plaques of PR8 Influenza virus following SIN-1 treatment in the presence of 2.5% BSA. **(B)** Infectivity of SIN-1 treatment of PR8 virus in presence of different concentrations of BSA. Statistical significance was determined by two-tailed unpaired t-test: (* $p<0.05$). Each graph in **B** was performed as a separate experiment.

proteins. To test this hypothesis, C57BL6 mice were vaccinated with 2µg of purified trimeric HA protein treated with 0.2mM SIN-1 for different lengths of time. Mice were boosted with an additional 2µg of protein at 2 weeks post-vaccination (Figure 5A). Sera were collected on day 0, day 14, and day 28 after the first vaccination. An Enzyme-Linked Immunosorbant Assay (ELISA) was performed with plated influenza virion to determine antibody responses following vaccination with HA protein. We observed

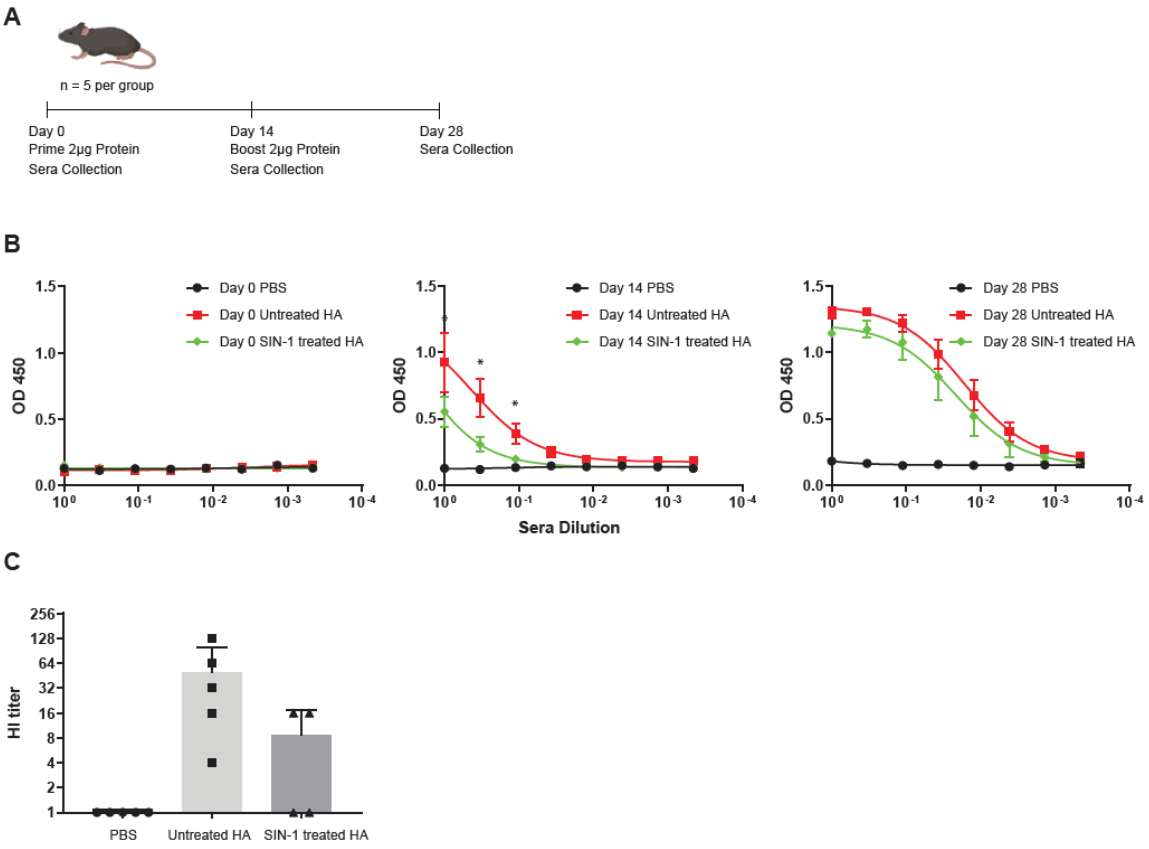

Figure 5. Reduced antibody responses to SIN-1-treated HA protein. (A) Schedule of mouse vaccinations with SIN1-treated or untreated HA protein, and sera collection (n=5 per group). **(B)** ELISA from mouse sera following vaccination with SIN1-treated HA protein. Unpaired t-test of significance for untreated vs 20-hour SIN-1 for all dilutions on Day 14: (*p<0.05). **(C)** Hemagglutination Inhibition assay results with sera from day 28 post-vaccination.

decreased antibody responses with increased SIN-1 treatment (Supplemental Figure 1) with a significant decrease in antibody responses observed after 20 hours of treatment with SIN-1 (Figure 5B). The decrease was most pronounced following the first vaccination. After boosting, antibody titers remained lower in the mice given SIN-1 treated HA, but only slightly. Additionally, significantly reduced antibody responses to HA were observed when purified HA protein was treated with different concentrations of

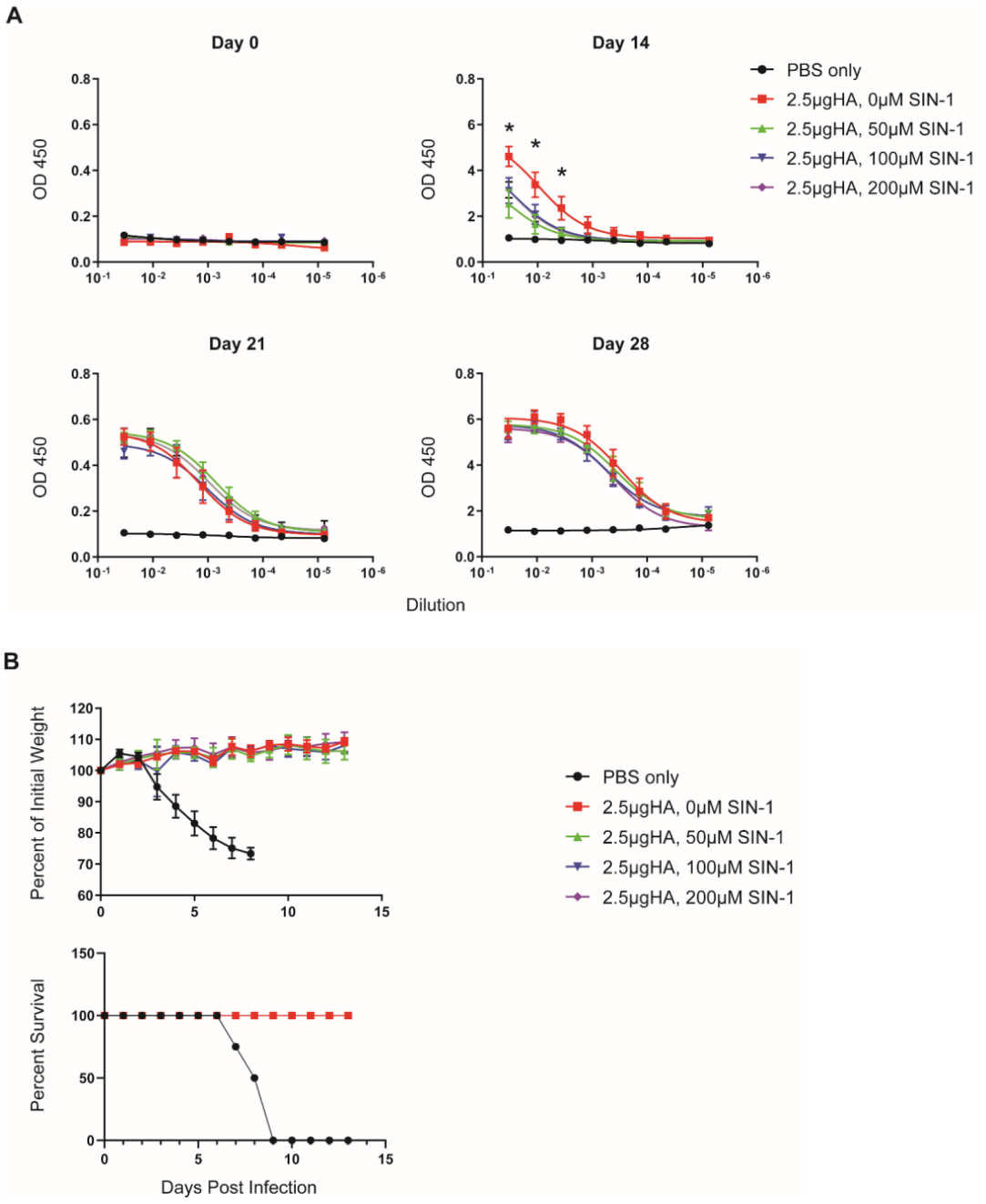

Figure 6. Responses to vaccination with SIN-1-treated HA in mice. **(A)** Mice (n=5 per group) were vaccinated with 2.5μg of SIN-1 treated HA and boosted on days 14 and 21 post-vaccination. Sera were collected on days 0, 14, 21, and 28 post-vaccination. Antibody responses to influenza virion were determined by ELISA. **(B)** Weight loss and percent survival of the mice from the groups in **A** following challenge with a lethal dose of PR8.

SIN-1 for 1 hour at room temperature (Figure 6A, $p<0.05$). After boosting, the differences in antibody titers between the groups were not significant, and all the mice survived challenge with a lethal dose of parental PR8 virus (Figure 6B). Because our mass spec data identified nitration of tyrosine residues in the receptor-binding domain of HA (Figure 2), we further hypothesized that SIN-1 treatment of HA would result in decreased virus-neutralizing antibodies. We used sera from day 28 post-vaccination to determine hemagglutination inhibition antibody titers from mice vaccinated with SIN-1 treated or untreated HA protein. While the sera from mice vaccinated with the SIN-1 treated HA protein had reduced hemagglutination inhibition titers compared to mice vaccinated with untreated HA protein, the difference was not statistically significant (Figure 5C, $p=0.14$). In summary, *in vitro* nitration of influenza HA protein is associated with decreased antibody responses to HA.

In vivo nitration of HA

To determine if influenza hemagglutinin protein is nitrated during influenza virus infection, we immunoprecipitated HA protein from the lungs of mice infected with 10,000 PFU of influenza A PR8 virus at day 5 post infection. The immunoprecipitated protein was detected by Western blot (Figure 7A). The band corresponding to the HA protein was excised from the gel and used for mass spec analysis for the detection of the following RNS-induced modifications: nitrotyrosine, aminotyrosine, cysteine-sulfinic acid, cysteine-sulfonic acid, and S-nitrosothiol. Detected peptides were checked against a mouse peptide library as a negative control. While we were able to detect the presence of the HA protein, nitrotyrosine modification of HA was not detected, and neither were

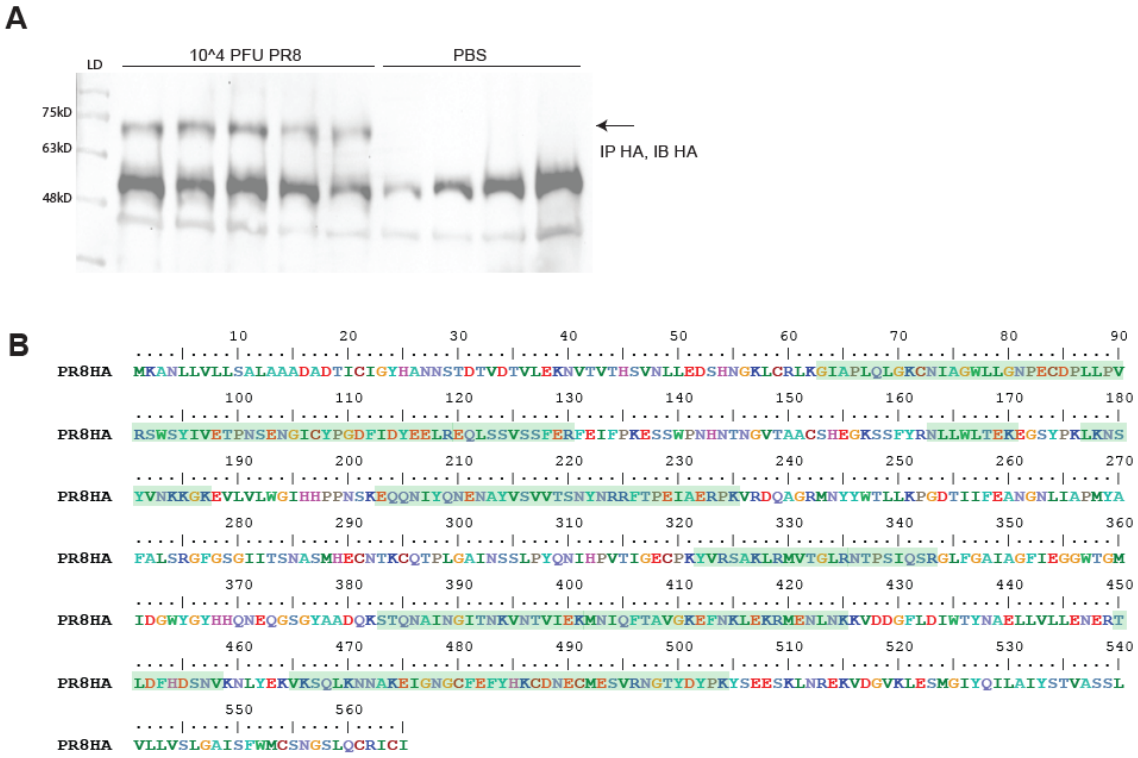

Figure 7. Immunoprecipitation and Mass spectrometry analysis of HA protein from mouse lung. (A) Western Blot for the detection of HA protein from mouse immunoprecipitations. Protein was immunoprecipitated with human α-HA antibody and blotted with mouse α-HA. Wells from left to right: Ladder, samples from 5 mice infected with 104 PFU of PR8 virus, samples from 4 uninfected mouse controls. (B) Coverage of HA protein mass spec analysis. Regions from detected peptides are shown in blue. (Protein accession number A0A6H1QXP1, 41.6% coverage, 24 unique peptides).

additional RNS modifications (Figure 7B). To check if host proteins were modified to nitrotyrosine following infection, the immunoprecipitated samples from Figure 6A were analyzed by mass spec against a mouse database. We were able to detect nitration of several different proteins, including Actin protein (Supplemental Figure 3).

DISCUSSION

We observed that influenza virus proteins are susceptible to nitration by peroxynitrite *in vitro*. Nitration modifications to the HA protein can occur in important

immunological domains and in the receptor binding domain. Nitration of influenza viruses reduces virus infectivity, resulting in lower virus titers *ex vivo*. Nitration of HA can also reduce titers of HA specific antibodies. While influenza virus is susceptible to nitration, nitration may not occur extensively enough to significantly impact virus titers or virus immunogenicity *in vivo*.

The decreased ability of influenza viruses to infect cells following SIN-1 treatment shows that, in principle, RNS modifications to influenza virus proteins can have a negative impact on virus infectivity and replication. However, the question remains as to whether these modifications happen extensively during *in vivo* infection. Blocking NO in a mouse model of influenza virus infection had no effect on virus titers in the mouse lungs[17,34]. Similarly, inhaled NO did not affect virus titers in mouse lungs[35]. This suggests that the effects of NO during infection are not a result of direct interaction with virus proteins. Our mass spec analysis of immunoprecipitated HA protein found no evidence of ROS and RNS-induced modifications to the HA protein. This does not rule out the possibility that influenza virus proteins may be modified *in vivo*. Nitrotyrosine can be detected in mouse lungs as early as day 3 post infection with influenza virus[18,36]. However, Akaike et al. have reported peak NO production in mouse lungs on day 7 post infection[17,37], and peak nitrotyrosine levels are typically seen around days 7 and 8 post infection[18,38]. We collected the lungs on day 5 post-infection. This earlier time point was chosen to maximize the amount of HA recovered from immunoprecipitation. A later timepoint may show nitration of the HA protein, but it is more challenging to perform this experiment as the virus starts to be cleared from the lungs and the mice may succumb

to the virus before reaching the desired day post-infection. Our immunoprecipitations of HA with lungs from Day 7 post-infection did not detect HA protein by western blot (data not shown). It may also be that the HA protein is modified below the limit of detection of our mass spec analysis. Additionally, we only checked the HA protein for modification, but other virus proteins may be more susceptible to nitration. However, the lack of RNS modifications to HA from our immunoprecipitation of HA from mouse lungs suggests that RNS modifications to influenza virus proteins may not occur to a significant extent *in vivo*.

One explanation for why influenza virus proteins may not be modified *in vivo* is that *in vivo* concentrations of peroxynitrite may be lower than the concentrations we used *in vitro*. While the transient and highly reactive nature of peroxynitrite makes determining its concentration *in vivo* challenging, estimates have suggested *in vivo* rates of peroxynitrite production around $5\mu Ms^{-1}$, which is difficult to convert to the actual concentrations of peroxynitrite used in our *in vitro* experiments[16,23,39,40]. Another explanation is that peroxynitrite is far more likely to contact and react with host molecules than viral molecules. During influenza virus infection, virion mass makes up only about 1% of the total dry mass of the cell[41,42]. Stoichiometrically, if there are more host proteins for the peroxynitrite to react with than viral proteins, modifications to viral proteins will be reduced and differences in virus titers will not be significant. This possibility is supported by our measurement of virus infectivity following SIN-1 treatment in the presence or absence of BSA. BSA is known to undergo nitration to nitrotyrosine following SIN-1 treatment, and SIN-1 treatment of influenza virus in the

presence of excess BSA did not affect virus infectivity (Figure 4). This suggests that when other macromolecules are present to act as targets for RNS modification, modifications of virus molecules are reduced, and virus infectivity and replication are unimpeded. This suggestion is somewhat at odds with the growth curve results we obtained with infected cells in the presence of SIN-1 (Figure 3B). We observed a decrease in virus titers in the presence of SIN-1 in virus-infected cells when an abundance of host proteins was also present. While this might suggest a direct role for peroxynitrite in inhibiting influenza replication, results could also be the result of SIN-1-induced pH changes in the culture media or direct damage to the cells from the peroxynitrite. While influenza virus growth curves are typically done in our lab with media containing buffers such as HEPES[43], HEPES can interfere with peroxynitrite production from SIN-1[44], so it was not included in our growth curve media. This resulted in lower pH in SIN-1-treated wells compared to untreated wells at 72 hours post-infection, and this lower pH could account for the lower viral titers in the growth curves.

The decreased antibody responses we observed to SIN-1-treated HA protein shows that, in principle, RNS-induced modifications to virus proteins can reduce antibody responses to native virus. However, the reduced antibody responses were seen principally following the first vaccination. Boosting the mice resulted in no differences in antibody responses between mice vaccinated with SIN-1 treated HA and mice vaccinated with untreated HA. One possible explanation for this is that the nitration of the HA protein is occurring randomly at different amino acid side changes. In this case, the vaccinations include a mixture of HA proteins modified at different positions. While the

initial vaccination may include enough modifications to reduce antibody responses to native virus, because the modifications occur randomly, there is no guarantee that boosting would contain the same mixture of modified epitopes as the original vaccination. There is also no guarantee that each mouse is getting the same mixture of modified epitopes. Boosting would then preferentially increase antibody responses to unmodified epitopes. This could explain why antibody responses in the mice vaccinated with SIN-1 treated HA were more similar to wild-type after the boost. This also raises the question whether RNS-induced modifications to virus proteins *in vivo* are extensive enough to significantly alter antibody responses. The conclusions reached in the previous paragraph also apply to our results obtained from vaccinating with the SIN-1-treated HA protein. While in principle RNS modifications may reduce antibody responses to HA proteins, modifications likely do not occur extensively enough to make a significant difference to antibody responses *in vivo*. Peak nitrotyrosine production may occur at a point when virus protein levels are already in decline, which would suggest that most virus protein produced is not modified extensively *in vivo.* However, as iNOS has roles in immune signaling, the NO and peroxynitrite may still impact antiviral antibody levels indirectly. Jayasekera et al. reported increased IgG2a antibody responses in mice lacking iNOS, but attributed this to altered interferon levels and T-cell profiles in the iNOS knock-out mice, rather than to a loss of nitration of influenza virus proteins[8]. These indirect effects may have a more significant role in determining antibody titers than direct nitration of virus proteins.

While levels of peroxynitrite in healthy animals are low, preexisting inflammatory conditions may elevate levels of peroxynitrite. Circulating levels of peroxynitrite in sera are increased in animal models of hypertension, and iNOS expression is increased in the lungs of mice acutely exposed to cigarette smoke[14,45,46]. It is possible that exposure to influenza virus proteins from either infection or vaccination under conditions with high preexisting levels of peroxynitrite may increase the likelihood of nitration of influenza virus proteins, which may lead to some of the effects of nitration observed in this study, such as lower antibody responses.

In summary, influenza viruses are susceptible to protein nitration, and *in vitro* nitration of influenza virus proteins reduces virus infectivity and immunogenicity. However, nitration of virus proteins may not occur extensively *in vivo*. The impact of direct protein nitration in other pathogenic virus infections remains an area of ongoing research.

MATERIALS AND METHODS

Influenza Virus Strains and Purification of Influenza Virions

Growth curves following SIN-1 (3-morpholino-sydnonimine, Cayman Chemicals) treatment were performed with PR8 A/Puerto Rico/8/34(H1N1) virus, X31 mouse adapted H3N2 reassortant virus carrying the HA and NA genes of A/Hong Kong/1/1968 (H3N2) in the background of PR8, and NL09 A/Netherlands/602/2009 (H1N1) virus. All other experiments were performed with PR8 virus. 10 day old embryonated chicken eggs were infected with 50PFU of virus per egg in 100µL of PBS/BSA/Pen-Strep as previously described[45,46] and incubated at 37°C for 48 hours. Eggs were then kept at 4°C

overnight, and the allantoic fluid was collected. The allantoic fluid was spun down at 3000rpm for 30 min at 4°C and the supernatant was collected. Virion was purified from allantoic supernatant by 20% sucrose/NTE Buffer ultracentrifugation at 25,000rpm for 2 hours at 4°C. The resulting pellets were resuspended in 1mL PBS and virion concentration was determined by Bradford Assay.

Purification of HA protein

10 T175 flasks (Genesee Scientific) of 293T cells were polyethylenimine (PEI) transfected with 20µg of pCAGGS expression plasmid containing C-terminal trimerization domain and C-terminal 6xHis tagged PR8 HA lacking the intracellular and transmembrane domains. Cells were transfected in 10mL Opti/MEM media. 12 hours after transfection, the media was changed to 20mL DMEM media containing 10% FBS and cells were left at 37°C for 48 hours. After 48 hours, the supernatant was collected, and protein was purified with a 5mL HisTrap column (Cytiva). Eluted protein was diafiltrated with a 10kD cut-off column (Amicon Ultracel 10K centrifugal filters) and washed twice with PBS. Protein concentration was determined by Bradford Assay, and trimeric HA was separated from monomeric HA by size-exclusion chromatography.

In vitro nitration of influenza proteins with SIN-1 chloride

For the SIN-1 treatment of HA monomer, 9µg of purified HA monomer was added to PBS containing 200µM SIN-1 in 125µL total volume and left shaking overnight at 4°C. For the SIN-1 treatment of HA trimeric protein for mouse vaccinations, 100µL of HA trimer (93ug) was added to PBS containing SIN-1 in a final volume of 500µL. Samples were left overnight at 4°C and then diafiltrated with a 10kD cut-off column (Amicon

Ultracel 10K centrifugal filters) and washed twice with 5mL PBS to remove residual SIN-1 in solution. The protein concentration was then determined by Bradford Assay.

Coomassie Staining and Western Blots

Western Blots for HA protein were blocked with 5% milk in PBS containing 0.1% Tween 20, then blotted with PY102 HA mouse monoclonal antibody diluted 1:500 in blocking buffer. The antibody was a kind gift from Dr. Peter Palese at the Icahn School of Medicine at Mount Sinai. When performing western blots to detect nitrotyrosine, samples were added to 2x SDS-PAGE Loading Dye lacking beta-mercaptoethanol or other reducing agents to avoid reducing nitrotyrosine to aminotyrosine. Western Blots were blocked with 2% BSA in PBS containing 0.1% Tween 20, and then incubated with nitrotyrosine mouse monoclonal antibody (Cayman Chemicals) diluted 1:500 in blocking buffer. Blots were incubated with goat α-mouse IgG-HRP secondary antibody (Prometheus) diluted 1:10,000 in blocking buffer. Blots were visualized with BioRad ChemiDoc Touch Imaging system. Coomassie Gels were stained as previously described[47].

Mass Spectrometry Sample Preparation

For SIN-1 treated virus and protein samples, Vacuum-dried samples were resuspended in 50µL 100 mM Triethylammonium bicarbonate (TEAB, Sigma Aldrich, St. Louis, MO). Samples were reduced with the addition of 2.5µL of 500 mM tris(2-carboxyethyl)phosphine (Thermo Scientific, Rockford, IL) and incubated at 37°C for 1 hour, after which 3µL of 500 mM Iodoacetamide (Sigma Aldrich) was added. Samples were incubated in the dark at room temperature for 1 hour. Samples were diluted with the

addition of 250µL of water and 250µL of 100 mM TEAB. 1µL (200ng) of trypsin/lysC mix (Promega, Madison, WI) was added to the samples and the samples were digested at 37°C for 16 hours. 10µL of the digest was injected for LC-MS analysis.

For immunoprecipitation samples, bands corresponding to the size of full-length HA protein were cut out from the gel and in-gel digestion was performed by adding 500µL of 25% acetonitrile/50mM ammonium bicarbonate (ABC) for 10 minutes. Samples were sonicated for 15 minutes, then the solution was discarded and replaced with 500µL of 50% acetonitrile/50mM ABC. Samples were sonicated again for 15 minutes, then solution was discarded replaced with 500µL of 25% acetonitrile/50mM ABC. Samples were sonicated again for 15 minutes, then the solution was discarded and replaced with 500µL of 50% acetonitrile/50mM ABC. Samples were sonicated again for 15 minutes, then the solution was discarded and replaced with 500µL of 100% acetonitrile. Samples were sonicated for 10 minutes, then the solution was dried using a speed-vac. Samples were reduced with the addition of 400µL of 10mM Dithiothreitol (DTT)/ 50mM ABC, incubated at 37ºC for 1 hour, after which 49µL of 500mM Iodoacetamide was added. Samples were incubated in the dark at room temperature for 25 minutes. Samples were washed twice with 500µL of 100% acetonitrile with 5 minutes sonication, then dried using a speed-vac. Samples were then suspended in 100µL of trypsin solution and incubated at 37ºC overnight. 500µL of 25% acetonitrile/5% Hydrogen acetate (HAc) were then added to the trypsin digested samples and samples were sonicated for 20 minutes. An additional 300µL of 50% acetonitrile/5% HAc was added to the samples and samples were sonicated for 20 minutes. The solution was then dried using a speed-vac

and desalted using a C18 zip-tip (Waters). The peptide solution was then dried by speed-vac and stored at -80°C until LC-MS/MS analysis.

Mass Spectrometry Sample and Data Analysis

For SIN-1 treated virus and protein samples, Liquid chromatography was performed on a Waters nanoAcquity UPLC in single-pump trapping mode with a Thermo PepMap RSLC C18 EASY-spray column (2µm, 100 Å, 75µm x 25cm) and a Waters Symmetry C18 trap column (5µm, 100 Å, 180µm x 20 mm). Solvents used were A: water with 0.1% formic acid and B: acetonitrile with 0.1% formic acid. Samples were separated at 300nL/min with a 260-minute gradient starting at 3% B increasing to 30% B from 1 to 230 minutes, then to 85% B at 240 minutes hold for 10 minutes then back to 3% B in 10 minutes. Mass spectrometry data was acquired on a Thermo Orbitrap Fusion in data-dependent mode. A full scan was conducted using 60k resolution in the Orbitrap in positive mode. Precursors for MS2 were filtered by monoisotopic peak determination for peptides (this was set to small molecule for the analysis), intensity threshold 5.0e3, charge state 2-7, and 60 second dynamic exclusion after 1 analysis with a mass tolerance of 10 ppm. Collisionally induced dissociation spectra were collected in MS2 at 35% energy and isolation window 1.6 m/z. Results were searched individually in Proteome Discoverer 2.2 (Thermo Scientific) against a custom FASTA database with the his-tagged hemagglutinin sequence for purified protein samples. The precursor mass tolerance was set to 10ppm and fragment mass tolerance to 0.6 Da. Fixed modifications were carbamidomethyl (Cys +57.021 Da), and dynamic modifications included methionine oxidation (+15.995 Da) N-

terminal acetylation (+42.011 Da), and tyrosine nitration. Results were filtered to a strict 1% false discovery rate.

For HA immunoprecipitation samples, Liquid chromatography was performed on a Dionex Ultimate 3000 UPLC system. First, the peptide samples were loaded onto a pre-column (75μm in internal diameter and 4 cm in length) packed in-house with reversed-phase C18 material (ODS-AQ C18, 5μm in particle size, Dr. Maisch GmbH HPLC). The analytes were subsequently resolved on an analytical column (75μm I.D., 25 cm in length) packed with reversed-phase C18 material (ReproSil-Pur 120 C18-AQ, 3-μm in particle size, Dr. Maisch GmbH HPLC). Solvents used were A: water with 0.1% formic acid and B: acetonitrile with 0.1% formic acid. Samples were separated at 300nL/min with a gradient included 0-15 min, 95% A; 15-150 min, 95-63% A; 150-152 min, 63%-1% A; 152-179 min, 1% A; 179-179.01 min, 1%- 95% A; 179.01-200 min, 95% A. Mass spectrometry data was acquired on a Q Exactive Plus quadrupole-Orbitrap mass spectrometer (Thermo Fisher Scientific) in data-dependent mode, where one full-scan MS (m/z 300–2000) was followed by MS/MS scans on the 20 most abundant ions found in full-scan MS. Precursor ions were isolated at a width of 1.0 m/z unit, and dynamic exclusion was enabled with an exclusion time window of 60 s after a precursor ion was first selected for MS/MS acquisition. Intensity threshold 5.0e3, charge state 2-7, and 60 second dynamic exclusion after 1 analysis with a mass tolerance of 10 ppm. Collisionally induced dissociation spectra were collected in MS2 at 35% energy and isolation window 1.6 m/z. The raw data were processed and analyzed using MaxQuant (version 2.0.3.1) against a custom FASTA database with the hemagglutinin sequence for the PR8 HA

sequence. The precursor mass tolerance was set to 10 ppm and fragment mass tolerance to 0.6 Da. Fixed modifications were carbamidomethyl (Cys +57.021 Da), and dynamic modifications included methionine oxidation (+15.995 Da) N-terminal acetylation (+42.011 Da), and tyrosine nitration. Results were filtered to a strict 1% false discovery rate.

Virus Plaque Assays

Influenza virus plaque assays were performed as previously described[48]. Influenza viruses were serially diluted 10-fold in PBS/BSA containing 1% Pen/Strep. 250µL of virus dilution was added to a confluent monolayer of MDCK cells in a 12 well plate, and virus was allowed to infect cells for 1 hour at 37°C. Virus dilutions were replaced with Post-Transfection Media containing 3.7% Avicell RC-591 NF (FMC Corporation) and left at 37°C for 48 hours. Cells were fixed with 1mL of 3.7% formaldehyde for 1 hour at room temperature and stained with 1% crystal violet solution.

Virus Infectivity Following SIN-1 treatment

Purified influenza virion was diluted down to 2.75ng/µL in 125µL total volume in PBS with SIN-1. Samples were left shaking at 350rpm overnight at 4°C. After incubation, virus infectivity was determined by plaque assay. For SIN-1 treatment of virus in the presence of BSA, purified influenza virus was diluted down to 2.75ng/µL in 120µL total volume of PBS containing different concentrations of BSA, followed by the addition of 5µL of SIN-1 to final concentrations. Samples were left shaking at 350rpm overnight at 4°C. After incubation, virus infectivity was determined by plaque assay.

Growth Curve of Influenza Virus

For growth curves following SIN-1 treatment, virus stocks were diluted down to $2x10^3$ PFU/mL, 1mL total volume. 200µL of SIN-1 in PBS was added to final concentrations of SIN-1, then incubated overnight at 4°C with shaking. 250µL of each virus sample was used to infect a monolayer of MDCK cells in a 12 well plate. After allowing virus to infect the monolayer for 1 hour, media was changed to 1mL post infection medium (PIM) containing 0.5µg Trypsin TPCK. 100µL of supernatant was collected at 24, 48, and 72 hours post infection and replaced with 100µL fresh PIM. Virus titer at each time point post infection was determined by plaque assay. For growth curves in the presence of SIN-1, MDCK cells were infected with 500PFU of PR8 virus in a 12 well plate. Virus was allowed to infect cells for 1 hour, then media was changed to 1mL of post transfection medium (PTM) containing 0.5µg Trypsin TPCK with SIN-1. 60µL of fresh SIN-1 in PBS was added every 12 hours to restore initial SIN-1 concentrations, and 120µL of media was collected at 24, 48, and 72 hours post infection. Virus titers at each time point post infection was determined by plaque assay.

Mouse Vaccinations and Virus Challenges

Six-week-old female C57BL/6 mice were purchased from Jackson Labs and used for vaccination and challenge studies. SIN-1 treated influenza HA protein vaccine was diluted in PBS and added to equal volume of Addavax adjuvant. Mice were injected intramuscularly with 50µL of vaccine per injection in both back legs. Retro-orbital blood was collected and centrifuged for 10 minutes at 10,000g to separate out sera. Sera was collected and stored at -80°C for use in antibody studies. For the challenge study, mice

were anesthetized with isoflurane and challenged intranasally with a lethal dose of 1000 PFU of PR8 virus in 50µL solution. Mice were monitored for weight loss and mortality each day post infection for 14 days.

Mouse Lung Cell Preparation and Immunoprecipitation of HA protein

Mice were challenged with 10^4 PFU of PR8 virus and sacrificed humanely on day 5 post infection. Lungs were collected and added to 10mL of FACS Buffer (PBS, 2mM EDTA, 3%FBS). Lungs were macerated until pulp-like with razor blades and added to 3mL of lung digestion buffer (HBSS from Lonza containing 5% FBS, 1mg/mL collagenase A and 0.05mg/mL DNaseI). Lungs were digested for 30 min at 37°C, then passed through an 18g needle to break up remaining tissue. The digested cells were added to 10mL of fresh FACS buffer and spun down for 4 min at 400g. Cells were resuspended in 3mL of RBC lysis buffer (ACK buffer[49]) for 5 minutes at room temperature. The lysed cells were added to 10mL of FACS Buffer and spun down for 4 min at 400g. The cells were resuspended in 1mL RIPA Lysis Buffer and left at 4°C for 30 min. Cells were spun down at 10,000g for 5 min at 4°C and the supernatant was collected. A Bradford Assay was performed to determine the protein concentration of the supernatant. 800µg of supernatant was added to 15µL of Sepharose beads loaded with 5µg of 18A3 human anti-HA antibody[50] and left overnight rotating at 4°C. Samples were then spun down at 2000g for 5 min and washed 3x with RIPA buffer. Pelleted beads were then boiled for 10 minutes and used for Coomassie staining and Western Blots.

Enzyme-Linked Immunosorbent Assays (ELISAs)

Purified influenza virion was diluted to 5µg/mL and was used to coat the bottom of maxisorp 96 well ELISA plate (Thermofisher). Virus was allowed to bind to the plate overnight at 4°C, then the plate was blocked with blocking buffer (1% milk in PBST). Sera was diluted 1:100 in blocking buffer, then serially diluted 3-fold. Plates were incubated with sera for 2 hours, after which the plates were washed 3 times with blocking buffer. Plates were incubated with goat α-mouse IgG-HRP secondary antibody (Prometheus) diluted 1:3000 in blocking buffer and incubated for 1 hour. Plates were washed 3 times with blocking buffer, then incubated with 100µL of SigmaFast OPD substrate for 30 minutes. Substrate reaction was stopped with 25µL of 3M HCl, and absorbance was measured at 450nm with a Luminometer plate reader (Promega).

Hemagglutination Inhibition Assay

Sera were RDE-treated overnight as previously described[51] then diluted 2-fold in PBS. Virus was diluted down to 4×10^6 PFU/mL in PBS/BSA/Pen-Strep and 25µL of virus was added to equal volume of sera in a v-bottom well of a 96 well microtiter plate. Virus and sera were incubated for 1 hour at 37°C. 50µL of 0.5% chicken RBCs (Lampire) diluted in PBS was added to each well. Plates were incubated at 4°C for 1 hour, then checked for hemagglutination inhibition.

Figure graphics and Statistical Analysis

Student t-test statistical analysis was performed with GraphPad Prism 9.2.0 software. Figure graphs were generated with GraphPad Prism 9.2.0 software, structural images

were generated with Pymol, and BioRender was used to create the mouse graphic in Figure 4.

Ethics Statement

The animal study was reviewed and approved by University of California, Riverside Institutional Animal Care and Use Committee (IACUC).

REFERENCES

1. Levy, R. M., Prince, J. M. & Billiar, T. R. Nitric oxide: A clinical primer. *Critical Care Medicine* **33**, S492 (2005).

2. Ignarro, L. J. & Freeman, B. *Nitric Oxide: Biology and Pathobiology*. (Academic Press, 2017).

3. Zaki, M. H., Akuta, T. & Akaike, T. Nitric Oxide-Induced Nitrative Stress Involved in Microbial Pathogenesis. *J Pharmacol Sci* **98**, 117–129 (2005).

4. Xie, Q. W., Whisnant, R. & Nathan, C. Promoter of the mouse gene encoding calcium-independent nitric oxide synthase confers inducibility by interferon gamma and bacterial lipopolysaccharide. *Journal of Experimental Medicine* **177**, 1779–1784 (1993).

5. Weinberg, J. B. *et al.* Human Mononuclear Phagocyte Inducible Nitric Oxide Synthase (iNOS): Analysis of iNOS mRNA, iNOS Protein, Biopterin, and Nitric Oxide Production by Blood Monocytes and Peritoneal Macrophages. *Blood* **86**, 1184–1195 (1995).

6. Koesling, D., Russwurm, M. & Mergia, E. Chapter 8 - Regulation and Physiological Functions of NO-Sensitive Guanylyl Cyclase. in *Nitric Oxide: Biology and Pathobiology* 107–116 (Academic Press, 2017).

7. Ichinose, F. & Zapol, W. M. Chapter 25 - Inhaled Nitric Oxide—Current Practice and Future Potential Uses and Development. in *Nitric Oxide: Biology and Pathobiology* 339–353 (Academic Press, 2017).

8. Jayasekera, J. P., Vinuesa, C. G., Karupiah, G. & King, N. J. C. Y. 2006. Enhanced antiviral antibody secretion and attenuated immunopathology during influenza virus infection in nitric oxide synthase-2-deficient mice. *Journal of General Virology* **87**, 3361–3371.

9. Obermajer, N. *et al.* Induction and stability of human Th17 cells require endogenous NOS2 and cGMP-dependent NO signaling. *Journal of Experimental Medicine* **210**, 1433–1445 (2013).

10. Giordano, D., Draves, K. E., Li, C., Hohl, T. M. & Clark, E. A. Nitric oxide regulates B cell activating factor (BAFF) expression and T-cell independent antibody responses. *J Immunol* **193**, 1110–1120 (2014).

11. Saini, A. S., Shenoy, G. N., Rath, S., Bal, V. & George, A. Inducible nitric oxide synthase is a major intermediate in signaling pathways for the survival of plasma cells. *Nat Immunol* **15**, 275–282 (2014).

12. Ischiropoulos, H., Zhu, L. & Beckman, J. S. Peroxynitrite formation from macrophage-derived nitric oxide. *Archives of Biochemistry and Biophysics* **298**, 446–451 (1992).

13. Ríos, N., Prolo, C., Alvarez, M. N., Piacenza, L. & Radi, R. Chapter 21 - Peroxynitrite Formation and Detection in Living Cells. in *Nitric Oxide: Biology and Pathobiology* 271–288 (Academic Press, 2017).

14. Pacher, P., Beckman, J. S. & Liaudet, L. Nitric Oxide and Peroxynitrite in Health and Disease. *Physiol Rev* **87**, 315–424 (2007).

15. McDonagh, B. Detection of ROS Induced Proteomic Signatures by Mass Spectrometry. *Front. Physiol.* **8**, (2017).

16. Szabó, C., Ischiropoulos, H. & Radi, R. Peroxynitrite: biochemistry, pathophysiology and development of therapeutics. *Nat Rev Drug Discov* **6**, 662–680 (2007).

17. Akaike, T. *et al.* Pathogenesis of influenza virus-induced pneumonia: involvement of both nitric oxide and oxygen radicals. *Proceedings of the National Academy of Sciences* **93**, 2448–2453 (1996).

18. Vlahos, R. *et al.* Inhibition of Nox2 Oxidase Activity Ameliorates Influenza A Virus-Induced Lung Inflammation. *PLoS Pathog* **7**, e1001271 (2011).

19. Nin, N. *et al.* Lung histopathological findings in fatal pandemic influenza A (H1N1). *Med Intensiva* **36**, 24–31 (2012).

20. Zablockienė, B., Ambrozaitis, A., Kačergius, T. & Gravenstein, S. Implication of nitric oxide in the pathogenesis of influenza virus infection. *Biologija* **58**, (2012).

21. James, S. L. Role of nitric oxide in parasitic infections. *Microbiological reviews* **59**, 533–547 (1995).

22. Oliveira-Brito, P. K. M., Rezende, C. P., Almeida, F., Roque-Barreira, M. C. & da Silva, T. A. iNOS/Arginase-1 expression in the pulmonary tissue over time during Cryptococcus gattii infection. *Innate Immun* **26**, 117–129 (2020).

23. Zhu, L., Gunn, C. & Beckman, J. S. Bactericidal activity of peroxynitrite. *Archives of Biochemistry and Biophysics* **298**, 452–457 (1992).

24. de Souza, K. P. R. *et al.* Nitric oxide synthase expression correlates with death in an experimental mouse model of dengue with CNS involvement. *Virology Journal* **10**, 267 (2013).

25. Uehara, E. U., Shida, B. de S. & de Brito, C. A. Role of nitric oxide in immune responses against viruses: beyond microbicidal activity. *Inflamm. Res.* **64**, 845–852 (2015).

26. Saura, M. *et al.* An Antiviral Mechanism of Nitric Oxide: Inhibition of a Viral Protease. *Immunity* **10**, 21–28 (1999).

27. Persichini, T. *et al.* Nitric Oxide Inhibits the HIV-1 Reverse Transcriptase Activity. *Biochemical and Biophysical Research Communications* **258**, 624–627 (1999).

28. Åkerström, S., Gunalan, V., Keng, C. T., Tan, Y.-J. & Mirazimi, A. Dual effect of nitric oxide on SARS-CoV replication: Viral RNA production and palmitoylation of the S protein are affected. *Virology* **395**, 1–9 (2009).

29. Tate, M. D. *et al.* Playing Hide and Seek: How Glycosylation of the Influenza Virus Hemagglutinin Can Modulate the Immune Response to Infection. *Viruses* **6**, 1294–1316 (2014).

30. Wang, C.-C. *et al.* Glycans on influenza hemagglutinin affect receptor binding and immune response. *Proc Natl Acad Sci U S A* **106**, 18137–18142 (2009).

31. López-Alarcón, C. *et al.* Reactivity of 1,4-Dihydropyridines Toward SIN-1-Derived Peroxynitrite. *Pharm Res* **21**, 1750–1757 (2004).

32. Russell, R. J., Gamblin, S. J. & Skehel, J. J. Influenza glycoproteins: Hemagglutinin and neuraminidase. in *Textbook of Influenza* (eds. Webster, R. G., Monto, A. S., Braciale, T. J. & Lamb, R. A.) 67–100 (John Wiley & Sons, Ltd, 2013). doi:10.1002/9781118636817.ch5.

33. Caton, A. J., Brownlee, G. G., Yewdell, J. W. & Gerhard, W. The antigenic structure of the influenza virus A/PR/8/34 hemagglutinin (H1 subtype). *Cell* **31**, 417–427 (1982).

34. Karupiah, G., Chen, J.-H., Mahalingam, S., Nathan, C. F. & MacMicking, J. D. Rapid Interferon γ–dependent Clearance of Influenza A Virus and Protection from Consolidating Pneumonitis in Nitric Oxide Synthase 2–deficient Mice. *Journal of Experimental Medicine* **188**, 1541–1546 (1998).

35. Darwish, I., Miller, C., Kain, K. C. & Liles, W. C. Inhaled Nitric Oxide Therapy Fails to Improve Outcome in Experimental Severe Influenza. *Int J Med Sci* **9**, 157–162 (2012).

36. Suliman, H. B., Ryan, L. K., Bishop, L. & Folz, R. J. Prevention of influenza-induced lung injury in mice overexpressing extracellular superoxide dismutase. *American Journal of Physiology-Lung Cellular and Molecular Physiology* **280**, L69–L78 (2001).

37. Akaike, T. Role of free radicals in viral pathogenesis and mutation. *Rev. Med. Virol.* **11**, 87–101 (2001).

38. Akaike, T. *et al.* 8-nitroguanosine formation in viral pneumonia and its implication for pathogenesis. *Proc Natl Acad Sci U S A* **100**, 685–690 (2003).

39. Radi, R. Oxygen radicals, nitric oxide, and peroxynitrite: Redox pathways in molecular medicine. *Proc Natl Acad Sci USA* **115**, 5839–5848 (2018).

40. Ferrer-Sueta, G. & Radi, R. Chemical Biology of Peroxynitrite: Kinetics, Diffusion, and Radicals. *ACS Chem. Biol.* **4**, 161–177 (2009).

41. Mahmoudabadi, G., Milo, R. & Phillips, R. Energetic cost of building a virus. *PNAS* **114**, E4324–E4333 (2017).

42. Frensing, T. *et al.* Influenza virus intracellular replication dynamics, release kinetics, and particle morphology during propagation in MDCK cells. *Appl Microbiol Biotechnol* **100**, 7181–7192 (2016).

43. Karakus, U., Crameri, M., Lanz, C. & Yángüez, E. Propagation and Titration of Influenza Viruses. in *Influenza Virus: Methods and Protocols* (ed. Yamauchi, Y.) 59–88 (Springer, 2018). doi:10.1007/978-1-4939-8678-1_4.

44. Lomonosova, E. E., Kirsch, M., Rauen, U. & de Groot, H. The Critical Role of Hepes in SIN-1 Cytotoxicity, Peroxynitrite Versus Hydrogen Peroxide. *Free Radical Biology and Medicine* **24**, 522–528 (1998).

45. Seimetz, M. *et al.* Inducible NOS Inhibition Reverses Tobacco-Smoke-Induced Emphysema and Pulmonary Hypertension in Mice. *Cell* **147**, 293–305 (2011).

46. Dobrian, A. D., Schriver, S. D. & Prewitt, R. L. Role of Angiotensin II and Free Radicals in Blood Pressure Regulation in a Rat Model of Renal Hypertension. *Hypertension* **38**, 361–366 (2001).

47. Hai, R., García-Sastre, A., Swayne, D. E. & Palese, P. A reassortment-incompetent live attenuated influenza virus vaccine for protection against pandemic virus strains. *J Virol* **85**, 6832–6843 (2011).

48. Hai, R. *et al.* Influenza A(H7N9) virus gains neuraminidase inhibitor resistance without loss of in vivo virulence or transmissibility. *Nat Commun* **4**, 2854 (2013).

49. Hoffmann, A. B., Mazelier, M., Léger, P. & Lozach, P.-Y. Deciphering Virus Entry with Fluorescently Labeled Viral Particles. in *Influenza Virus: Methods and Protocols* (ed. Yamauchi, Y.) 159–183 (Springer, 2018). doi:10.1007/978-1-4939-8678-1_8.

50. Anchisi, S., Gonçalves, A. R., Mazel-Sanchez, B., Cordey, S. & Schmolke, M. Influenza A Virus Genetic Tools: From Clinical Sample to Molecular Clone. in *Influenza Virus: Methods and Protocols* (ed. Yamauchi, Y.) 33–58 (Springer, 2018). doi:10.1007/978-1-4939-8678-1_3.

51. ACK Lysis Buffer. *Cold Spring Harb Protoc* **2014**, pdb.rec083295 (2014).

52. Whittle, J. R. R. *et al.* Flow Cytometry Reveals that H5N1 Vaccination Elicits Cross-Reactive Stem-Directed Antibodies from Multiple Ig Heavy-Chain Lineages. *J Virol* **88**, 4047–4057 (2014).

53. Liu, W.-C., Nachbagauer, R., Krammer, F. & Albrecht, R. A. Assessment of Influenza Virus Hemagglutinin Stalk-Specific Antibody Responses. in *Influenza Virus: Methods and Protocols* (ed. Yamauchi, Y.) 487–511 (Springer, 2018). doi:10.1007/978-1-4939-8678-1_23.

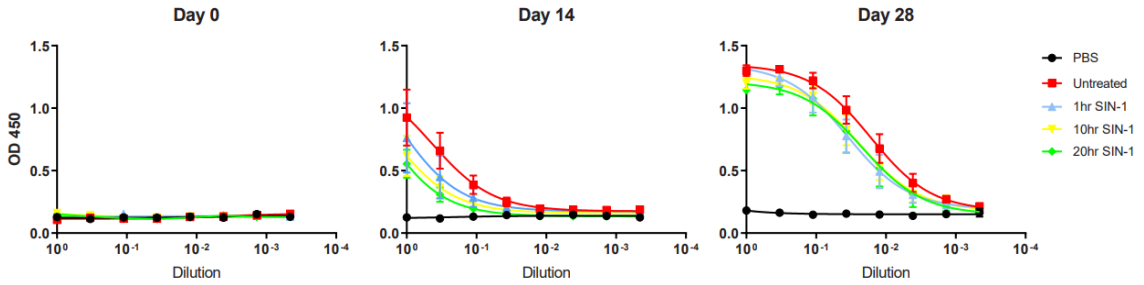

Supplemental Figure 1. Reduced Antibody responses to SIN-1 treated HA protein. Results are for vaccinations with HA protein treated with SIN-1 for 1 hour, 10 hours, or 20 hours. Untreated and 20 hour SIN-1 treated results are displayed in Figure 4B.

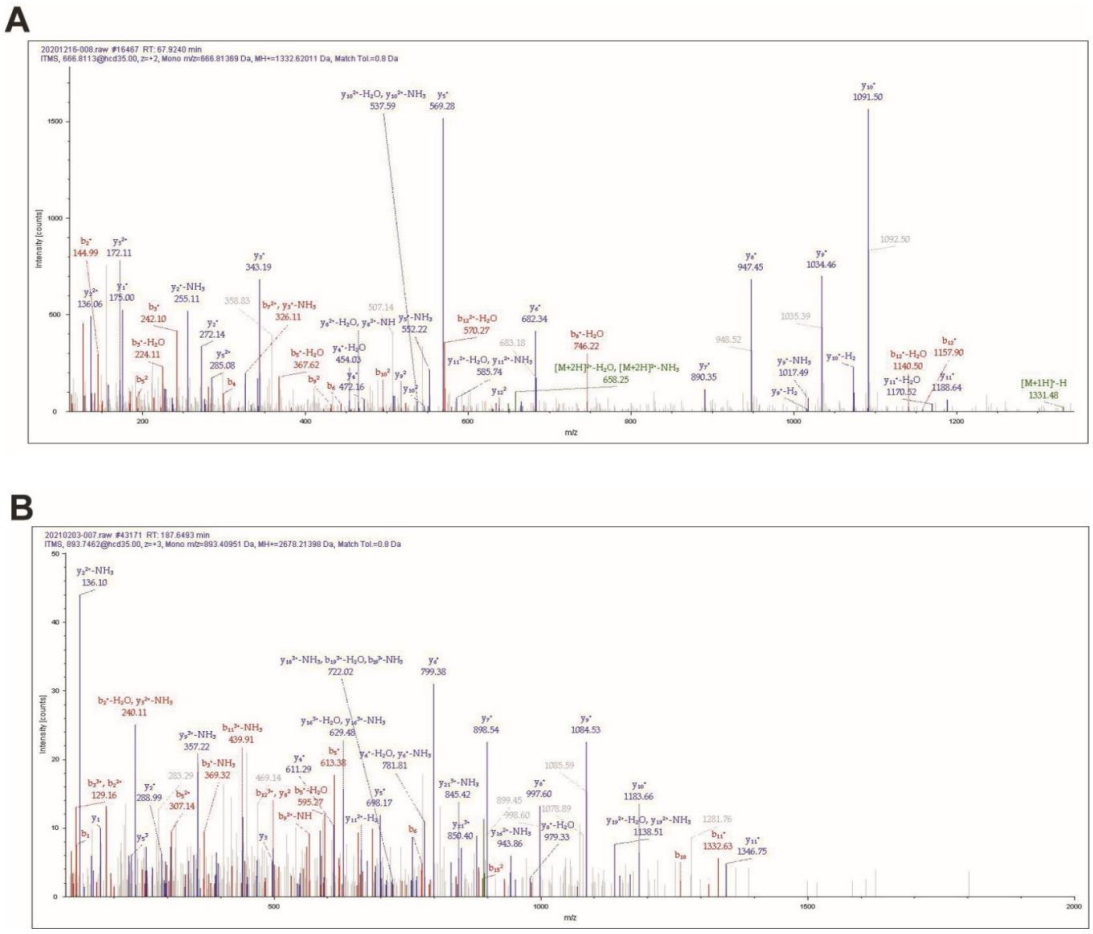

Supplemental Figure 2. (A) Representative MS2 mass spectra of nitrotyrosine-modified purified HA protein peptide GSPGSGY(Nitrotyrosine)IPEAPR. **(B)** Representative MS2 mass spectra of nitrotyrosine modified HA protein from PR8 virion peptide EQQNIYQNENAYVSVVTSNY(Nitrotyrosine)NR. y ions are shown in blue and b ions are shown in red.

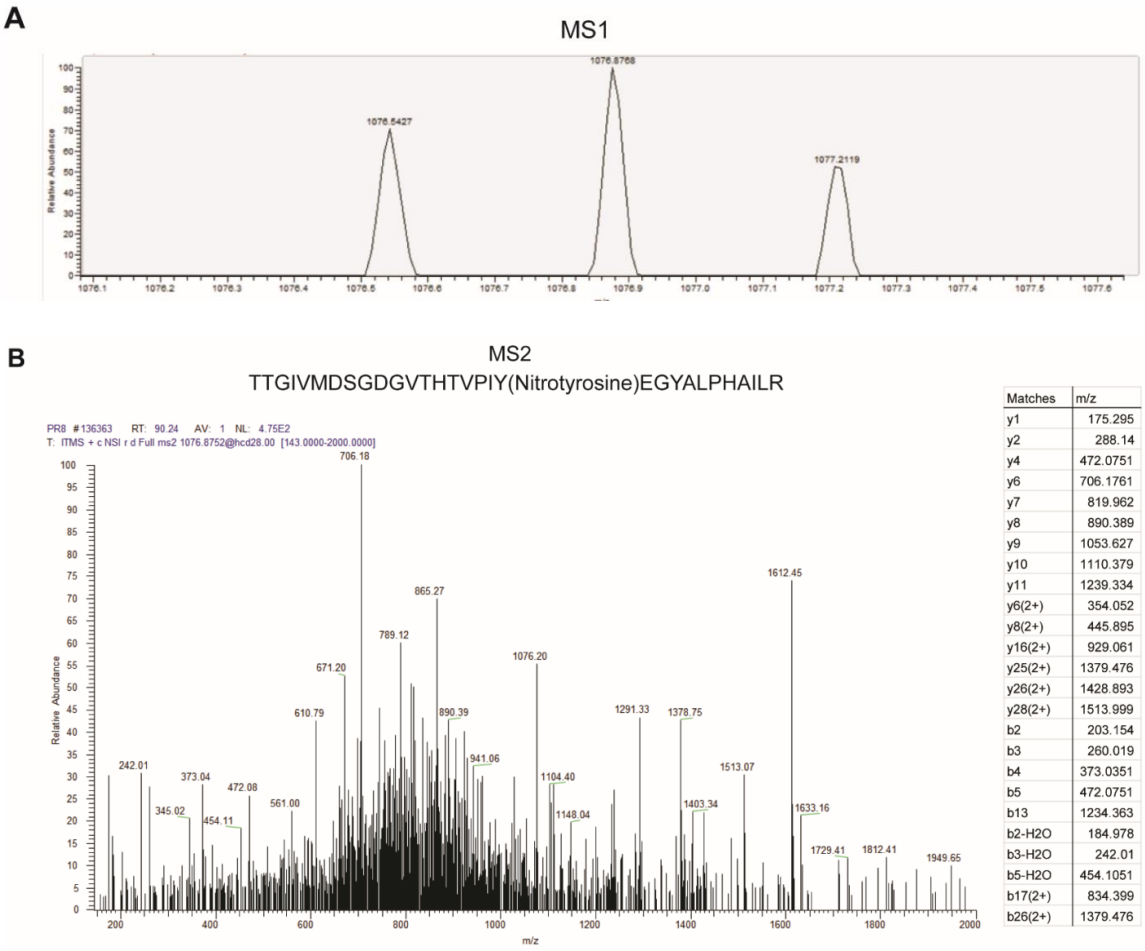

Matches	m/z
y1	175.295
y2	288.14
y4	472.0751
y6	706.1761
y7	819.962
y8	890.389
y9	1053.627
y10	1110.379
y11	1239.334
y6(2+)	354.052
y8(2+)	445.895
y16(2+)	929.061
y25(2+)	1379.476
y26(2+)	1428.893
y28(2+)	1513.999
b2	203.154
b3	260.019
b4	373.0351
b5	472.0751
b13	1234.363
b2-H2O	184.978
b3-H2O	242.01
b5-H2O	454.1051
b17(2+)	834.399
b26(2+)	1379.476

Supplemental Figure 3. MS1 and MS2 peptide spectra matched to nitrotyrosine-modified mouse Actin protein (Protein accession number P63260) from PR8 infected mice, 5 days post infection. MS1 spectra shows peptide peak at 1076.8768 m/z. MS2 spectra is for peptide sequence TTGIVMDSGDGVTHTVPIY(Nitrotyrosine)EGYALPHAILR.

Chapter 3:
Modification of Influenza Hemagglutinin Protein with Unnatural Amino Acids

ABSTRACT

Unnatural Amino Acids (unAAs) have emerged as useful biochemical tools in the last few decades. UnAAs are amino acids not part of the canonical 20 amino acids common to all living things or the noncanonical amino acids selenocysteine and pyrrolysine found in certain archaea. Incorporation of unAAs can endow proteins with new properties. Hundreds of unnatural amino acids have been synthesized and tested for their application in diverse scientific disciplines. Recently, unnatural amino acids containing aryl side chains have been shown to increase the immunogenicity of proteins such as mTNFα, mEGF, and mRBD4. This function of unnatural amino acids, however, has not yet been demonstrated for a virus protein. The development of novel vaccine strategies that provide enhanced protection against influenza viruses is highly desirable. We therefore tested the ability of unAAs to increase the immunogenicity of the influenza hemagglutinin protein. We succeeded in incorporating the unAAs 4-boronophenylalanine and p-nitrophenylalanine into the HA protein. However, the incorporation of the unAAs did not increase the immunogenicity of the HA protein. We conclude that the incorporation of unAAs into influenza virus proteins may not be a suitable approach for increasing the immunogenicity of virus proteins.

INTRODUCTION

Genetic code expansion to include unAAs began with the realization that the genetic code was flexible. In the 1960s, random mutagenesis produced premature TAG

amber termination codons in bacteria and viruses.[1] Random mutagenesis also produced mutants that were able to "suppress" the loss-of-function TAG mutants, resulting in the production of full-length protein[2]. Amino acid sequencing of the generated proteins revealed that a different amino acid had been substituted into the TAG site. Additional sequencing revealed that the anticodon of a particular tRNA had been mutated so that it now recognized the amber codon. By matching the mutated tRNA to the incorporated amino acid, scientists could match amino acids to specific anticodon sequences, thus determining the genetic code.[3]

The suppressor mutants showed it was possible to change the genetic code by mutating the anticodon of a tRNA so that it now coded for a different amino acid. Based on this finding, it was logical that the genetic code could be expanded to include unAAs. The expansion involves converting a codon (typically the amber stop codon) from its natural termination role to coding for an unAA. This requires mutating the anticodon of a particular tRNA so that it recognizes the amber stop codon, as well as aminoacylation of the mutant orthogonal tRNA with the unAA. Initially, the aminoacylation was done *in vitro*[4], but the creation of orthogonal tRNA synthetases (RS) that recognize the unAA allows for aminoacylation *in vivo*.[5] The creation of orthogonal tRNA/RS pairs has been covered in several excellent reviews by Peter Schultz[6–8]. The first step is the selection of the genes for conversion to orthogonal tRNA/RS. The orthogonal tRNA should be as specific as possible for recognition by the orthogonal RS, so that the orthogonal tRNA is not recognized by naturally occurring RS. Likewise, the orthogonal RS should be as specific as possible for the unAA and the orthogonal tRNA, so that it does not charge the

orthogonal tRNA with a natural amino acid or charge natural tRNAs with the unAA. To keep the reaction as specific as possible, tRNA/RS pairs from the archaea *Methanococcus jannaschii* were used[9], as they are evolutionarily distant from the bacterial and eukaryotic model organisms. Most orthogonal pairs have used archaea genes, from organisms like *Methanosarcina barkeri* and *Methanosarcina mazei*[10], though orthogonal pairs from *Saccharomyces cerevisiae*, *E.coli*, *Pyrococcus horikoshii*, *Methanobacterium thermoautotrophicum*, *Pyrococcus horikoshii*, and *Bacillus stearothermophilus* have also been reported.[6]

Once the tRNA/RS genes are cloned, the anticodon of the tRNA is mutated so that it recognizes the amber stop codon. The mutant tRNA sequence is then cloned into a plasmid containing an antibiotic resistance gene with a premature TAG codon. Next, a library of RS sequences containing mutations in the amino acid binding pocket is generated. The plasmids containing the library and the tRNA are then used to transform bacteria in the presence of the unAA. The cells will survive in the presence of antibiotic if the RS can aminoacylate the tRNA. The RS that passes this positive selection step is then transformed into E. coli with the mutant tRNA in the presence of a mutant gene for barnase containing several TAG mutations. Barnase is toxic to bacteria. If the RS charges the tRNA in the absence of the unAA, that indicates the RS can use a native amino acid to charge the tRNA, and those candidates are discarded. The candidates that pass this negative selection test can then be used for several rounds of selection to find the most efficient and stringent RS.

While the genetic code expansion system using the amber stop codon is impressive, it has many hurdles that must be overcome for efficient unAA incorporation into protein. Firstly, the tRNA/RS pair must be specific for the unAA so that the tRNA is not charged with native amino acids. The selection protocols outlined above help overcome this limitation.[6] Secondly, the unAA-charged tRNA faces competition from the host translation termination machinery in recognizing the amber stop codon. In bacteria, this problem is avoided by disrupting release factor 1 (RF1)[11], which is specific for the amber codon. In eukaryotes, mutations in eukaryotic release factor 1 (eRF1) can inhibit eRF1's ability to recognize the amber codon, giving the advantage to the unAA-charged tRNA.[12] Thirdly, there is the potential for off-target incorporation of the unAA at naturally occurring amber stop codons, which could potentially result in the readthrough of many genes. An amber-codon free E. coli strain has been created to circumvent this problem in E. coli.[13] The amber stop codon is used the least frequently among the different termination codons, and the presence of the orthogonal translation machinery seems well-tolerated in mammalian systems.[14] Selective addition of the unAA to the cell media and the use of inducible promoters for the tRNA/RS system could also minimize off-target incorporation of the unAA. Fourthly, the presence of the premature termination codon makes the mRNA a target for degradation by nonsense mediated decay (NMD). Yeast strains lacking the UPF1 protein, critical for NMD, have shown increased unAA incorporation.[15]

In addition to the amber stop codon, quadruplet frame-shift codons have been used to expand the genetic code. Like the suppressor mutants of amber stop codons,

suppressor mutants that could overcome frameshift mutations were an indication that the genetic code could be expanded to include quadruplet codons[16]. Recoding quadruplet tRNA/RS pairs to recognize unAAs is done in a manner similar to the amber stop codon[17]. However, poor incorporation efficiencies have also led to the optimization of other components of the translation machinery for quadruplet codon usage[18]. Using a genetic code of four bases rather than three greatly increases the number of unique codons available for recoding to unAAs, and these codons have been used in cell free, bacterial, and mammalian systems for incorporation of unAAs[18,20,21].

One potential use of unAAs is their ability to break immune tolerance. The immune system generates potent antibody and T-cell responses to foreign antigens but is tolerant of self-antigens. Self-tolerance is broken in many different autoimmune diseases, and this has also been associated with an increase in the presence of 3-nitrotyrosine and anti-nitrotyrosine antibodies. It was hypothesized that the incorporation of nitroaryl-containing unAAs into self-proteins would be able to break immune tolerance. Peter Shultz's group incorporated the unAA p-nitrophenylalanine (pNO2Phe) into mouse TNFα, which was then used to vaccinate mice.[19] The unAA-modified protein generated a strong antibody response against wild-type mouse TNFα. The group then went on to demonstrate the same effect for other self-proteins, including mRBP4 and mEGF.[20]

Others have built upon the original work of Peter Schultz's group to expand the application of unAAs to generate strong antibody responses. Tong et al. used pNO2Phe modified antigen to generate human monoclonal antibodies against hTNFα and against human BAFF protein *in vitro*.[21] Li et al. also used pNO2Phe-modified RANKL to break

immune tolerance to RANKL in a mouse model of bone loss[22] and collagen-induced arthritis[23], and Kessel et. al used pNO2Phe-modified C5a to break immune tolerance to C5a in a mouse model of arthritis.[24] These experiments confirmed that pNO2Phe modification of proteins is a reliable and reproducible method for breaking immune tolerance to self-proteins. However, it remained to be determined if pNO2Phe could be used to not just break immune tolerance, but to increase antibody responses to an already immunogenic protein. Tian et al. addressed this question by incorporating pNO2Phe into different amino acid positions of the universal helper T cell epitope PADRE fused to HER2.[25] The HER2-PADRE fusion protein was by itself immunogenic. They tested antibody responses to the pNO2Phe-modified fusion proteins in C57BL6 mice. They found unAA modification could increase the immunogenicity of HER2, but this enhancement effect was position dependent. Mutating certain amino acid positions of the T cell-epitope decreased antibody responses to HER2, while mutating other positions increased antibody responses to HER2. This position dependent effect on increased immunogenicity was also observed by Gauba et al. in their experiments with unAA modification of mTNFα to break immune tolerance.[26]

Understanding the mechanism behind how unAAs break immune tolerance shed light on understanding why the observed increased immunogenicity was position dependent. Gauba et al. showed that the generation of new helper T cell epitopes was the mechanism behind autoantibody responses to mTNFα following immunization with unAA-modified mTNFα.[26] First, they observed that the breakage of immune tolerance following immunization with unAA-modified protein was MHC-restricted. They

observed that breakage of immune tolerance was dependent on the strain of the immunized mouse. A mutation to unAA at amino acid position 11 in mTNFα broke immune tolerance in B6 mice but not FVB/N mice. Conversely, a mutation to unAA at amino acid position 21 in mTNFα broke immune tolerance in FVB/N mice but not B6 mice. Hypothesizing that these observations could be the result of differences in MHC class II, the authors vaccinated congenic mice that differed only in their MHC class II expression. Mice expressing the H-2^b allele generated an autoantibody response following vaccination with mTNFα modified with unAA at amino acid position 11, while mice expressing the H-2^q allele did not. After showing the MHC restriction of unAA-breakage of immune tolerance, the authors demonstrated that the unAA modification created new peptides displayed to $CD4^+$ T cells in MHC class II. The authors synthesized a panel of mTNFα peptides containing the unAA modification at amino acid position 11. CD4 T cells were isolated from mice immunized with the unAA-modified mTNFα and were cocultured with antigen-presenting cells in the presence of the unAA-containing peptides. The T cells were activated by the unAA-containing peptides, but not by peptides from native mTNFα. With the new understanding of how breaking immune tolerance could be achieved, the authors also showed that point mutations to natural aryl amino acids were sufficient to break immune tolerance. A lysine to tyrosine mutation at position 11 of mTNFα and a tyrosine to phenylalanine mutation at position 29 of mEGF were both immunogenic, generating strong antibody responses to their wild-type counterparts.

Since our aim was increasing the immunogenicity of the influenza virus HA protein, an already immunogenic protein, we hypothesized that our unAA mutations

would result in changes in immunogenicity similar to those seen with PADRE[25]. We hypothesized that the changes in immunogenicity would be position dependent. We therefore sought to make a wide range of mutations in HA at different amino acid positions. We incorporated the unAAs 4-boronophenylalanine (4BorPhe) and p-nitrophenylalanine (pNO2Phe) into multiple positions of the HA protein. We also generated a system for the creation of live but replication-incompetent viruses containing unAAs incorporated into HA. However, the incorporation of the unAAs into the HA protein did not increase the immunogenicity of HA. This chapter concludes with a discussion of future prospects for unAAs in vaccine design.

RESULTS

UnAA incorporation into the HA protein

Since it was hypothesized that only a subset of mutations to HA would show increased immunogenicity, we selected a total of 18 amino acid codon positions in the sequence of PR8 HA for mutagenesis to TAG for unAA incorporation (Figure 8A). Known glycosylation sites as well as the fusion peptide of HA were avoided. Beyond those criteria, the mutations were grouped into 4 categories: 1) Mutations that flank the highly conserved fusion peptide of HA 2) Mutations of natural amino acids that are structurally similar to aryl unAAs 3) Mutations in known antigenic sites of HA 4) Mutations predicted to increase binding of HA peptides to MHC class II I-Ab allele (Figure 8B)[27].

A

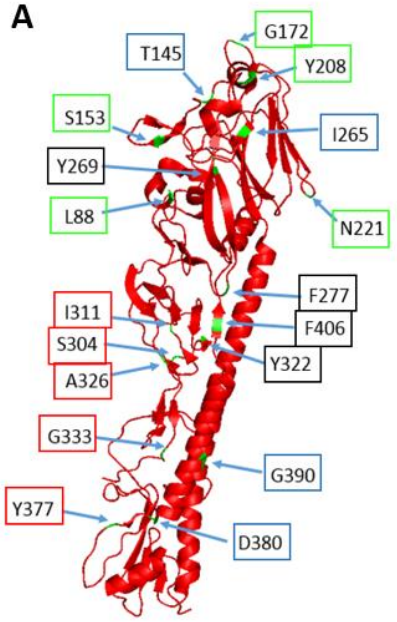

B

Mutant	Binding Prediction of WT Peptide by SMM-align	Binding Prediction of Mutant Peptide by SMM-align
T145	11.91	1.27
G333	21.74	9.63
D380	36.48	3.82
G390	25.56	7.46

Figure 8. Premature stop codon mutations in PR8 HA. (A) Amino acid positions targeted for mutation to the amber stop codon. Red: Mutations that flank the highly conserved fusion peptide of HA. Black: Mutations of natural amino acids that are structurally similar to aryl unAAs. Green: Mutations in known antigenic sites of HA. Blue: Mutations predicted to increase binding to MHC class II I-Ab allele. (B) Using Tyr as a substitute for the unAA mutation, mutant HA peptides were assigned a percentile rank based on their predicted ability to bind to MHC-II I-A^b. Low percentile rank = stronger binding. Neo-epitopes are those that are predicted to cross the threshold of 11.00 (the predicted binding of class-II-associated invariant chain).

To confirm the incorporation of unAAs into the HA protein, we co-transfected 293T cells with a plasmid containing an orthogonal tRNA/RS pair derived from *E. coli* tyrosyl tRNA and synthetase[28] in the presence or absence of unAAs. Incorporation of the unAA was confirmed by western blot (Representative mutations shown in Figure 9A). In the absence of the orthogonal translation machinery, the TAG codon functions as a stop codon and full-length HA protein is not produced. In the presence of the unAA and the orthogonal translation machinery, full-length HA protein can be observed. There was a small amount of full-length HA produced in the presence of the orthogonal translation

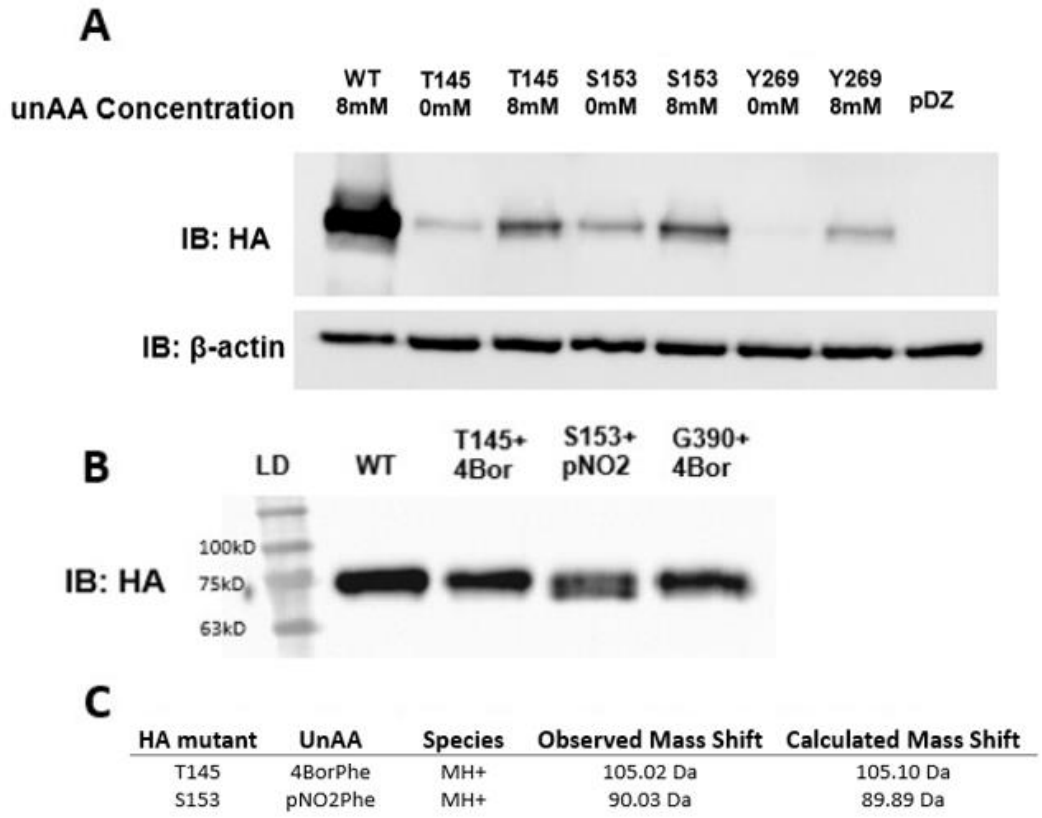

HA mutant	UnAA	Species	Observed Mass Shift	Calculated Mass Shift
T145	4BorPhe	MH+	105.02 Da	105.10 Da
S153	pNO2Phe	MH+	90.03 Da	89.89 Da

Figure 9. UnAA modification of HA. (A) 293T cells co-transfected with HA mutants in the presence or absence of 4BorPhe. Cells were lysed and used for a western blot for the detection of different HA mutants (T145, S153, and Y269). Results are representative of the other mutants and of pNO2Phe incorporation. (**B**) Western blot for detection of purified HA6xHis protein from 293T cells. (**C)** LC-MS analysis of purified mutant HA6xHis protein.

machinery alone, suggesting the orthogonal translation machinery has some affinity for a natural amino acid. Nevertheless, the amount of full-length HA produced was greatly increased in the presence of unAA. To further confirm the incorporation of unAA into the protein, the mutant HA proteins were purified by Ni-affinity chromatography (Figure 9B) and analyzed by mass spectrometry (mass spec). Mass spec analysis confirmed the incorporation of unAA into the HA protein. (Figure 9C).

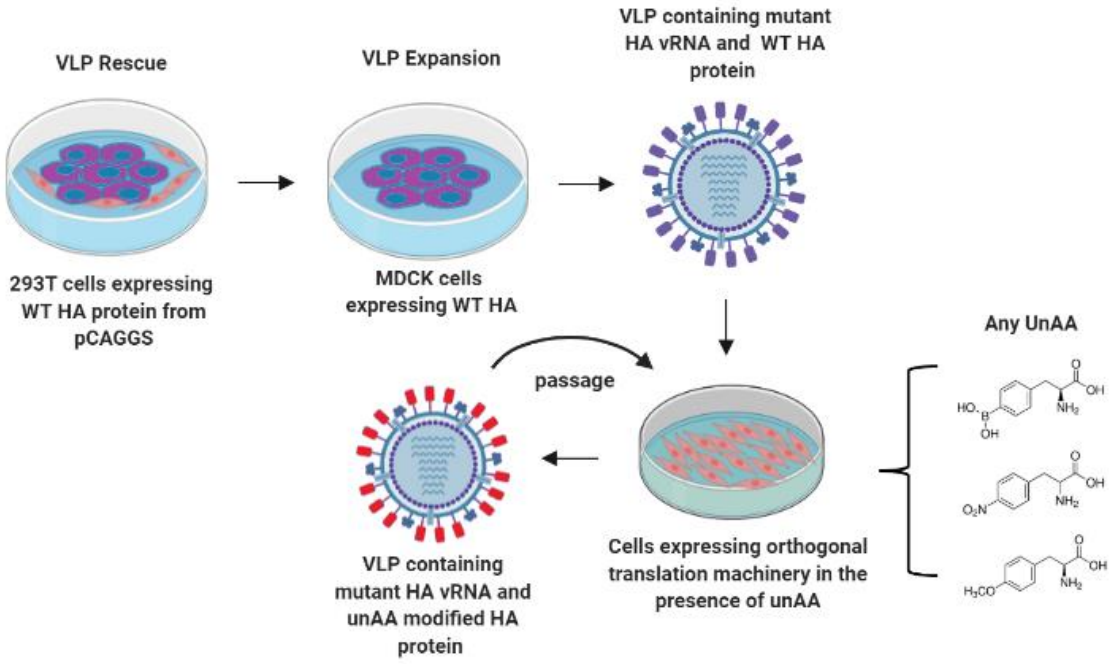

Figure 10. Strategy for production of live but replication-incompetent influenza VLPs containing unAA-modified HA protein.

Influenza VLPs containing unAA incorporated into HA

To increase the efficiency of the production of influenza VLPs containing unAA-modified HA, we devised a strategy that split the production of VLPs into two steps (Figure 10). First, the VLPs are rescued in 293T cells by transfecting the mutant HA-pDZ plasmid, pDZ plasmids encoding the 7 additional viral gene segments, and a WT HA-pCAGGS plasmid. The mutant HA-pDZ plasmid supplies the viral RNA segment containing the TAG mutant codon for unAA incorporation but does not make functional HA at this step. Instead, WT HA protein is provided by the HA-pCAGGS plasmid to form the virus particle. VLPs from the rescue are expanded in MDCK cells constitutively expressing WT HA protein to generate VLPs containing WT HA protein and mutant HA

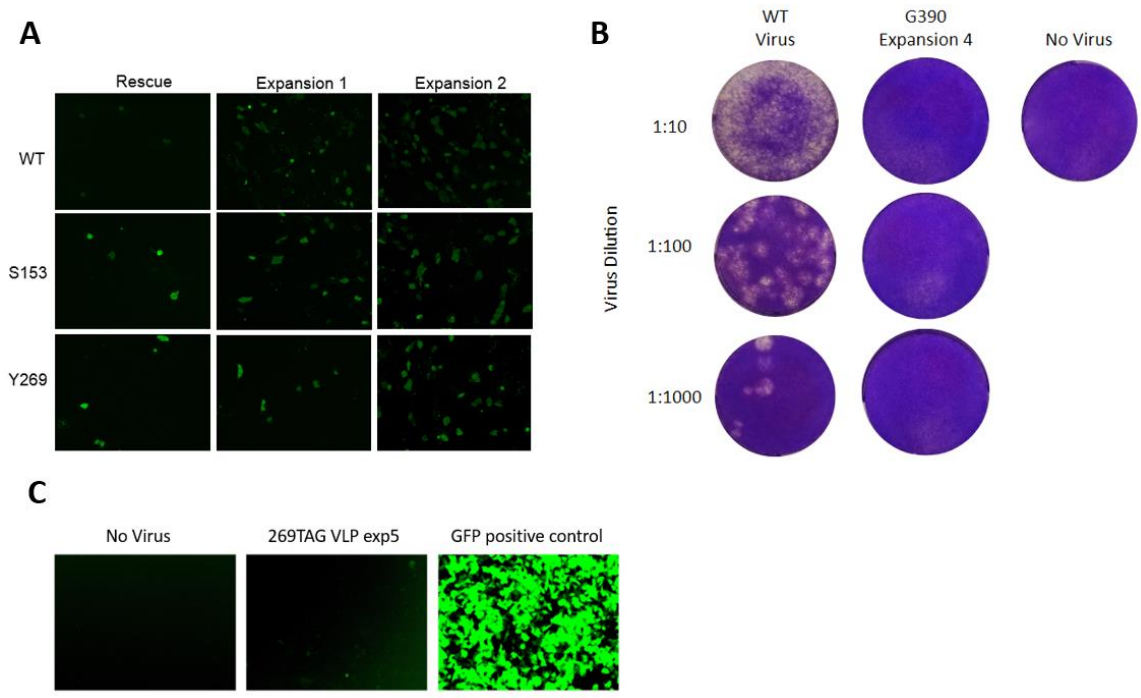

Figure 11. Production of VLPs for unAA-incorporation into influenza HA protein. **(A)** Representative FFU assay results for VLP rescues in 293T cells and expansions in HA-MDCK cells. **(B)** Representative Plaque Assay result of VLP expansions. **(C)** Representative FFU assay result for production of VLPs containing the unAA in 293T cells expressing the orthogonal translation machinery in the presence of 8mM 4BorPhe. GFP positive control represents cells transfected with pCAGGS plasmid containing a mutant version of GFP with a pre-mature stop codon at amino acid position 39.

RNA segment. These VLPs can then be used as a base for the incorporation of different unAAs at specific sites of the HA protein. The VLPs are used to infect cells expressing the orthogonal translation machinery in the presence of the unAA. The VLPs produced contain the unAA-modified HA protein and mutant HA viral RNA segment. We implemented this strategy and generated VLPs containing pre-mature stop codon mutations at nine different amino acid positions (T145, S153, Y269, F277, S304, I311, A326, Y377, and G390). The presence of VLPs was confirmed by a Fluorescence Forming Unit Assay (FFU assay) (Figure 11A). The VLPs were shown to be replication

incompetent by plaque assay (Figure 11B). However, infection of 293T cells constitutively expressing the orthogonal translation machinery in the presence of unAA did not produce VLPs (Figure 11C).

Mouse sera antibody responses to HA following vaccination with unAA-modified HA

To test if the unAA modifications could alter antibody responses to WT HA protein, purified unAA-modified HA protein was used to vaccinate mice. Three unAA-modified HA proteins were used: HA containing 4BorPhe at amino acid position 145 (T145_4BorPhe), HA containing pNO2Phe at amino acid position 153 (S153_pNO2Phe), and HA containing 4BorPhe at amino acid position 390 (G390_4BorPhe). Mice were vaccinated with 15µg of either WT HA protein, T145_4BorPhe HA, S153_pNO2Phe HA, G390_4BorPhe HA, or PBS. Sera were collected on Day 1 and Day 21 post-vaccination. Mice were boosted on Day 21 with an additional 15ug of protein and sera were collected 3 weeks later, on Day 42 post-vaccination. Sera antibody titers against WT HA were determined by ELISA. Of the three mutants tested, none showed increased antibody responses to WT HA, while the G390_4BorPhe mutant showed decreased antibody responses to WT HA on Day 21 post-infection (Figure 12). However, on Day 42 post-infection, all three mutants showed no significant difference in IgG titers compared to WT protein, though all were elevated over PBS.

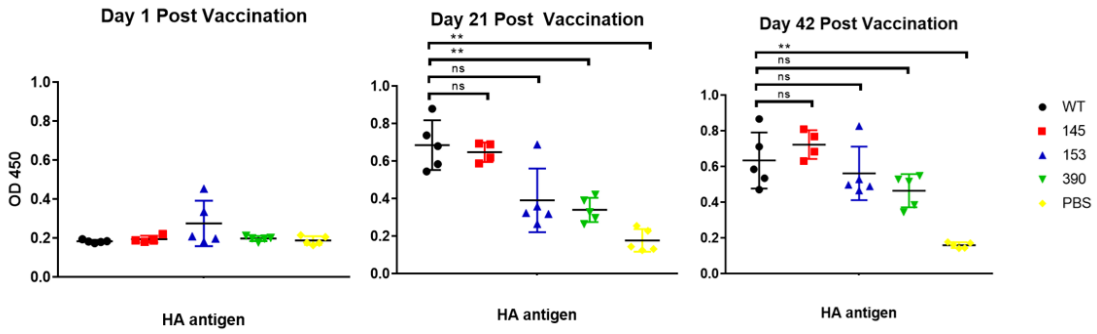

Figure 12. Mouse Sera IgG responses to vaccination with unAA modified HA. Sera was collected on Day 1, Day 21, and Day 42 after the initial vaccination with 15µg of either WT HA protein, T145_4BorPhe HA, S153_pNO2Phe HA, G390_4BorPhe HA, or PBS (5 mice per group). Mice were boosted on Day 21 after the initial vaccination with an additional 15µg of protein. 5ug of purified WT PR8 virus was used for the ELISA antigen.

DISCUSSION

In summary, unAAs can be incorporated into HA protein at specific positions to produce unAA-modified HA, though the production of the modified HA is not as efficient as the production of WT HA. We designed a strategy for the efficient production of infectious but replication-incompetent influenza VLPs containing unAA modifications at specific positions of the HA protein. This procedure splits the production of unAA-modified VLPs into two steps. The first step produces VLPs with WT HA protein and amber stop codon mutations for unAA incorporation. These VLPs can serve as a base for the incorporation of any unAA of choice. The VLPs from the first step can be used to infect cells expressing the orthogonal translation machinery. These cells then produce the final unAA-modified VLPs. Although we did not observe production of unAA-modified VLPs when we infected 293T cells constitutively expressing the orthogonal translation machinery, this is likely due to the inefficiency of the orthogonal translation system (see

Figure 9) rather than a problem with the experimental design. Incorporating a more efficient translation system into our method in Figure 10 is likely to produce VLPs. Finally, to test if the unAA modifications could alter antibody responses to WT HA protein, we vaccinated mice with purified unAA modified HA protein and determined sera antibody responses to WT HA. None of the unAA-modified HA proteins increased antibody responses to WT HA protein. This was not surprising, as we expected any mutations that increased the immunogenicity of HA would be position dependent and would represent only a subset of the mutations tested. Since we only tested 3 mutants, it was not surprising that we did not observe any mutations with increased immunogenicity. Testing additional mutations at different HA positions may eventually determine which unAA-modifications can increase immunogenicity to HA. However, reflecting on the mechanism behind unAA-increased immunogenicity provides insights into why this may not be the best strategy.

The mechanistic understanding that breaking immune tolerance with unAAs is achieved by the creation of novel helper T-cell epitopes creates two problems. First, it suggests that unAAs are not necessary for the generation of autoantibodies. Notably, the unAAs used in all the papers described so far contain aromatic side chains, a property that makes them particularly good anchor residues for binding the MHC class II binding pocket. If the introduction of an aromatic side chain to a peptide is all that is required for breaking immune tolerance, as implied by Gauba et al.'s results, the introduction of the natural amino acids tyrosine or phenylalanine would be a much easier task for breaking immune tolerance. However, there are two potential properties of unAAs that might make

them the preferred method for breaking immune tolerance. The first is that the nitroaryl side chains may have a stronger binding affinity for germline antibody combining sites compared to aryl side chains, which could increase antibody recognition of the antigen[29,30]. The second is that mutating to bulky side chain amino acids like Phe and Tyr could drastically alter the shape of the antigen, which would prevent recognition of native epitopes by antibodies. Mutating native Phe or Tyr to pNO2Phe avoids making large structural changes to the antigen. Li et al.[22] and Kessel et al.[24] both showed mutating Tyr to the unAA pNO2Phe is sufficient to generate an increased antibody response to WT protein compared to vaccination with WT protein. This change occurred without a corresponding change in the aromatic ring of the amino acid side chain, suggesting the breakage of immune tolerance goes beyond substituting an aromatic side chain.

The mechanism proposed by Gauba et al. introduces a second problem, namely the diversity of MHC molecules. Gauba et al. demonstrated that the increased immunogenicity of unAA-modified proteins was MHC restricted. The effect was only observed in specific genetic backgrounds with particular MHC alleles[26]. The human population contains thousands of different HLA alleles, and each individual can have up to 12 different isoforms. Finding the site-specific mutation in a protein that increases immunogenicity in every MHC genetic background is a major challenge for using unAAs to break immune tolerance. Tian et al. addressed this problem by incorporating pNO2Phe into different positions of the universal T-cell epitope PADRE to see if any could increase immunogenicity against HER2[25]. The results of their study again showed position-dependent increased immunogenicity, but several mutation sites eliminated the

immunogenicity of the protein entirely. This highlights the fact that the unnatural amino acid by itself is not immunogenic. Rather, it is the context-specific interaction of the unnatural amino acid-modified protein with the immune system that dictates whether there is an increased adaptive immune response. The authors were able to identify a position that, when mutated to pNO2Phe, increased immunogenicity to HER2 in multiple mouse genetic backgrounds, and in a separate paper, they further showed that the same position exhibited increased immunogenicity of HER2 in vitro with human PBMCs of different genetic backgrounds[31]. However, more studies need to be done to determine if this increased immunogenicity is observed with other immunogenic proteins.

Lin et al. provided the first example of incorporation of unAAs into live viruses.[32] Using hepatitis D virus, they were able to generate virus-like particles and live viruses containing pyrrolysine analog-modified L proteins using the genetic code expansion system in human hepatocytes. They also did not test the virus as a vaccine, but their paper highlights again the importance of site-specificity when incorporating unAAs into proteins. In testing the production of their VLPs, incorporation of unAA at position S280 in the L protein produced VLPs at a level slightly lower but comparable to WT, and not at all in the absence of unAA. However, when they used the same mutation site for the production of live viruses carrying the unAA modification, virus production was greatly reduced compared to WT. Further analysis showed modification at the S280 position suppressed virus infectivity, while modification of other sites did not. This experimental evidence demonstrates the potential of unAA modifications to alter protein function, which can also attenuate viruses.

Wang et al. introduced expanded genetic code technology for the purpose of making virus vaccines when they incorporated unnatural amino acids into HIV.[33] They reasoned that genetic code expansion could function as a genetic switch to control virus production, which is only on in the presence of unAA. Since the cells of the vaccine recipient would not have the orthogonal translation machinery or the unAA, production of virus protein would stop, and the virus would be unable to replicate. Using a virus rescue system for HIV, they incorporated premature amber stop codons into the gene for the HIV Gag protein. They then tested production of HIV virus in the presence of the orthogonal translation machinery and tyrosine analog unAAs. The result was very little production of virus. Virus production was measured by a p24 assay. Absorbance values for virus production in the presence of unAA were 0.453. While above the background absorbance of 0.001 in the absence of unAA, this was far less than the 6.181 absorbance units seen with wild type virus. Thinking the problem may have been readthrough of virus genes that naturally use the amber stop codon, the authors compared production of WT virus in the presence or absence of the orthogonal translation machinery and unAA. The production of WT virus was the same, with or without unAA, indicating the machinery was not interfering with production of the other virus proteins. Furthermore, they took an HIV-1 strain containing GFP and inserted an amber stop codon into GFP. They then compared GFP expression to the strain not containing the amber stop codon, and found that it was similar, indicating there was no problem with unAA incorporation. As it was possible the modification interfered with Gag protein function, the authors tested multiple mutation sites for unAA incorporation into Gag. While some sites gave

better virus production than others, all were greatly reduced compared to WT, indicating the low virus production may have been due to decreased Gag protein function following unAA insertion. To increase the presence of orthogonal translation machinery, Yuan et al. built upon the design of the mutant HIV viruses by generating HIV strains containing the orthogonal translation machinery in the virus genome.[34] However, this virus also showed reduced infectivity compared to WT. $TCID_{50}$ values for the mutant were $2.56x10^3$ and $5.20x10^7$ for WT virus. Lastly, in addition to amber stop codons, quadruplet codons have been used to incorporate unAAs into HIV proteins[35]. Chen et al. introduced a UAGA codon into the coding sequence of the p17 matrix protein of HIV and were able to detect virus production above background. The authors noted that the quadruplet codon may be preferable to the amber codon to produce safe infectious but replication incompetent vaccines. Amber codons have the potential to revert to sense codons by base substitution, which could allow for reversion back to infectious virus. However, reversion to sense codons from a quadruplet codon requires insertion or deletions, which are far less frequent compared to base substitutions and may make quadruplet codons a better choice for producing attenuated virus vaccines. Thus far, HIV virus produced by genetic code expansion technology has not been tested as a vaccine in an animal model.

In 2016, Si et al. were able to overcome many of the challenges of producing a live but replication incompetent virus using genetic code expansion technology.[36] They generated stable 293T cell lines expressing the orthogonal translation system for incorporation of the unAA NAEK. They then were able to rescue influenza viruses containing premature amber codons in different gene segments. The viruses could be

produced at titers similar to WT virus. However, the viruses containing only one premature termination codon were susceptible to reversion, and escape frequencies after 20 passages in the transgenic cells were high. This reversion is a real problem for using these viruses as vaccines, as the revertant viruses could be pathogenic. The authors then constructed a panel of viruses containing 1 to 8 total premature termination codons. Each extra amber stop codon reduced the escape frequency of the virus, though it also reduced the virus replication kinetics. The authors selected a virus containing 4 mutations in the virus gene NP, PA, PB1, and PB2 to use for the remaining studies, which they called PTC4A virus. The vaccine was shown to be safe and well tolerated by the animals. No weight loss was observed following vaccination with PTC4A. They showed that PTC4A generated antibody responses comparable to CAIV vaccination in mice, ferrets, and guinea pigs. The PTC4A viruses were 100% effective at preventing mortality against homologous challenge after 1 vaccine dose, and 100% effective at preventing weight loss after 2 doses. This is the first demonstration of the protective efficacy of a live-attenuated vaccine produced by genetic code expansion.

In summary, the ability of unAA mutations to break immune tolerance is now well established and has been reported in many different systems and proteins. However, we did not observe increased antibody responses to unAA modified HA. The mechanism behind breakage of immune tolerance raises the question of whether unAA modification is the best tool to use for vaccines designed to increase antibody responses to virus proteins. The presence of the unAA by itself is not sufficient to break immune tolerance. The interaction of the unAA-modified peptide with the immune system, specifically it's

interaction with MHC molecules, determines whether immune tolerance will be broken, and those interactions are dependent on which amino acid is mutated to unAA. The MHC restriction of the modifications makes translating findings from genetically identical mouse models to the clinic difficult. Future studies should address MHC restriction by testing vaccine candidates in multiple genetic backgrounds and with mutations at multiple amino acid positions. Guaba et al. have shown that the breakage of immune tolerance can be achieved by mutating to natural amino acids rather than unAAs. Additionally, while mutations in RANKL to pNO2Phe can be used to generate a vaccine against RANKL, Ko et al. have also shown that making natural amino acid mutations in RANKL is sufficient to generate increased antibody responses to RANKL compared to vaccination with WT protein[37]. Making substitutions to natural amino acids is simpler than unAA incorporation into proteins and seems sufficient for vaccine design.

MATERIALS AND METHODS

Cloning TAG mutations into the HA gene segment

Site-directed mutagenesis was performed using the HA gene of A/PR8/8/34 (H1N1) strain of influenza. Primers containing the TAG mutation were used to amplify the gene segments, after which overlapping PCR was performed to produce the full-length HA insert, which was ligated into either the pCAGGS plasmid for protein purification or the pDZ plasmid for VLP production using InFusion ligation (Takara Bio).

Prediction of HA epitope binding to MHC class II I-Ab allele

The Immune Epitope Database (IEDB) SMM-align program[38] was used to predict epitope binding to MHC class II I-A^b allele. The I-A^b allele was chosen as this is the only

allele of MHC class II found in C57BL/6 mice, which were the mice used for vaccination. Since the database does not include predictions for unAAs, we used Tyrosine mutations in the HA protein as substitutes for unAAs, since Tyrosine is most similar in structure to the aryl amino acids used in our study. Amino acid sequences were generated that contained a single mutation to Tyrosine at every amino acid position of the PR8 HA protein sequence (Uniprot ID P03452). These sequences were analyzed by the SMM-align program, and resulting peptides were given a percentile rank based on their predicted ability to bind to MHC class II I-A^b. Lower percentile rank indicates predicted increased binding to MHC class II I-A^b. A threshold percentile rank of 11 (the predicted binding of class-II-associated invariant chain) was chosen to determine predicted neo-epitopes.

Production of unAA-modified HA from 293T cells

12 T175 flasks of 293T cells were plated the day before transfection and media was replaced to 10mL OptiMEM on the day of transfection. 293T cells were PEI (polyethylenimine) transfected with 15ug of pCAGGS plasmid containing the TAG-mutant HA gene and 8ug pMAH-poly-eRF1 plasmid per flask. The HA gene contained a C-terminal 6xHis tag and trimerization domain and lacked a trans-membrane domain to allow for protein secretion. 6 hours after transfection, the transfection media was replaced with 20mL filter-sterilized 293T media containing 8mM of either 4BorPhe or pNO2Phe unAA. Cells were incubated at 37°C for 48 hours, then supernatants were collected for purification. Protein was purified with a 5mL HisTrap column (Cytiva). Eluted protein

was diafiltrated with a 10kD cut-off column (Amicon Ultracel 10K centrifugal filters) and washed twice with PBS. Protein concentration was determined by Bradford Assay.

Western Blots

Western Blots for HA protein were blocked with 5% milk in PBS containing 0.1% Tween 20, then blotted with PY102 HA mouse monoclonal antibody diluted 1:500 in blocking buffer. The antibody was a kind gift from Dr. Peter Palese at the Icahn School of Medicine at Mount Sinai. Blots were incubated with goat α-mouse IgG-HRP secondary antibody (Prometheus) diluted 1:10,000 in blocking buffer. Blots were visualized with BioRad ChemiDoc Touch Imaging system.

Mass Spec Sample Preparation and Sample Analysis

Vacuum-dried samples were resuspended in 50µL 100 mM Triethylammonium bicarbonate (TEAB, Sigma Aldrich, St. Louis, MO). Samples were reduced with the addition of 2.5µL of 500mM tris(2-carboxyethyl)phosphine (Thermo Scientific, Rockford, IL) and incubated at 37°C for 1 hour. Following incubation, 3µL of 500mM Iodoacetamide (Sigma Aldrich) was added. Samples were incubated in dark at room temperature for 1 hour. Samples were diluted with the addition of 250µL of water and 250µL of 100mM TEAB. 1µL (200ng) of trypsin/lysC mix (Promega, Madison, WI) was added and samples were digested at 37°C overnight (16 hours). 10µL of the digest was injected for LC-MS analysis. Liquid chromatography was performed on a Waters nanoAcquity UPLC in single-pump trapping mode with a Thermo PepMap RSLC C18 EASY-spray column (2µm, 100 Å, 75µm x 25cm) and a Waters Symmetry C18 trap column (5µm, 100 Å, 180µm x 20mm). Solvents used were A: water with 0.1% formic

acid and B: acetonitrile with 0.1% formic acid. Samples were separated at 300 nL/min with a 260-minute gradient starting at 3% B increasing to 30% B from 1 to 230 minutes, then to 85% B at 240 minutes hold for 10 minutes then back to 3% B in 10 minutes. Mass spectrometry data was acquired on a Thermo Orbitrap Fusion in data-dependent mode. A full scan was conducted using 60k resolution in the Orbitrap in positive mode. Precursors for MS2 were filtered by monoisotopic peak determination for peptides (this was set to small molecule for the 4-Boronophenylalanine mutant analysis), intensity threshold 5.0e3, charge state 2-7, and 60 second dynamic exclusion after 1 analysis with a mass tolerance of 10 ppm. Collisionally induced dissociation spectra were collected in MS2 at 35% energy and isolation window 1.6 m/z.

Mass Spec Data Analysis

Results were searched individually in Proteome Discoverer 2.2 (Thermo Scientific) against a custom FASTA database with the his-tagged hemagglutinin sequence. The precursor mass tolerance was set to 10 ppm and fragment mass tolerance to 0.6 Da. Fixed modifications were carbamidomethyl (Cys +57.021 Da), and dynamic modifications included methionine oxidation (+15.995 Da) N-terminal acetylation (+42.011 Da), and synthetic amino acid substitutions Y->4Bor (+28.012 Da) and S->pNO2 (+105.021 Da). Results were filtered to a strict 1% false discovery rate.

Influenza VLP rescues and expansions

Influenza VLP rescues were performed similar to previously described influenza virus rescue procedures, with the following modifications. Since the HA gene segment contained a premature TAG stop codon, a helper HA-pCAGGS plasmid was included in

the rescue plasmid mix to supply the HA protein, while the mutant HA-pDZ plasmid provided the viral RNA. Since the resulting VLPs contained HA genes with premature TAG stop codons, the VLPs were expanded in MDCK cells constitutively expressing HA protein. The resulting VLPs contained mutant HA gene segments and WT HA protein.

Plaque Assays

Influenza virus plaque assays were performed as previously described[39]. Influenza viruses or VLPs were serially diluted 10-fold in PBS/BSA containing Penn/Strep. 250µL of virus dilution was added to a confluent monolayer of MDCK cells in a 12 well plate, and virus was allowed to infect cells for 1 hour at 37°C. Virus dilutions were replaced with Post-Transfection Media containing 3.7% Avicell and left at 37°C for 48 hours. Cells were fixed with 1mL of 3.7% formaldehyde for 1 hour at room temperature and stained with 1% crystal violet solution.

Mouse Vaccinations

Six-week-old female C57BL/6 mice were purchased from Jackson Labs and used for vaccinations. HA protein vaccine was diluted in PBS and added to equal volume of Addavax adjuvant. Mice were injected intramuscularly with 50µL of vaccine per injection in both back legs, 15ug per mouse, 5 mice per group. Retro-orbital blood was collected and centrifuged for 10 minutes at 10,000g to separate out sera. Sera was collected and stored at -80°C for ELISAs.

Enzyme-Linked Immunosorbent Assays (ELISAs)

Purified influenza virion was diluted to 5µg/mL and was used to coat the bottom of maxisorp 96 well ELISA plate (Thermofisher). Virus was allowed to bind to the plate

overnight at 4°C, then the plate was blocked with blocking buffer (1% milk in PBST). Sera was diluted 1:100 in blocking buffer, then serially diluted 3-fold. Plates were incubated with sera for 2 hours, after which the plates were washed 3 times with blocking buffer. Plates were incubated with goat α-mouse IgG-HRP secondary antibody (Prometheus) diluted 1:3000 in blocking buffer and incubated for 1 hour. Plates were washed 3 times with blocking buffer, then incubated with 100µL of SigmaFast OPD substrate for 30 minutes. Substrate reaction was stopped with 25µL of 3M HCl, and absorbance was measured at 450nm with a Luminometer plate reader (Promega).

Statistical Analysis

Statistical analysis was performed with GraphPad Prism 9.2.0 software. Student T-tests were used to compare ELISA values at specific dilutions.

REFERENCES

1. Benzer, S. & Champe, S. P. A Change From Nonsense To Sense In The Genetic Code. *Proc Natl Acad Sci U S A* **48**, 1114–1121 (1962).

2. Garen, A., Garen, S. & Wilhelm, R. C. Suppressor genes for nonsense mutations: I. The Su-1, Su-2 and Su-3 genes of Escherichia coli. *Journal of Molecular Biology* **14**, 167–178 (1965).

3. Weigert, M. G. & Garen, A. Amino acid substitutions resulting from suppression of nonsense mutations: I. Serine insertion by the Su-1 suppressor gene. *Journal of Molecular Biology* **12**, 448–455 (1965).

4. Hecht, S. M., Alford, B. L., Kuroda, Y. & Kitano, S. "Chemical aminoacylation" of tRNA's. *Journal of Biological Chemistry* **253**, 4517–4520 (1978).

5. Wang, L., Brock, A., Herberich, B. & Schultz, P. G. Expanding the Genetic Code of Escherichia coli. *Science* **292**, 498–500 (2001).

6. Xie, J. & Schultz, P. G. A chemical toolkit for proteins — an expanded genetic code. *Nature Reviews Molecular Cell Biology* **7**, 775–782 (2006).

7. Liu, C. C. & Schultz, P. G. Adding New Chemistries to the Genetic Code. *Annu. Rev. Biochem.* **79**, 413–444 (2010).

8. Young, D. D. & Schultz, P. G. Playing with the Molecules of Life. *ACS Chem. Biol.* **13**, 854–870 (2018).

9. Wang, L. & Schultz, P. G. A general approach for the generation of orthogonal tRNAs. *Chemistry & Biology* **8**, 883–890 (2001).

10. Wan, W., Tharp, J. M. & Liu, W. R. Pyrrolysyl-tRNA synthetase: An ordinary enzyme but an outstanding genetic code expansion tool. *Biochimica et Biophysica Acta (BBA) - Proteins and Proteomics* **1844**, 1059–1070 (2014).

11. Johnson, D. B. F. *et al.* RF1 knockout allows ribosomal incorporation of unnatural amino acids at multiple sites. *Nature Chemical Biology* **7**, 779–786 (2011).

12. Schmied, W. H., Elsässer, S. J., Uttamapinant, C. & Chin, J. W. Efficient Multisite Unnatural Amino Acid Incorporation in Mammalian Cells via Optimized Pyrrolysyl tRNA Synthetase/tRNA Expression and Engineered eRF1. *Journal of the American Chemical Society* **136**, 15577–15583 (2014).

13. Lajoie, M. J. *et al.* Genomically recoded organisms expand biological functions. *Science* **342**, 357–360 (2013).

14. Sakamoto, K. *et al.* Site-specific incorporation of an unnatural amino acid into proteins in mammalian cells. *Nucleic Acids Research* **30**, 4692–4699 (2002).

15. Wang, Q. & Wang, L. Genetic Incorporation of Unnatural Amino Acids into Proteins in Yeast. *Methods Mol Biol* **794**, 199–213 (2012).

16. Riddle, D. L. & Carbon, J. Frameshift Suppression: a Nucleotide Addition in the Anticodon of a Glycine Transfer RNA. *Nature New Biology* **242**, 230–234 (1973).

17. Niu, W., Schultz, P. G. & Guo, J. An Expanded Genetic Code in Mammalian Cells with a Functional Quadruplet Codon. *ACS Chem. Biol.* **8**, 1640–1645 (2013).

18. Neumann, H., Wang, K., Davis, L., Garcia-Alai, M. & Chin, J. W. Encoding multiple unnatural amino acids via evolution of a quadruplet-decoding ribosome. *Nature* **464**, 441–444 (2010).

19. Grünewald, J. *et al.* Immunochemical termination of self-tolerance. *PNAS* **105**, 11276–11280 (2008).

20. Grünewald, J. *et al.* Mechanistic studies of the immunochemical termination of self-tolerance with unnatural amino acids. *Proc Natl Acad Sci U S A* **106**, 4337–4342 (2009).

21. Tong, Y., Zhong, S., Shan, Z., Yao, W. & Tian, H. A novel human anti-BAFF neutralizing monoclonal antibody derived from in vitro immunization. *Biomedicine & Pharmacotherapy* **119**, 109430 (2019).

22. Li, F. *et al.* A new vaccine targeting RANKL, prepared by incorporation of an unnatural Amino acid into RANKL, prevents OVX-induced bone loss in mice. *Biochemical and Biophysical Research Communications* **499**, 648–654 (2018).

23. Wu, T. *et al.* A novel recombinant RANKL vaccine prepared by incorporation of an unnatural amino acid into RANKL and its preventive effect in a murine model of collagen-induced arthritis. *International Immunopharmacology* **64**, 326–332 (2018).

24. Kessel, C. *et al.* A Single Functional Group Substitution in C5a Breaks B Cell and T Cell Tolerance and Protects Against Experimental Arthritis. *Arthritis & Rheumatology* **66**, 610–621 (2014).

25. Tian, H. *et al.* Nitrated T helper cell epitopes enhance the immunogenicity of HER2 vaccine and induce anti-tumor immunity. *Cancer Letters* **430**, 79–87 (2018).

26. Gauba, V. *et al.* Loss of CD4 T-cell–dependent tolerance to proteins with modified amino acids. *Proc Natl Acad Sci U S A* **108**, 12821–12826 (2011).

27. Russell, R. J., Gamblin, S. J. & Skehel, J. J. Influenza glycoproteins: Hemagglutinin and neuraminidase. in *Textbook of Influenza* (eds. Webster, R. G., Monto, A. S., Braciale, T. J. & Lamb, R. A.) 67–100 (John Wiley & Sons, Ltd, 2013). doi:10.1002/9781118636817.ch5.

28. Chen, Z., Ren, W., Wright, Q. E. & Ai, H. Genetically Encoded Fluorescent Probe for the Selective Detection of Peroxynitrite. *J. Am. Chem. Soc.* **135**, 14940–14943 (2013).

29. Wedemayer, G. J., Wang, L. H., Patten, P. A., Schultz, P. G. & Stevens, R. C. Crystal structures of the free and liganded form of an esterolytic catalytic antibody11Edited by I. A. Wilson. *Journal of Molecular Biology* **268**, 390–400 (1997).

30. An, Y., Bloom, J. W. G. & Wheeler, S. E. Quantifying the π-Stacking Interactions in Nitroarene Binding Sites of Proteins. *J. Phys. Chem. B* **119**, 14441–14450 (2015).

31. Jiang, L. *et al.* Efficient Acquisition of Fully Human Antibody Genes against Self-Proteins by Sorting Single B Cells Stimulated with Vaccines Based on Nitrated T Helper Cell Epitopes. *Journal of Immunology Research* **2019**, e7914326 (2019).

32. Lin, S. *et al.* Site-Specific Engineering of Chemical Functionalities on the Surface of Live Hepatitis D Virus. *Angewandte Chemie International Edition* **52**, 13970–13974 (2013).

33. Wang, N. *et al.* Construction of a Live-Attenuated HIV-1 Vaccine through Genetic Code Expansion. *Angew Chem Int Ed Engl* **53**, 4867–4871 (2014).

34. Yuan, Z. *et al.* Controlling Multicycle Replication of Live-Attenuated HIV-1 Using an Unnatural Genetic Switch. *ACS Synthetic Biology* **6**, 721–731 (2017).

35. Chen, Y. *et al.* Controlling the Replication of a Genomically Recoded HIV-1 with a Functional Quadruplet Codon in Mammalian Cells. *ACS Synth. Biol.* **7**, 1612–1617 (2018).

36. Si, L. *et al.* Generation of influenza A viruses as live but replication-incompetent virus vaccines -Suplemental. *Science* **354**, 1170–1173 (2016).

37. Ko, Y. J. *et al.* A novel modified RANKL variant can prevent osteoporosis by acting as a vaccine and an inhibitor. *Clin Transl Med* **11**, (2021).

38. Nielsen, M., Lundegaard, C. & Lund, O. Prediction of MHC class II binding affinity using SMM-align, a novel stabilization matrix alignment method. *BMC Bioinformatics* **8**, 238 (2007).

39. Anchisi, S., Gonçalves, A. R., Mazel-Sanchez, B., Cordey, S. & Schmolke, M. Influenza A Virus Genetic Tools: From Clinical Sample to Molecular Clone. in *Influenza Virus: Methods and Protocols* (ed. Yamauchi, Y.) 33–58 (Springer, 2018). doi:10.1007/978-1-4939-8678-1_3.

Chapter 4:
A Chimeric Influenza Virus NP And SARS-CoV-2 Spike RBD Protein Vaccine for Increased Immunity to Spike

ABSTRACT

Vaccination remains the most effective intervention to prevent COVID-19 morbidity and mortality. Antibodies targeting the spike protein receptor-binding domain (RBD) can neutralize virus particles. SARS-CoV-2 vaccines that generate strong neutralizing antibodies against the spike RBD domain are therefore highly desirable. Authorized coronavirus vaccines targeting spike produce high neutralizing antibody titers against SARS-CoV-2. However, these vaccines require at least two doses to produce high titers of neutralizing antibodies. The current SARS-CoV-2 vaccines have low efficacy against disease following a single vaccination, and individuals remain vulnerable to severe disease in between the first and second vaccinations. We therefore wished to design a vaccine candidate that would produce increased protective immune responses following the first vaccine dose. We hypothesized that antibodies against the RBD domain of the SARS-CoV-2 coronavirus spike protein could be increased by drawing upon immunity to a previous infection. We generated a fusion protein containing the NP protein of the PR8 strain of influenza A virus and the RBD domain of SARS-CoV-2 coronavirus. Mice with or without previous immunity to PR8 were then vaccinated with the NP/RBD fusion protein. Two weeks after vaccination, sera antibodies against the spike protein were checked by ELISA. Among mice that received the NP/RBD vaccine, we observed significantly increased antibody responses against spike in mice with previous immunity to PR8 compared to mice without previous immunity to PR8 at this

timepoint. A chimeric NP/RBD protein vaccine has the potential to provide increased protection against COVID-19 following a single dose of vaccine, and this vaccine strategy is highly valuable in a pandemic scenario where it is desirable to generate protective immunity in the population as quickly as possible.

INTRODUCTION

Since the start of the 21st century, the world has seen the emergence of three novel human coronaviruses. SARS-CoV-1 was first identified in China in November 2002, and MERS-CoV was identified in June of 2012. Then at the end of 2019, SARS-CoV-2 was identified as a novel human coronavirus in China. The rapid spread of the virus quickly caused a global pandemic on a scale not seen since the 1918 Influenza pandemic. To date, SARS-CoV-2 has killed over 6 million people globally and is the cause of countless cases of disease (https://covid19.who.int/). The rollout of effective vaccines against the virus has greatly reduced the overall burden of Coronavirus disease 2019 (COVID-19) morbidity and mortality. However, the emergence of more transmissible virus variants capable of evading vaccine-derived immune responses has driven new surges of disease[1–6]. It is therefore likely that SARS-CoV-2 infections will persist for some time, and vaccines will therefore continue to be needed to combat the virus. Additionally, the emergence of three novel human coronaviruses in less than two decades makes it likely another novel human coronavirus will emerge in the future. Vaccine strategies for future pandemic scenarios are therefore an important area of research and development.

The main vaccine strategies against SARS-CoV-2 target the virus spike glycoprotein. Spike is the main surface antigen of SARS-CoV-2 that exists as a trimer on the surface of the virus particle, with each monomer consisting of a protein approximately 180kD in size made up of S1 and S2 subunits[7–9]. During virus infection, spike binds to ACE2 receptors on the surface of host cells. Binding to ACE2 triggers internalization of the virus into the cell, and also triggers conformational changes in the spike protein to allow for fusion of the virus envelope with the host membrane, allowing for release of the virus genome into the cytoplasm. Within the S1 subunit of the spike protein is the Receptor Binding Domain (RBD), which contains the contact points for spike binding to ACE2[10]. Vaccines targeting the RBD domain of spike produce RBD-specific antibodies in mice, non-human primates, and humans. These RBD-specific antibodies can neutralize SARS-CoV-2 viruses and are protective in disease models[11–19]. RBD-based vaccines have been authorized for use in humans. The ZF2001 vaccine has received emergency use authorization in China and Uzbekistan, and the Corbevax vaccine has been approved for use in India.[20–22]

While the current vaccine strategies against SARS-CoV-2 have been remarkably effective at controlling the virus, one of the limitations of current vaccines is poor immune responses from a single vaccine dose. Neutralizing antibodies against WA1 strain of SARS-CoV-2 were detected in only 79% of individuals vaccinated with the Moderna mRNA-1273 vaccine at 4 weeks after a single dose, compared to 100% of individuals 2 weeks after a second dose[23]. Similarly, neutralizing antibody titers against SARS-CoV-2 were detected in only 73% of individuals vaccinated with 30ug of

BNT162b1 at 3 weeks after a single dose, compared with 100% of individuals 2 weeks after a second dose[24], and this difference was also observed with the BNT162b2 vaccine[25]. In a study of non-human primates vaccinated with the mRNA-1273 vaccine, neutralization assays with a pseudotyped lentivirus reporter showed 50% inhibitory dilution (ID50) geometric mean titers (GMT) of 63 at 4 weeks after the first vaccination, compared with GMT of 103 by 4 weeks after the second vaccination[26]. These lower antibody responses are associated with lower protection against disease. A study in Qatar found 83% effectiveness of the mRNA-1273 vaccine in 2021 against severe disease and death among individuals receiving only one dose of vaccine, compared to 97% vaccine effectiveness among individuals receiving two doses of vaccine[27]. A study of vaccine effectiveness against emerging variants found that vaccine effectiveness against symptomatic disease following infection with the Delta variant was only 30.7% among individuals who received a single dose of the BNT162b2 vaccine, while vaccine effectiveness was 79.6% among individuals who received two doses. This study also observed only 30.0% vaccine effectiveness among individuals who received a single dose of the ChAdOx1 vaccine, while vaccine effectiveness was 67% among individuals who received a second dose of the ChAdOx1 vaccine.[28] Taken together, these studies point to a weakness of COVID-19 vaccines during the period after a single vaccine dose.

A limiting factor in the production of neutralizing antibodies following vaccination is a lack of expanded spike-specific helper T cells. Activation of antigen-specific B cells requires T cell help (see Figure 1 in Chapter 1)[29–31]. Following recognition of antigen by the B cell receptor, the antigen is internalized and processed

into antigenic peptides in the lysosome. Antigenic peptides are displayed on the surface of the B cell bound to MHC class II molecules for presentation to helper T cells. Recognition of antigenic peptide bound to MHC class II by T cells with antigen-specific T cell receptors (TCRs) leads to activation of the T cell, which provides stimulatory signals to the B cell, leading to B cell activation and antibody secretion. T and B cell activation leads to clonal expansion of both cell types. The majority of expanded cells become effector cells, while a subset become memory cells. Individuals encountering a novel antigen have naïve populations of both antigen-specific B and T cells, but these populations have not expanded yet. Therefore, the number of spike-specific helper T cells available to provide help to spike-specific B cells is low at the point of first exposure to antigen.

We hypothesized that these limitations could be overcome by drawing on immunity to a previous immunization to increase antibody responses to spike. Specifically, we hypothesized antibody responses to spike could be increased in animals with preexisting immunity to influenza virus by vaccinating with a fusion protein containing the influenza NP protein and the SARS-CoV-2 RBD protein. Theoretically, spike-specific B cells recognizing the NP/RBD vaccine would be able to present both NP and RBD antigenic peptides, which would allow the B cell to derive help from a population of previously expanded NP-specific helper T cells. Additionally, we theorized that NP-specific antibodies from a previous immunization would be able to bind to the NP/RBD protein. NP specific antibodies could then facilitate the Fc receptor-mediated uptake of NP/RBD by antigen-presenting cells (APCs), which would allow for faster

presentation of antigen to RBD-specific helper T cells. When we vaccinated mice with or without previous immunity to influenza virus, we found NP/RBD vaccination produced higher spike-specific antibodies in mice with previous influenza immunity compared to mice without previous influenza immunity 14 days post-vaccination. These results represent a novel vaccine strategy with important implications for the future of pandemic vaccines.

RESULTS

Expression of NP/RBD and predicted structure

We used the baculovirus/SF9 cell expression system to express our chimeric NP/RBD protein vaccine. The gene for the chimeric protein was cloned into the pFastBac plasmid for baculovirus rescue and contained an N-terminal secretion signal from the gene for hemagglutinin protein of influenza virus WSN strain. PR8 influenza NP protein was included adjacent to the C terminal end of the signal peptide and was fused to the receptor binding domain (RBD) domain of the WA1 strain of SARS-CoV-2 coronavirus (amino acids 330-528). A 6xHis tag was included at the C terminal end for protein purification with a 5mL Ni column (Figure 13A). The size of the purified protein was verified by Coomassie Blue stain and Western Blot with an RBD-specific antibody (Figure 13B). We also wanted to have some indication that the NP and RBD proteins maintained their shape after fusing the proteins together. We used the Alphafold program to predict the structure of the NP/RBD protein (Figure 13C)[32]. The predicted protein structure showed NP and RBD folding separately, with RBD maintaining its original

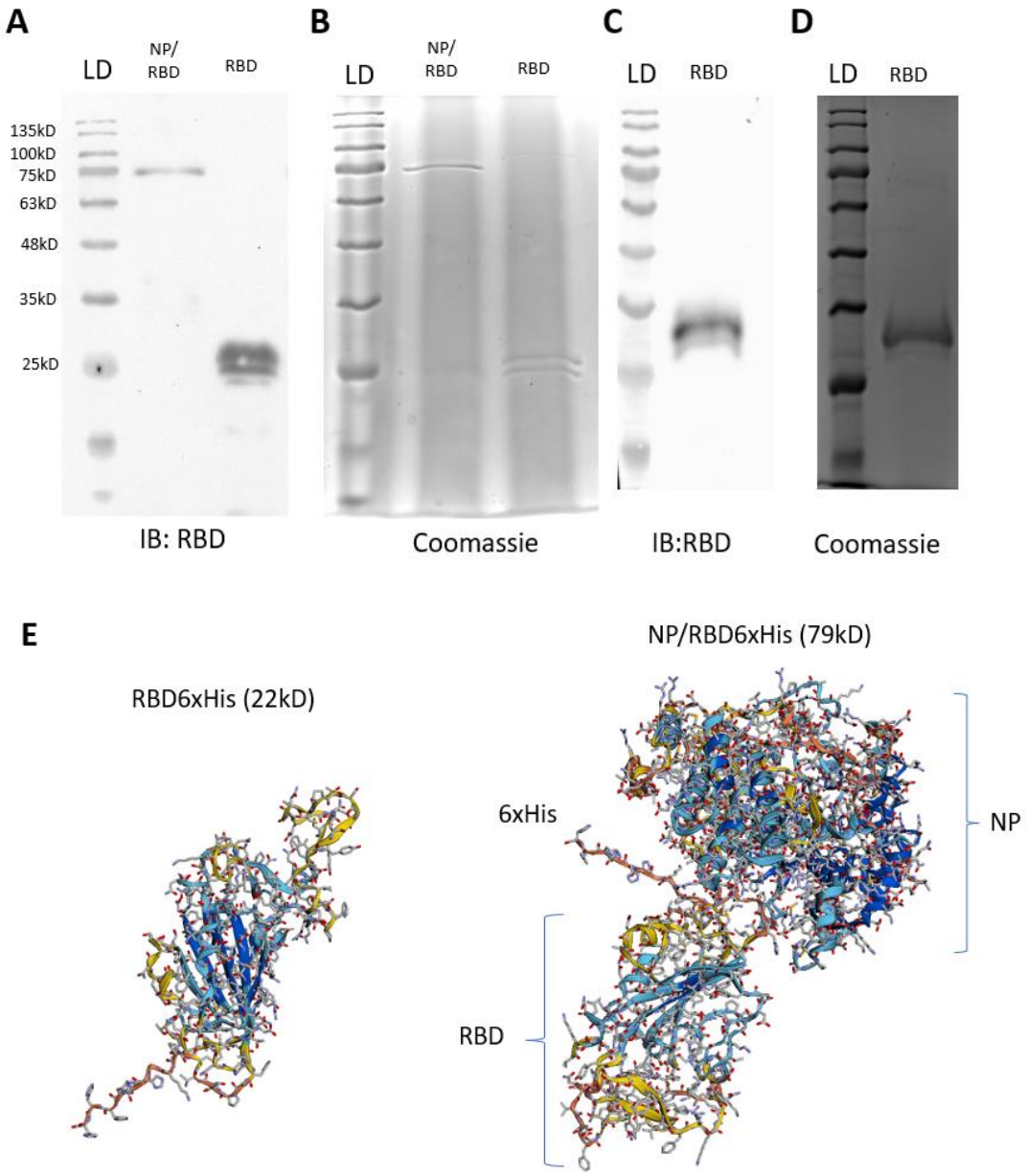

Figure 13. Purification and structure of NP/RBD protein and RBD protein. (A) Western Blot of purified NP/RBD6xHis (1ug) and RBD6xHis amino acids 330-528 (0.28ug). **(B)** Coomassie stain of purified NP/RBD6xHis (1ug) and RBD6xHis amino acids 330-528 (1ug). **(C)** Western Blot of purified RBD6xHis amino acids 319-528 (0.3ug). **(D)** Coomassie stain of purified RBD6xHis amino acids 319-528 (1ug). **(E)** AlphaFold predicted structure of RBD6xHis and NP/RBD6xHis.

shape. After confirming the purity of the purified NP/RBD protein, we proceed to test its immunogenicity in a mouse model.

Antibody responses to vaccination with NP/RBD in mice previously infected with PR8

To establish pre-existing immunity to PR8 influenza virus, C57BL/6 mice were infected with 100PFU of virus or PBS and allowed to recover. 16 days post-infection, sera was collected, and the mice were vaccinated with equal molar amount of either the NP/RBD protein, RBD protein (amino acids 330-528), or PBS (Figure 14A). On the day of vaccination, the mice had strong NP antibody responses to PR8 infection, and these antibody responses were found to also bind the NP/RBD fusion protein (Figure 14B,C). Sera was collected 14 days post vaccination, and IgG antibody responses to purified WA1 SARS-CoV-2 spike protein (amino acids 22-1208) were determined by ELISA. The NP/RBD protein produced strong antibody responses to spike, while the purified RBD protein was poorly immunogenic. Antibody responses to spike were greatly increased in the mice previously infected with PR8 compared to mock infected mice (Figure 14D,E). This increase was observed when the ELISA was repeated with purified RBD as the ELISA antigen (Figure 14F). We further tested the ability of the antibodies elicited by our NP/RBD vaccine to neutralize live WA1 SARS-CoV-2 virus. Antibodies from mice with pre-existing PR8 immunity neutralized SARS-CoV-2 virus to a significantly greater extent than mice without pre-existing PR8 immunity (Figure 14G). Mice with pre-existing immunity to PR8 were boosted with purified RBD protein (amino acids 330-528). Antibodies levels from sera and nasal washes were analyzed with

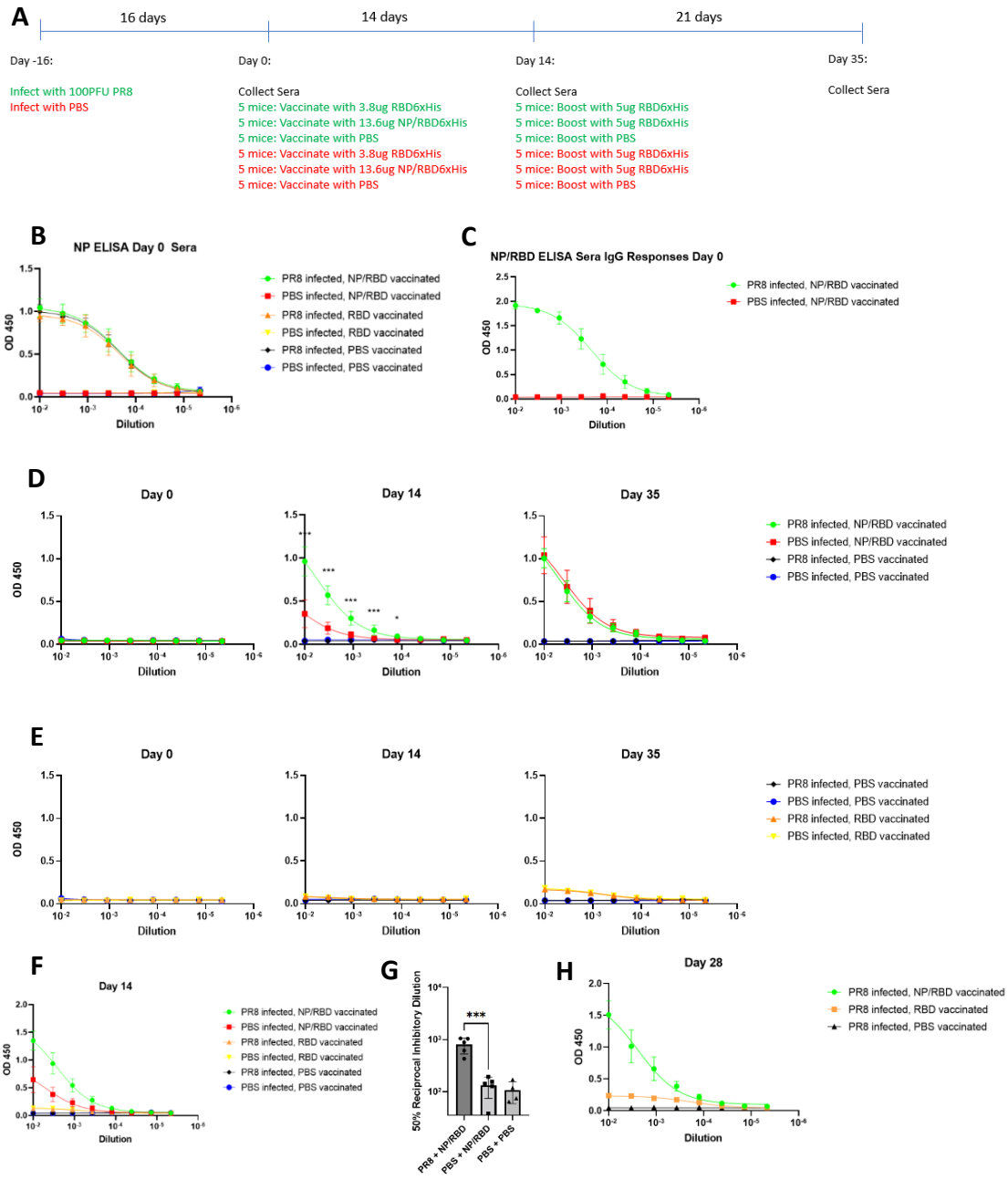

Figure 14. Antibody responses to vaccination with NP/RBD in mice previously infected with PR8. (A) Mouse vaccination schedule. **(B)** ELISA of sera PR8 NP IgG antibody responses on Day 0. **(C)** ELISA of sera NP/RBD IgG antibody responses on Day 0. **(D)** ELISA of sera spike IgG antibody responses on Day 14 post vaccination with NP/RBD or PBS. **(E)** ELISA of sera spike IgG antibody responses on Day 14 post vaccination with NP/RBD or PBS. **(F)** ELISA of sera RBD IgG antibody responses on Day 14. **(G)** Neutralization of WA1 SARS-CoV-2 with sera from Day 14 post-vaccination. **(H)** ELISA of sera spike IgG antibody response on Day 28.

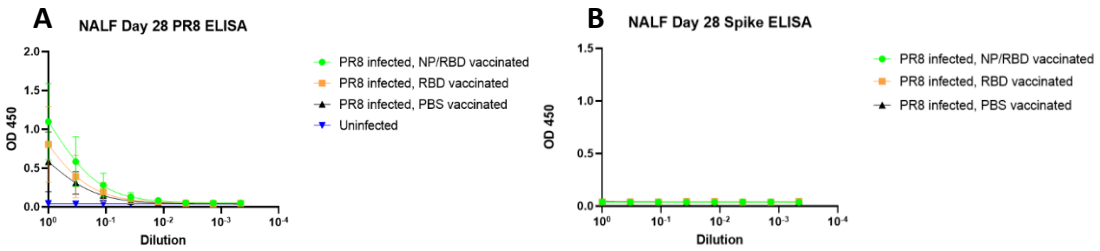

Figure 15. Mucosal IgA Antibody responses to vaccination with NP/RBD in mice previously infected with PR8. (A) ELISA of nasal wash PR8 IgA antibody responses on Day 28 post-vaccination. **(B)** ELISA of nasal wash spike IgA antibody responses on Day 28 post-vaccination.

samples taken 14 days post-boost (day 28 after initial vaccination). Antibody responses to spike remained high (Figures 14H). IgA responses to spike in the nasal washes were not observed, though the mice did have detectable IgA responses to PR8 virus (Figure 15B, C). This was expected, since our vaccine was delivered intramuscularly, and the mice had been infected with PR8 virus. We further examined the spike-specific IgG responses from 3 weeks post boost with RBD. Spike-specific antibodies were again high in the mice originally vaccinated with NP/RBD. However, antibodies to spike were similar in the mice with or without previous immunity to PR8 (Figure 14D,E). In summary, these results demonstrate the ability of NP/RBD to provide a neutralizing antibody response, and this ability is increased in the presence of pre-existing immunity to PR8 at an early timepoint.

Antibody responses to vaccination with NP/RBD in mice previously vaccinated with UV-inactivated PR8

One possible explanation for the increased antibody responses to spike observed in Figure 14 was that overall immune activation from the virus infection was driving the

increase in antibody production. The increased cytokine production and priming of the innate immune system during infection may have set up the adaptive immune system to respond faster to our NP/RBD vaccine. If this was the case, this would mean our increased antibody responses were not due to a specific interaction of adaptive immune responses to PR8 with our NP/RBD vaccine. To rule out non-specific immune activation as the cause of our observed increased immunity in Figure 14, we established pre-existing immunity in mice to either PR8 or the B/Victoria/2/1987 strain of Influenza B virus (IBV) by vaccinating mice with equal microgram amounts of UV-inactivated purified virus (Figure 16A). 16 days post-vaccination with inactivated virus, mice were vaccinated with either NP/RBD protein or PBS. Mice were boosted 14 days post-vaccination with purified RBD protein (amino acids 330-528), and sera were collected on Day 0, Day 14, and Day 35 after initial vaccination. IBV NP and PR8 NP protein share only approximately 30% amino acid identity, and no IgG antibodies to PR8 NP were detected in IBV vaccinated mice at Day 0 (Figure 16B). We again observed that antibody responses to spike were significantly elevated in mice that had pre-existing immunity to PR8 at Day 14, but not in mice that had pre-existing immunity to IBV or PBS (Figure 16C). Sike antibody responses at Day 35 post-vaccination were again similar between NP/RBD vaccine group (Figure 16D). These results demonstrate that NP/RBD vaccination can draw on immunity established by a specific previous exposure to influenza virus to increase the speed of antibody responses to spike at an early timepoint post-vaccination.

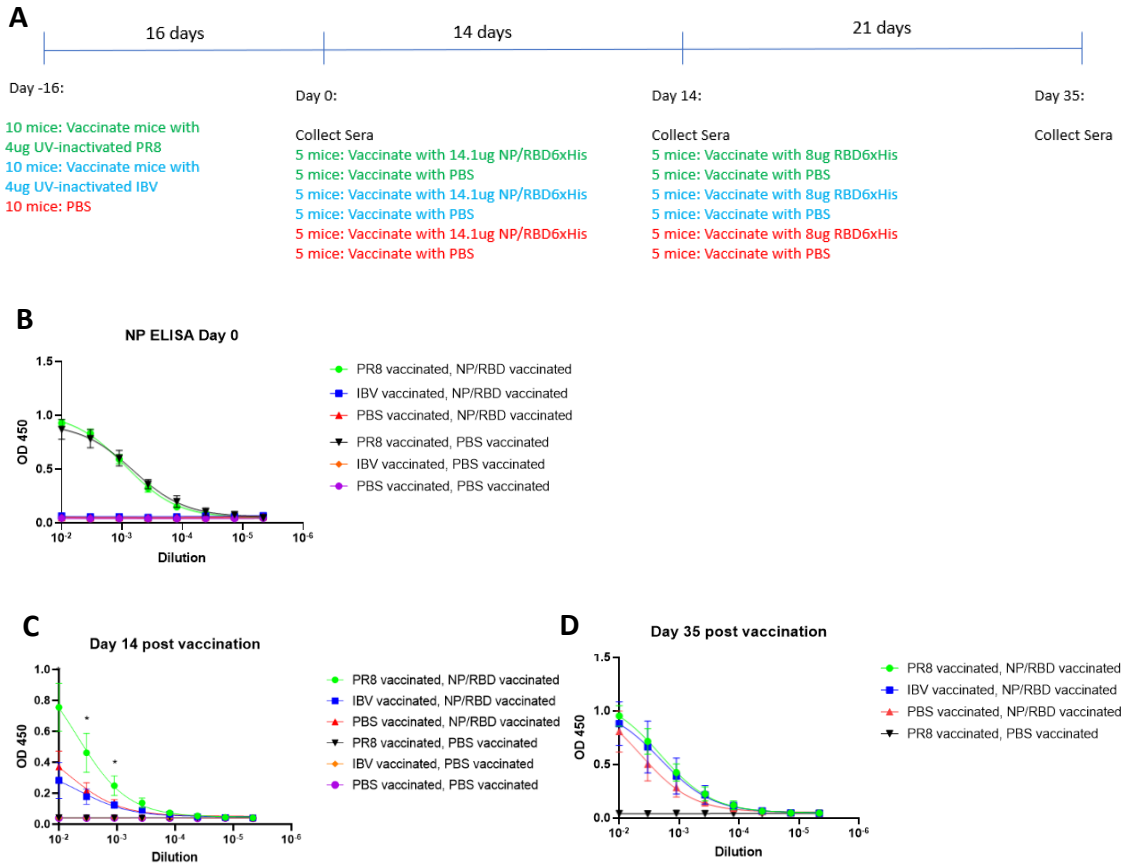

Figure 16. Antibody responses to vaccination with NP/RBD in mice previously vaccinated with UV-inactivated PR8. (A) Mouse vaccination schedule. **(B)** PR8 NP ELISA with sera from Day 0. **(C)** Spike ELISA with sera from Day 14. **(D)** Spike ELISA with sera from Day 35.

Splenocyte stimulations from mice vaccinated with NP/RBD

T cell responses are an important protective adaptive immune response in addition to antibodies. We therefore wished to check if our vaccine regimen with NP/RBD produced RBD-specific T cell responses. Mice that were vaccinated with either NP/RBD or RBD followed by boosting with RBD were sacrificed 2 weeks after boost and spleens were collected for splenocyte stimulation assays (Figure 17A). RBD protein was used to stimulate splenocytes, and IFNγ production was measured by ELISA as an output for T

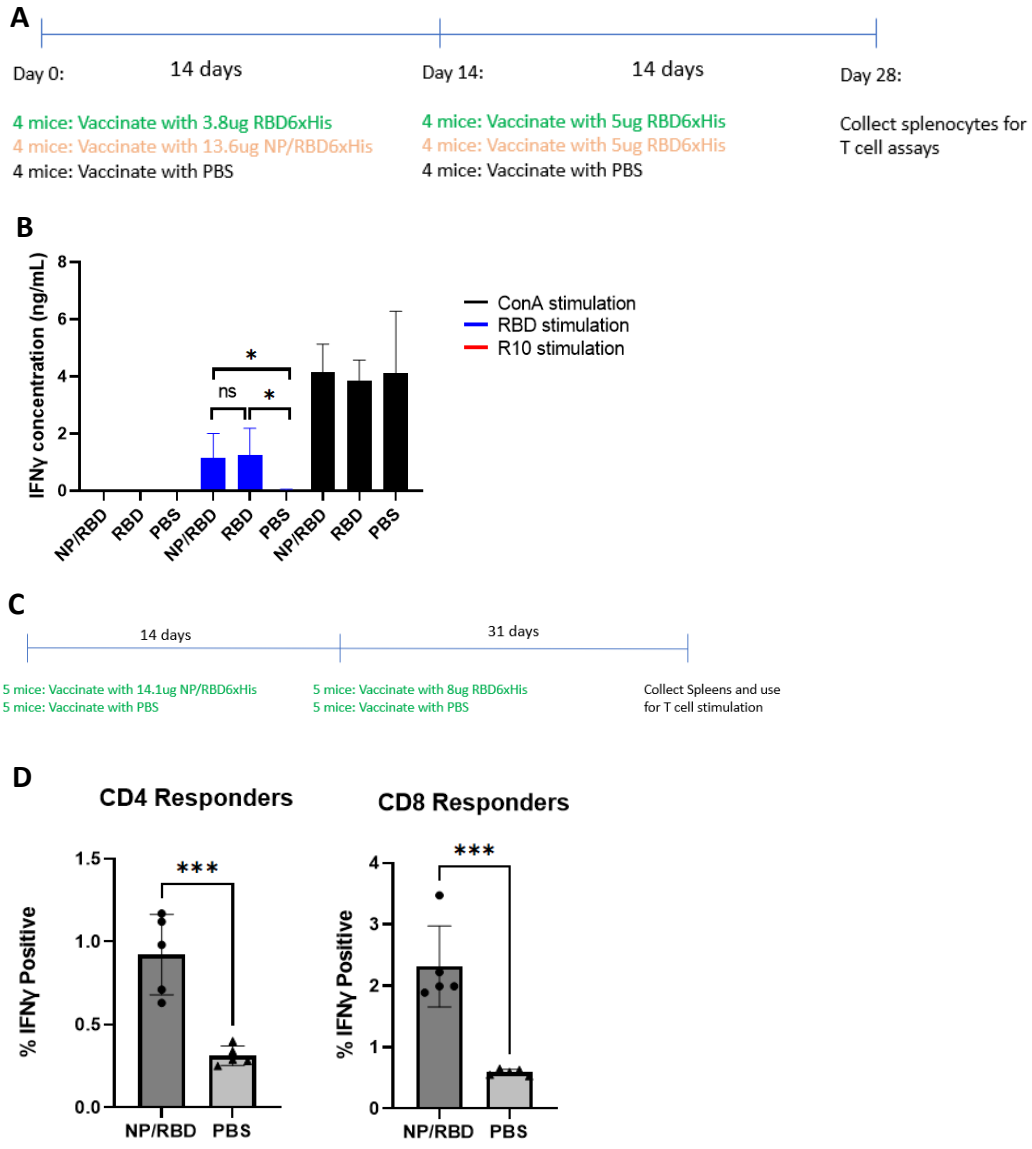

Figure 17. T cell responses to vaccination with NP/RBD and boosting with RBD. (A) Mouse vaccination schedule for data in (B). (B) IFNγ ELISA with the supernatants from splenocytes taken from Day 28, stimulated with RBD, ConA as a positive control, or R10 media as a negative control. (C) Mouse vaccination schedule for data in (D). (D) Intracellular cytokine staining after RBD stimulation of CD4 and CD8 positive lymphocytes for IFNγ in mice vaccinated with either NP/RBD and boosted with RBD or mice vaccinated with PBS.

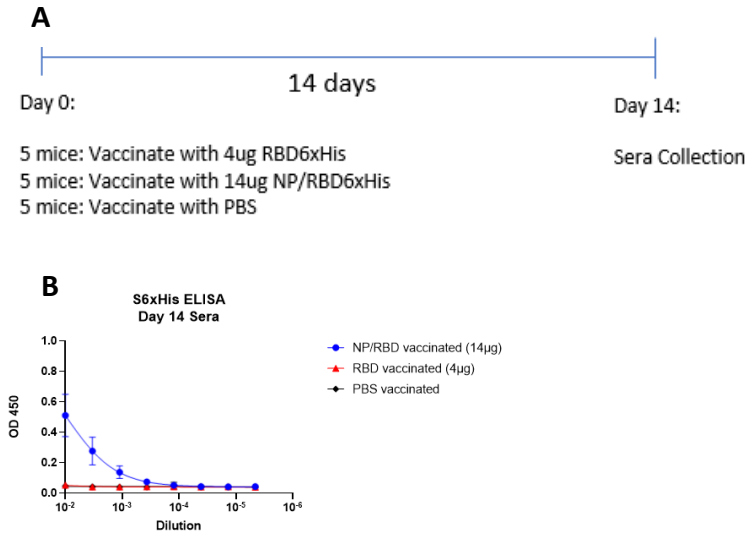

Figure 18. Comparison of antibody responses following vaccination with NP/RBD and RBD (amino acids 319-528). (A) Mouse vaccination schedule. **(B)** Spike ELISA with sera collected 14 days after vaccination.

cell activation. Both vaccine groups showed comparable splenocyte activation following stimulation with RBD over unvaccinated mice (Figure 17B). In a separate experiment to check RBD-specific T cell responses, mice vaccinated with NP/RBD followed by boosting with RBD were sacrificed 31 days after boost (Figure 17C). RBD protein was used to stimulate splenocytes, and IFNγ production was measured by intracellular cytokine staining. Flow cytometric analysis of stained lymphocytes showed significantly increased RBD-specific CD4 and CD8 positive cells in mice vaccinated with NP/RBD compared to unvaccinated mice (Figure 17D, Supplemental Figure 4). Taken together, these results demonstrate that a vaccine strategy that utilizes NP/RBD is capable of producing RBD-specific T cell responses.

Comparison of sera antibody responses in mice vaccinated with NP/RBD or RBD protein

We speculated that the poor immunogenicity of the RBD may have been due to its poor glycosylation owing to the inclusion of a glycosylation site at amino acid position 331, very close to the N-terminus of our protein[33,34]. We therefore purified a second version of the RBD protein containing amino acids 319-528 (Figure 12C,D). Mice were vaccinated with either NP/RBD or RBD (aa 319-528) protein at equal molar amounts of RBD (Figure 18A). 14 days post-vaccination, sera was collected and IgG antibody responses to spike were determined by ELISA. The NP/RBD protein again produced greatly increased antibody responses to spike, while the purified RBD protein was again not immunogenic (Figure 18B). In summary, vaccination with the NP/RBD protein shows superior immunogenicity compared to vaccination with RBD alone.

DISCUSSION

We devised a vaccine strategy to utilize pre-existing immunity to influenza virus with the goal of increasing antibody responses to SARS-CoV-2. We purified a fusion protein of the influenza NP protein and SARS-CoV-2 RBD protein as a vaccine candidate against SARS-CoV-2. Vaccination with the NP/RBD protein produced high levels of spike-specific antibodies after a single dose, and antibodies were significantly higher in mice with pre-existing immunity to influenza virus at this time point. Vaccination with NP/RBD also produced significantly higher antibody responses compared to equal-molar vaccinations with RBD protein, which was not greatly immunogenic under our vaccination conditions. Antibody responses to NP/RBD in mice with pre-existing immunity to influenza showed greater neutralization of SARS-CoV-2

virus than antibodies produced in mice without pre-existing immunity. Furthermore, NP/RBD vaccination followed by boosting with RBD protein was also shown to produce RBD-specific splenocyte activation as measured by IFNγ ELISA and durable RBD-specific T cell responses. These results demonstrate proof-of-principle that antibody responses to a novel pathogen can be increased by drawing on previous immunity to an unrelated pathogen. Furthermore, this shows the benefits of an NP/RBD vaccine candidate against SARS-CoV-2.

At the conception of this project, we hypothesized three possible outcomes regarding the immunogenicity of NP/RBD. 1) NP/RBD would show increased immunogenicity in mice with pre-existing immunity to PR8 compared to mice without pre-existing immunity 2) NP/RBD would show decreased immunogenicity in mice with pre-existing immunity to PR8 compared to mice without pre-existing immunity 3) NP/RBD would show similar immunogenicity in mice with or without pre-existing immunity to PR8. While the pre-existing CD4 positive T cell immunity to NP was expected to boost antibody responses to RBD after NP/RBD vaccination, pre-existing antibodies to NP could have been expected to decrease antibody responses to RBD after NP/RBD vaccinations due to the well-described phenomenon of original antigenic sin[35–38]. In original antigenic sin, antibody responses are preferentially boosted to epitopes from a previous immunization at the expense of antibody responses to novel epitopes. We speculated that NP-specific B cells expanded during PR8 immunization could outcompete spike-specific B cells for access to NP/RBD antigen and for space in lymphatic tissue. However, our results demonstrate that the presence of NP-specific B

cells and NP-specific antibodies did not result in a decrease in spike-specific antibodies compared to mice without NP immunity.

The ability of NP to form oligomers likely contributes to the increased immunogenicity of NP/RBD over monomer RBD, and many vaccine platforms with RBD have made use of dimerized RBD or incorporated RBD into nanoparticle structures.[12,14,17,18] The oligomerization of NP/RBD could enhance its stability and allow for crosslinking of B-cell receptors upon antigen recognition for greater B cell stimulation[18,39]. The ability of NP/RBD to have enhanced immunogenicity not just from its structure but also from its engagement with immune responses to influenza makes it an ideal vaccine candidate against SARS-CoV-2.

The vaccine strategy outlined in the report has the potential to be incorporated into other vaccine strategies, such as mRNA or DNA vaccines. Additionally, the strategy of targeting preexisting immunity to increase antibody responses to a novel pathogen does not necessarily have to work with influenza and COVID-19. Vaccine strategies that draw on immunity to pathogens other than influenza are worth exploring, and this platform could potentially be used to increase antibody responses to pathogens other than SARS-CoV-2. There remain many future directions of investigation with this vaccine strategy, especially experiments designed to compare NP/RBD to the current approved vaccines, but our initial results demonstrate the beneficial effects of using an NP/RBD vaccine against SARS-CoV-2.

MATERIALS AND METHODS

Cloning

The genes for the extracellular domain of WA1 spike protein (amino acids 22-1208), WA1 spike RBD domain (amino acids 330-528), and NP/RBD were cloned into the pFastBac plasmid for baculovirus rescue with an N-terminal secretion signal sequence derived from the gene for WSN Influenza Hemagglutinin and a C-terminal 6xHis Tag for protein purification. pFastBac plasmid was digested with HindIII and BamHI restriction enzymes and genes of interest were inserted into the plasmid by InFusion ligation. Plasmid sequences were verified by Sanger Sequencing and purified plasmids were used for baculovirus rescue.

The gene for RBD (amino acids 319-528) was cloned into the pCAGGS plasmid with an N-terminal secretion signal derived from the gene for WSN Influenza Hemagglutinin and a C-terminal 6xHis Tag for protein purification. pCAGGS plasmid was digested with EcoRI and XhoI restriction enzymes and the RBD gene was inserted into the plasmid by InFusion ligation. Plasmid sequences were verified by Sanger Sequencing and purified plasmids were used for protein expression in 293T cells.

Baculovirus Rescue

Baculovirus rescues for protein expression were performed using the Bac-to-Bac Baculovirus Expression System according to the manufacturer's instructions (Invitrogen). Rescued virus was amplified twice in SF9 cells to produce P2 virus. Western Blots were performed with the cells used to produce the P2 virus to verify expression of the protein of interest. Verified P2 stocks were used to infect SF9 cells for protein purification.

Protein Purification

WA1 spike, spike RBD (amino acids 330-528), and NP/RBD protein were purified with the baculovirus expression system. 200mL of SF9 cells at a density of 1x10^6 cells/mL were infected with 20mL of P2 baculovirus containing the gene of interest. 48 hours after infection, the cells were collected and spun down at 500g for 5 minutes. The supernatants were collected and passed through a 0.2 micron filter, and PMSF protease inhibitor was added to the filtrate. The filtrate was then passed through a 5mL HisTrapFF Ni column (Cytiva) at a flow rate of 5mL per minute. The column was washed with 50mL of wash buffer containing 20mM imidazole, then protein was eluted from the column with 20mL of elution buffer containing 250mM imidazole. Eluted protein was diafiltrated and concentrated with a 15mL 10kD cut-off column (Amicon Ultracel 10K centrifugal filters), and the column was washed twice with PBS. Protein concentration was determined by Bradford Assay.

Spike RBD (amino acids 319-528) was purified by transfection of 293T cells with the RBD-pCAGGS plasmid. 5 T175 flasks (Genesee Scientific) of 293T cells were polyethylenimine (PEI) transfected with 30µg of pCAGGS expression plasmid in Opti/MEM media (Thermo Fisher) at a ratio of 3uL PEI:1ug DNA. 6 hours after the addition of DNA/PEI to the cells, the media was changed to 20mL DMEM media containing 10% FBS and cells were left at 37°C for 48 hours. After 48 hours, the supernatant was collected, and protein was purified with a 5mL HisTrap column (Cytiva). Eluted protein was diafiltrated with a 10kD cut-off column (Amicon Ultracel 10K centrifugal filters) and washed twice with PBS. Protein concentration was determined by

Bradford Assay. The eluted protein was further purified by size exclusion chromatography (Cytiva) with an AKTAgo system. The fraction corresponding to the RBD protein was collected and verified by Western blot and Coomassie Blue stain. Protein concentration was determined by Bradford Assay.

Western Blots and Coomassie Blue stains

Western Blots for RBD-containing proteins were blocked with 2% BSA in PBS containing 0.1% Tween20 (PBST), then blotted with anti-SARS-CoV-2 spike RBD Monoclonal Antibody (R&D Systems, Catalog # MAB10540) diluted 1:500 in 2% BSA/PBST for 1 hours. Blots were then incubated with goat α-mouse IgG-HRP secondary antibody (Prometheus) diluted 1:10,000 in blocking buffer for 1 hour. Blots were visualized with BioRad ChemiDoc Touch Imaging system. Coomassie Gels were stained as previously described[40].

Alphafold Prediction

Predicted protein structures for the RBD (amino acids 330-528) and NP/RBD were determined with the AlphaFold Colab based on AlphaFold v2.1.0 using the AlphaFold model parameters[32].

Mouse Infections and Vaccinations

The animal studies in this paper all made use of six-week-old female C57BL/6 mice purchased from Jackson Labs. Mice were infected intranasally with 100PFU of PR8 virus (A/Puerto Rico/8/34 strain) in 50uL PBS containing 0.4% BSA and 1% Pen-Strep antibiotic to establish pre-existing immunity to PR8. Purified virion of PR8 and IBV (B/Victoria/2/1987 strain) diluted in PBS were UV-inactivated on ice for 30 minutes and

added to equal volume of Addavax adjuvant for vaccinations. Mice were injected intramuscularly with 50µL of vaccine per injection in both back legs.

IgG and IgA ELISAs

ELISA to determine IgG antibody responses to PR8 NP protein, SARS-CoV-2 spike protein, and SARS-CoV-2 spike RBD protein were performed as follows. Maxisorp 96 well ELISA plates (Thermofisher) were coated with 50uL of purified target antigen at a concentration of 2.5ug/mL. Antigen was allowed to bind to the plate overnight at 4°C, then the plate was blocked with blocking buffer (1% milk in PBST). Sera was diluted 1:100 in blocking buffer, then serially diluted 3-fold. Plates were incubated with sera for 2 hours, after which the plates were washed 3 times with blocking buffer. Plates were incubated with goat α-mouse IgG-HRP secondary antibody (Prometheus) diluted 1:3000 in blocking buffer and incubated for 1 hour. Plates were washed 3 times with blocking buffer, then incubated with 100µL of SigmaFast OPD substrate for 30 minutes. Substrate reaction was stopped with 25µL of 3M HCl, and absorbance was measured at 450nm with a Luminometer plate reader (Promega). ELISAs to determine IgA antibody responses were performed in a similar manner. The starting dilution of nasal washes was undiluted sample, followed by serial 3-fold dilutions in blocking buffer. Plates were incubated with nasal wash for 2 hours, washed with blocking buffer 3 times, then incubated with goat anti-mouse IgA-HRP antibody (Southern Biotech) for 1 hour. Substrate addition and absorbance measurements were performed as with IgG responses.

Splenocyte Stimulations

Mice were euthanized with carbon dioxide on the day of splenocyte collection. Spleens were mashed through a 40 micron cell strainer and washed with 10mL R10 media (RPMI media containing 1% Glutamine, 1% Pen/Strep, 1% HEPES, and 10% FBS). Splenocytes were spun down at 1200rpm for 10 minutes, then resuspended in 3mL of ACK red blood cell lysis buffer for 5 minutes, after which 10mL of R10 media was added to the cells, and the cells were spun down again at 1200rpm for 10 minutes. Cells were resuspended in 4mL of R10 media and counted with a hemocytometer. $3x10^6$ cells per sample were added to each well of a 96 well plate in 50µL of R10 media. An additional 50uL of R10 media, R10 media containing RBD at 30ug/mL, or R10 media containing ConA were added to the cells. Cells were stimulated for 48 hours for IFNγ ELISAs or overnight for intracellular cytokine staining.

Intracellular Cytokine Staining and Flow Cytometry

Stimulated splenocytes were collected and blocked with Fc block for 5 minutes, then stained with CD4, CD8, and CD3 antibodies for 30 minutes at room temperature: anti-mouse CD8a FITC (Invitrogen 11-0081-81), anti-mouse CD4 APC-eFlour780 (Invitrogen 47-0041-82), and anti-mouse PerpCP-Cyanine 5.5 (Invitrogen 45-0031-82). Cells were then washed twice with 200µL FACS buffer (PBS, 2mM EDTA, 3%FBS). Cells were fixed and permeabilized with eBioscience Fixation/Permeabilization solution (00-5123), then stained with IFNγ antibody anti-mouse IFNγ PE (Invitrogen 12-7311-81) for 30 minutes at room temperature. Cells were washed twice with 200µL FACS buffer and analyzed by Flow Cytometry with a BD FACSCantoII system. 5,000 events were

recorded for each compensation control and 60,000 events were recorded for each sample. Gating and sample analysis was performed with FlowJo software v10.8.

Statistical Analysis

Unpaired t-tests for significance were performed with GraphPad Prism 9.2.0 software.

ETHICS STATEMENT

The animal studies were reviewed and approved by University of California, Riverside Institutional Animal Care and Use Committee (IACUC).

REFERENCES

1. Tian, D., Sun, Y., Xu, H. & Ye, Q. The emergence and epidemic characteristics of the highly mutated SARS-CoV-2 Omicron variant. *Journal of Medical Virology* **94**, 2376–2383 (2022).

2. Tao, K. *et al.* The biological and clinical significance of emerging SARS-CoV-2 variants. *Nat Rev Genet* **22**, 757–773 (2021).

3. Harvey, W. T. *et al.* SARS-CoV-2 variants, spike mutations and immune escape. *Nat Rev Microbiol* **19**, 409–424 (2021).

4. Yu, J. *et al.* Neutralization of the SARS-CoV-2 Omicron BA.1 and BA.2 Variants. *New England Journal of Medicine* **386**, 1579–1580 (2022).

5. Zhou, B. *et al.* SARS-CoV-2 spike D614G change enhances replication and transmission. *Nature* **592**, 122–127 (2021).

6. Zhang, L. *et al.* SARS-CoV-2 spike-protein D614G mutation increases virion spike density and infectivity. *Nat Commun* **11**, 6013 (2020).

7. Walls, A. C. *et al.* Structure, Function, and Antigenicity of the SARS-CoV-2 spike Glycoprotein. *Cell* **181**, 281-292.e6 (2020).

8. Yurkovetskiy, L. *et al.* Structural and Functional Analysis of the D614G SARS-CoV-2 spike Protein Variant. *Cell* **183**, 739-751.e8 (2020).

9. Cai, Y. *et al.* Distinct conformational states of SARS-CoV-2 spike protein. *Science* **369**, 1586–1592 (2020).

10. Lan, J. *et al.* Structure of the SARS-CoV-2 spike receptor-binding domain bound to the ACE2 receptor. *Nature* **581**, 215–220 (2020).

11. Tai, W. *et al.* A novel receptor-binding domain (RBD)-based mRNA vaccine against SARS-CoV-2. *Cell Res* **30**, 932–935 (2020).

12. An, Y. *et al.* A tandem-repeat dimeric RBD protein-based covid-19 vaccine zf2001 protects mice and nonhuman primates. *Emerging Microbes & Infections* **11**, 1058–1071 (2022).

13. Yang, J. *et al.* A vaccine targeting the RBD of the S protein of SARS-CoV-2 induces protective immunity. *Nature* **586**, 572–577 (2020).

14. Alleva, D. G. *et al.* Development of an IgG-Fc fusion COVID-19 subunit vaccine, AKS-452. *Vaccine* **39**, 6601–6613 (2021).

15. Dai, L. *et al.* Efficacy and Safety of the RBD-Dimer–Based Covid-19 Vaccine ZF2001 in Adults. *New England Journal of Medicine* **0**, null (2022).

16. Sun, S. *et al.* Interferon-armed RBD dimer enhances the immunogenicity of RBD for sterilizing immunity against SARS-CoV-2. *Cell Res* **31**, 1011–1023 (2021).

17. Ma, X. *et al.* Nanoparticle Vaccines Based on the Receptor Binding Domain (RBD) and Heptad Repeat (HR) of SARS-CoV-2 Elicit Robust Protective Immune Responses. *Immunity* **53**, 1315-1330.e9 (2020).

18. Liu, Z. *et al.* RBD-Fc-based COVID-19 vaccine candidate induces highly potent SARS-CoV-2 neutralizing antibody response. *Sig Transduct Target Ther* **5**, 1–10 (2020).

19. Yang, S. *et al.* Safety and immunogenicity of a recombinant tandem-repeat dimeric RBD-based protein subunit vaccine (ZF2001) against COVID-19 in adults: two randomised, double-blind, placebo-controlled, phase 1 and 2 trials. *The Lancet Infectious Diseases* **21**, 1107–1119 (2021).

20. China IMCAS's COVID-19 vaccine obtained emergency use approval in China. *Reuters* (2021).

21. Perappadan, B. S. Covid vaccine update | Corbevax, Covaxin get drug regulator nod for use in children between 5 and 12. *The Hindu* (2022).

22. Uzbekistan approves Chinese-developed COVID-19 vaccine. *Reuters* (2021).

23. Pegu, A. *et al.* Durability of mRNA-1273 vaccine–induced antibodies against SARS-CoV-2 variants. *Science* **373**, 1372–1377 (2021).

24. Mulligan, M. J. *et al.* Phase I/II study of COVID-19 RNA vaccine BNT162b1 in adults. *Nature* **586**, 589–593 (2020).

25. Walsh, E. E. *et al.* Safety and Immunogenicity of Two RNA-Based Covid-19 Vaccine Candidates. *New England Journal of Medicine* **383**, 2439–2450 (2020).

26. Corbett, K. S. *et al.* Evaluation of the mRNA-1273 Vaccine against SARS-CoV-2 in Nonhuman Primates. *New England Journal of Medicine* **383**, 1544–1555 (2020).

27. Abu-Raddad, L. J., Chemaitelly, H. & Bertollini, R. Waning mRNA-1273 Vaccine Effectiveness against SARS-CoV-2 Infection in Qatar. *New England Journal of Medicine* **386**, 1091–1093 (2022).

28. Lopez Bernal, J. *et al.* Effectiveness of Covid-19 Vaccines against the B.1.617.2 (Delta) Variant. *New England Journal of Medicine* **0**, null (2021).

29. Parker, D. C. T Cell-Dependent B Cell Activation. *Annual Review of Immunology* **11**, 331–360 (1993).

30. Noelle, R. J. & Snow, E. C. T helper cell-dependent B cell activation. *The FASEB Journal* **5**, 2770–2776 (1991).

31. Ise, W. & Kurosaki, T. Plasma cell generation during T-cell-dependent immune responses. *International Immunology* **33**, 797–801 (2021).

32. Jumper, J. *et al.* Highly accurate protein structure prediction with AlphaFold. *Nature* **596**, 583–589 (2021).

33. Shajahan, A., Supekar, N. T., Gleinich, A. S. & Azadi, P. Deducing the N- and O-glycosylation profile of the spike protein of novel coronavirus SARS-CoV-2. *Glycobiology* **30**, 981–988 (2020).

34. Watanabe, Y., Allen, J. D., Wrapp, D., McLellan, J. S. & Crispin, M. Site-specific glycan analysis of the SARS-CoV-2 spike. *Science* **369**, 330–333 (2020).

35. Brown, E. L. & Essigmann, H. T. Original Antigenic Sin: the Downside of Immunological Memory and Implications for COVID-19. *mSphere* **6**, e00056-21 (2021).

36. East, I. J., Todd, P. E. E. & Leach, S. J. Original Antigenic Sin: Experiments with a defined antigen. *Molecular Immunology* **17**, 1539–1544 (1980).

37. Vatti, A. *et al.* Original antigenic sin: A comprehensive review. *Journal of Autoimmunity* **83**, 12–21 (2017).

38. Zhang, A., Stacey, H. D., Mullarkey, C. E. & Miller, M. S. Original Antigenic Sin: How First Exposure Shapes Lifelong Anti–Influenza Virus Immune Responses. *The Journal of Immunology* **202**, 335–340 (2019).

39. Dai, L. *et al.* A Universal Design of Betacoronavirus Vaccines against COVID-19, MERS, and SARS. *Cell* **182**, 722-733.e11 (2020).

40. Hoffmann, A. B., Mazelier, M., Léger, P. & Lozach, P.-Y. Deciphering Virus Entry with Fluorescently Labeled Viral Particles. in *Influenza Virus: Methods and Protocols* (ed. Yamauchi, Y.) 159–183 (Springer, 2018). doi:10.1007/978-1-4939-8678-1_8.

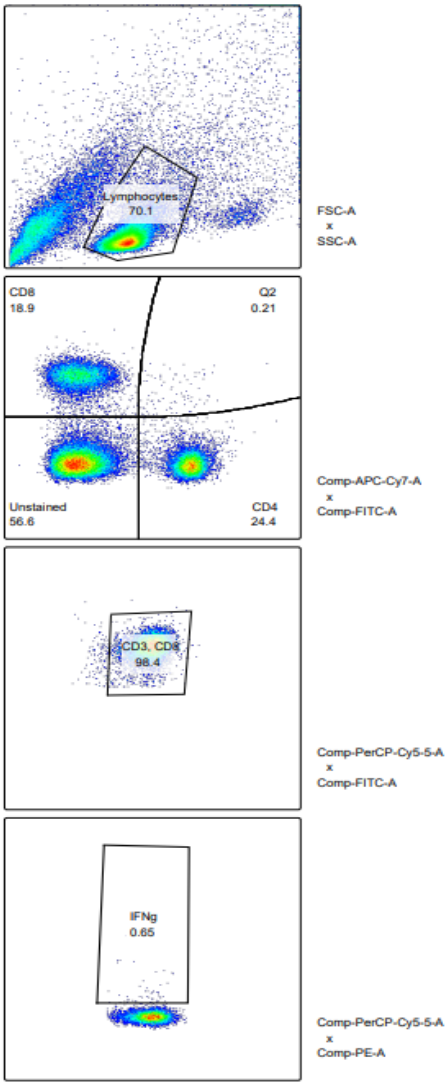

Supplemental Figure 4. Gating strategy for intracellular cytokine staining in Figure 16D. The top panel shows forward scatter on the x-axis and side scatter on the y-axis. The second panel from the top shows CD4 staining on the x-axis and CD8 staining on the y-axis. The third panel from the top shows CD3 staining on the x-axis and CD4 staining on the y-axis. The bottom panel shows CD3 staining on the x-axis and IFNγ staining on the y-axis.

Chapter 5:
Conclusions

This dissertation has focused on strategies to optimize immunity against influenza viruses and SARS-CoV-2 viruses. The experiments presented in Chapter 2 provide evidence that influenza viruses are susceptible to nitration, which reduces virus infectivity and immunogenicity. While nitration of virus proteins may not occur extensively in healthy individuals, future experiments designed to test the nitration of influenza virus proteins in individuals with chronic inflammatory conditions would be helpful. The experiments presented in Chapter 3 provide evidence that unnatural amino acid modifications have the potential to decrease immunogenicity of virus proteins. Because the strategy of using unnatural amino acids to create live but replication incompetent virus vaccines is promising, considerations should be made for the potential effects incorporating the unnatural amino acid has on virus protein immunogenicity. Finally, the experiments presented in Chapter 4 provide evidence that harnessing immunity to a previous influenza virus immunization can speed up the production of antibody responses to SARS-CoV-2. This is an exciting new vaccination strategy that has implications not only for SARS-CoV-2 and influenza viruses. Future experiments should focus on whether immunity to other pathogens can also speed up antibody production, the extent to which antibody or T cell responses to previous infection contribute to the increased antibody responses to spike, and whether this vaccine strategy can be adapted to other vaccine platforms such as virus-vectored or RNA vaccines. As we continue to face the threat of emerging viruses, new discoveries like those presented here will be invaluable in the goal of keeping the world safe from virus diseases.